Institute of Thermoelectricity, Academy of Sciences and Ministry of Education and Science of Ukraine

Journal of THERMOELECTRICITY

International Research

Founded in December, 1993

published 6 times a year

No. 1 *2020*

Editorial Board

International Editorial Board

Founders – National Academy of Sciences, Ukraine
Institute of Thermoelectricity of National Academy of Sciences and Ministry of Education and Science of Ukraine

Certificate of state registration № КВ 15496-4068 ПР

Approved for printing by the Academic Council of Institute of Thermoelectricity of the National Academy of Sciences and Ministry of Education and Science, Ukraine

Address of editorial office:
Ukraine, 58002, Chernivtsi, General Post Office, P.O. Box 86.
Phone: +(380-372) 90 31 65.
Fax: +(380-3722) 4 19 17.
E-mail: jt@inst.cv.ua
http://www.jt.inst.cv.ua

Signed for publication 26.03.2020. Format 70×108/16. Offset paper №1. Offset printing.
Printer's sheet 11.5. Publisher's signature 9.2. Circulation 400 copies. Order 5.

Printed from the layout original made by "Journal of Thermoelectricity" editorial board
in the printing house of "Bukrek" publishers,
10, Radischev Str., Chernivtsi, 58000, Ukraine

CONTENTS

General problems

V.I. Fediv, O.Yu. Mykytiuk, O.I. Olar, V. V. Kulchynskyj, T.V. Biryukova, O.P. Mykytiuk The role of microcalorimetric research in medicine and pharmacy 5

Theory

*Gorskyi P.V.*On the fundamental difference between thermoelectric composites and doped thermoelectric materials and the consequences it implies 25

Metrology and stardardization

V.G. Kolobrodov, V.I.Mykytenko. G.S.Tymchyk Polarization model of thermal contrast observation objects 36

Thermoelectric products

R.G. Cherkez, I.A.Konstantynovych. Generalized theory of thermoelectric energy conversion for permeable thermoelements 50

*Anatychuk L.I., Vikhor L.M., Kotsur M.P, Romaniuk I.F., Soroka A.V.*Optimal control of transient thermoelectric cooling process in the mode of minimum power consumption 61

*A.V. Prybyla, L.I.Anatychuk*Influence of miniaturization on the efficiency of a space-purpose thermoelectric heat pump 76

New

Casian A. I..

V.I. Fediv, *doc. phys.– math. sciences, professor*
O.Yu. Mykytiuk, *cand. phys.– math. sciences, assoc. professor*
O.I. Olar, *cand. phys.– math. sciences, assoc. professor*
V. V. Kulchynskyj, *cand. phys.– math. sciences, assist. professor*
T.V. Biryukova, *cand. techn. sciences, assoc. professor*
O.P. Mykytiuk, *cand. med. sciences, assoc. professor*

Higher State Educational Establishment of Ukraine
"Bukovinsky State Medical University"
Teatralna Square, 2 , Chernivtsi, 58002, Ukraine
e-mail: fediv.volodymyr@bsmu.edu.ua

THE ROLE OF MICROCALORIMETRIC RESEARCH IN MEDICINE AND PHARMACY

The article is devoted to an overview of some practical applications of microcalorimetric research methods for the needs of medical and pharmaceutical science and practice. The laws of thermodynamics are the main regulator of chemical processes, i.e. the processes of metabolism in biological systems. Biological thermodynamics deals with the quantitative study of the energy transformations occurring in living organisms, structures and cells, or the nature and function of the chemical processes underlying these transformations. Microcalorimetry is an indispensable tool for determining the thermodynamic parameters of a system, which is necessary both in the study of the structure of the biological system and the processes occurring in the system. The effects of drugs on the biological system and the processes of creating new drugs are also characterized by changes in thermodynamic parameters. Bibl. 43.
Key words: microcalorimetry, thermodynamics, phase transitions, medicine, pharmacy

Introduction

Microcalorimeters are devices for measuring the small amount of heat that occurs in closed volumes, called reaction chambers. Microcalorimetric studies are important in medicine and pharmacy, since most physico-chemical and biological processes are accompanied by thermal effects, yielding fundamental information on the nature of energy conversion in the system. Microcalorimeters are used to study the phase transitions in solid and liquid states, the formation of complexes, equilibrium constants, to study the interactions between solids and gases and liquids, to measure the heat of hydration, dissolution, adsorption, enthalpy, heat, and thermal conductivity. Also, important is the ability to study the thermogenesis of microorganisms, metabolic processes at different levels of living system organization, etc. [1].

Microcalorimeters are classified by thermal measurement conditions and by the interaction of the reaction chamber with the environment [2].

Main part

Thermodynamics of biological systems

The laws of thermodynamics have been developed for many years as fundamental rules that are satisfied when energy is exchanged in a thermodynamic system. The implications of the laws of thermodynamics are relevant to almost every aspect of scientific research.

Such concepts as thermal energy, temperature, heat transfer, thermodynamic process are handled to understand the laws of thermodynamics [3]. The laws of thermodynamics do not take into account the specific nature of heat transfer at the atomic or molecular level, but characterize the total energy and thermal transitions in the system [4].

A living organism is an energy system where the same laws of thermodynamics apply as in inanimate nature. There are various energy processes in the biosystems: breathing, photosynthesis, muscle contraction, transport of substances, etc. Processes that take place in biosystems are irreversible (non-equilibrium), that is, when the system goes from one state to another, it is impossible to return to the initial state without additional energy flow from the outside. The study of the biological process presents the following three tasks: the transfer of energy, which depends solely on the initial and final state of the system; the mechanism of reactions involved; the speed of these reactions.

According to the first law of thermodynamics, different types of energy can pass from one kind to another, but with these transformations energy does not disappear and does not appear from nothing. The implementation of the first law of thermodynamics for biological systems was proved in 1780 by Antoine Lavoisier and Pierre Laplace. They measured the amount of heat (at the rate of snow melting) and carbon dioxide released by the guinea pig during its life, and compared these values with the thermal effect of combustion reactions on CO_2 products. The results showed that there was no difference between the internal energy of the consumption products and the heat that was emitted. This proves that living organisms are not independent suppliers of energy, but merely transform one type of energy into another. The application of the first law of thermodynamics to living systems is that the energy supplied to living organisms by food is distributed in the process of consumption into two parts:

- released into the environment in the form of heat and energy contained in life products;
- deposited in cellular material.

The sum of these two parts is equal to the internal energy of the food supplied to the body [5].

The first law of thermodynamics of biological systems indicates that an arbitrary biological system (cell, human body, etc.) is an open thermodynamic system. This law establishes quantitative relationships between the amount of heat, the work, and the change in the internal energy of a thermodynamic system, but does not determine the direction of thermodynamic processes.

The energy balance of the body is studied by direct and indirect calorimetry. In the former case, a person is placed in an isolated chamber, in which the amount of heat radiated by a living organism during various processes of normal physiological activity is determined. Indirect calorimetry is based on calculation methods using respiratory coefficients (the ratio between the amount of carbon dioxide that is released and the amount of oxygen that is absorbed, for carbohydrates it is 1.0, for proteins - 0.8, for fats - 0.7) and the caloric equivalent of oxygen (the amount of heat released at a flow rate of 1 liter of oxygen, for carbohydrates it is 21.2 kJ, for proteins - 20.09 kJ, for fats - 19.6 kJ).

Enthalpy is often used to describe thermal effects in biological systems (showing the total heat content of the system), since all processes in cells occur at constant pressure:

$$\Delta H = \Delta U + p \cdot \Delta V,$$

here, $p \cdot \Delta V$ is a "non-mechanical work.

Enthalpy reflects the ability of systems to perform non-mechanical work and release heat, as well as the number and types of chemical bonds in reagents and reaction products. Enthalpy is a function of state, so it is impossible to determine the absolute value of enthalpy, but the enthalpy change associated with the thermodynamic process can be measured accurately. In the isochoric process, all the heat received by the system goes to a change in internal energy, that is, $Q_V = \Delta U$. Therefore, the change in internal energy in a certain process can be measured when it flows in a calorimeter at a constant volume. In an isobaric process, the system spends heat to perform work, therefore $Q_P = \Delta H$.

Sufficient accuracy in measuring the energy balance is achieved if the body does not perform mechanical work and does not accumulate biomass. In this case, the energy changes ΔH in the biological system can be accurately recorded by a calorimeter when measuring the heat released. If $H > 0$, the heat is absorbed and the reaction is called endothermic. If $\Delta H < 0$, then the system releases heat, and the reaction is called exothermic. Most metabolic reactions are exothermic. .

All the energy entering the body turns into heat. During the formation of ATP, only part of the energy is stored, most of it is dissipated in the form of heat. If ATP energy is used by the functional systems of the body, then most of this energy is also converted into heat. Part of the energy left in the cells is spent on the functions they perform, but it still turns into heat. For example, the energy used by muscle cells is spent on overcoming the forces of viscous resistance of muscles and other tissues. Viscous movement causes friction, which causes the formation of heat, for example, the expenditure of energy transmitted by the heart to the blood flow. During the movement of blood through the vessels, all energy is converted into heat due to friction between the layers of blood and between the blood and the walls of the vessels. So, in fact, all the energy that has been expended by the body ultimately turns into heat, with the exception of the case when the muscles perform work with external bodies [6].

For a long time, it was believed that only processes that are accompanied by a decrease in the energy of the system (exothermic) proceed spontaneously. However, many unauthorized endothermic processes (for example, dissolution of some salts, decomposition of carbonic acid, etc.) are known in which heat is absorbed. At low temperatures, mainly exothermic reactions occur.

In chemical reactions, under the action of the same principle, atoms tend to merge into such molecules, the formation of which leads to the release of energy (coupling reaction). But more likely are those reactions that result in an increase in the number of particles (decomposition reactions). Thus, unauthorized processes that occur without a change in energy state occur only in the direction in which disorder in the system increases and it passes to a more probable state.

Among the thermodynamic functions characterizing the energy state of a biological object, entropy plays an important role. Entropy characterizes energy costs usually in the form of heat during irreversible processes. Thus, entropy reflects that part of the energy of the system that has been dissipated, degraded in thermal form, and cannot be used to carry out work at a constant temperature. In reverse processes the entropy change is zero ($\Delta S = 0$), and in the case of irreversible it is positive ($\Delta S > 0$). Therefore, the smaller the energy gradients in a system and the more heat dissipated in the form of degraded energy, the greater its entropy.

Energy is spent on ordering the system, so an ordered system has a certain amount of energy and can do the work. This energy supply will inevitably be wasted due to insufficient isolation of the system from the environment.

According to the Boltzmann-Planck formula, the entropy of a system is related to the probability:

$$S=k\cdot\ln W,$$

where S is entropy, k is the Boltzmann constant, W is thermodynamic probability.

If we artificially create a closed isolated system with a very unlikely structure and leave it on its own, then it will evolve into a more probable structure. Therefore, we conclude that probability has a natural tendency to increase, as well as entropy. Entropy can be interpreted as a measure of disorder in a physical system or as a measure of a lack of information about the structure of a system. Since information can only be obtained as a result of energy expenditure, any experience that provides information about the physical system or arbitrary physical measurements of system parameters can be made as a result of increasing the entropy of the system or its environment. Moreover, the average entropy increase according to the second law of thermodynamics is always greater than the information obtained [7].

Entropy has positive values associated with increasing disorder and vice versa. In particular, the release of structured water molecules surrounding the binding surfaces is generally considered to be a source of positive entropy due to increased system disorder. Conversely, an increase in system ordering due to, for example, the introduction of conformational constraints in the binding complex is reflected by the negative entropy values [8].

The practical absence of reversible processes in biological systems causes the fact that all the processes that occur in them are accompanied by an increase in entropy. So, in biosystems, not all the free energy consumed by a particular process passes into useful work. Part of it dissipates in the form of heat. The ratio of the amount of work done to the amount of free energy expended on it is called the efficiency of the biological process.

Thus, muscle contraction is carried out with an efficiency of ~ 30%, glycolysis ~ 36%. However, there are also processes that are close to the reverse, that is, the efficiency of which is high. For example, the luminescence of some tropical insects has an efficiency of 98-99%, the discharge of electric fish - 98%. The reason for this highly efficient use of free energy is not yet fully understood. Thus, the more significant is the increase in entropy in a given process, the more probable is the irreversibility of this process.

Living organisms retain low levels of entropy over time because they receive energy from the environment in the form of food. This energy is released during the oxidation of the substance, which is accompanied by the consumption of oxygen and the release of carbon dioxide.

The second law of thermodynamics implies the principle that total entropy must increase steadily. Although thermodynamics does not independently describe processes as a function of time, the second law of thermodynamics determines the direction in which the value of total entropy increases.

The question is can the arbitrary process be reversed? The second law of thermodynamics answers that this is possible by creating an equivalent or even greater disorder elsewhere. A clear example is photosynthesis. Carbon dioxide, water, and other nutrients are absorbed by plants, and complex molecules of carbohydrates are synthesized at their expense. This process is accompanied by a decrease in entropy. Photosynthesis is impossible without sunlight. Therefore, the decrease in entropy in the synthesis of carbohydrates in plants is offset by the increase in entropy in the Sun. Many other important biochemical processes are also carried out with the reduction of entropy - the formation of biopolymers (proteins, nucleic acids, etc.), the active transport of ions through cell membranes, etc. But a living organism is an open system, and in it entropy can grow, remain unchanged or decrease depending on the amount of entropy generated inside the system, its inflow

from the outside or outflow into the environment. Our Universe is also not an isolated system, and therefore it does not face "thermal death" - a state of maximum entropy.

Entropy is a driving force for the unfolding of proteins. The natural state of a protein is characterized by a low value of entropy, since its conformation is very limited. On the other hand, the expanded form can exist in many different conformations, even if each amino acid takes only three positions, the polypeptide chain of 100 amino acids can take 3^{100} or 10^{47} different conformations. Since the result of the unfolding reaction of a protein can be in a large number of equivalent states in comparison with the natural state, entropy increases during the unfolding reaction. During protein folding, entropy loss must be balanced by the contribution of enthalpy to the free energy that promotes folding. Significant non-covalent forces of hydrogen bonds and other physical interactions compensate for small entropy. Changes in the entropy of the solvent - water - play an important role in compensating for the loss of conformational entropy. In the natural state, many non-polar amino acid residues, which are packed in protein, are sequestered (separated) away from water. In the unfolded form, these residues are treated with water molecules that are formed around nonpolar residues into cellular structures. The hydrogen bond network is reorganized so that the number of hydrogen bonds remains. This ordering of water molecules reduces its entropy. When the protein folds, these water molecules are released and the non-polar residues are separated from the water. The resulting recovery of entropy through water is a dominant force in protein folding, and this effect is generally known as the hydrophobic effect. Therefore, the solvent has a significant effect on biological reactions.

Entropy plays an important role in enzymatic catalysis. Usually, the reactions in solution are slow due to the entropic cost of bringing the reagents and catalyst together. Two or more molecules combined together into one entails significant entropy loss. On the other hand, when enzymes bind to the substrate, the released bond energy is used to compensate for the entropy losses caused by the formation of low-probability enzyme-substrate complexes as the enzyme-catalytic groups are very precisely oriented. This is due to an increase in the dissociation constant of enzyme-substrate complexes. Small losses of entropy occur during the stages of the chemical reaction, since the catalytic groups are already properly oriented in the enzyme – substrate complexes, and therefore their effective concentration is very high compared to the corresponding biochemical reactions that occur freely in solution [9].

According to the second law of thermodynamics, spontaneous chemical reactions, which in biological processes typically occur at constant temperature and pressure, are always accompanied by a decrease in free energy. Free energy is the energy spent to perform useful work. All reactions occur in the direction of the equilibrium state (where the free energy decreases no longer).

The stability of any isolated system is determined by the ratio of enthalpy and entropy factors. The former characterizes the system's desire for ordering, since this process is accompanied by a decrease in internal energy, the second - shows a tendency to disorder, since this situation is most likely. So, if in the process $\Delta S = 0$ - the degree of disorder does not change, then the process goes in the direction of decreasing enthalpy, that is, $\Delta H < 0$. If in the process no energy changes occur ($\Delta H = 0$), then the process goes towards increasing entropy, that is, $\Delta S > 0$.

As a criterion of arbitrariness in non-isolated systems, a new state function was introduced that takes into account both of these factors. This state function for isobaric processes is called Gibbs energy or isobaric isothermal potential G:

$$\Delta G = \Delta H - T\Delta S.$$

For isochoric processes, a similar Helmholtz energy or isochoric isothermal potential F is introduced:

$$\Delta F = \Delta U - T\Delta S.$$

At a constant temperature and pressure, only those processes can occur arbitrarily for which the change in the Gibbs (or Helmholtz) energy is negative [8].

Lost free energy appears as heat (enthalpy) or an increase in entropy. Thus, spontaneous chemical reactions on which life depends can occur with heat consumption, but only at the cost of an increase in free energy. For example, protein unfolding consumes a large amount of heat and is an example of a reaction caused by an increase in entropy. From the definition of entropy, when considering a biological process at constant temperature, the entropy change is equal to the heat given by the heat divided by the temperature. Since the heat of the protein unfolding is positive because it is consumed, the entropy changes are always positive.

Pharmaceutical materials, crystalline and amorphous, absorb water from the atmosphere, which affects critical drug development factors, such as the isolation of the crystalline form of the drug, compatibility with excipients, dosage form selection, packaging and shelf life. In order to improve knowledge of pharmaceutical materials and to bypass potential problems by studying the thermodynamics of the interaction of solids with sorbed water, a study was conducted [10].

In the study of increasing the bioavailability of an effective therapeutic and prophylactic agent of lovastatin, which blocks the initial stages of cholesterol synthesis, the thermodynamic parameters (ΔG, ΔH, ΔS) characterizing the process of solubility of lovastatin in aqueous solution were systematically determined along with other characteristics. The data obtained will ultimately enable the development of the desired highly soluble, effective and safer lovastatin preparations [11].

The review [12] discusses the role of thermodynamics in allosteric mechanisms, that is, when behavior in one part of a molecule changes due to a change that has occurred in another part of it. Conformational changes are accompanied by a significant increase in entropy. The effect of point mutations on the thermodynamic parameters of binding and function may reveal the energy pairing of neighboring (and distant) amino acid residues upon activation.

The determination of whether the interaction of a particular ligand-receptor in equilibrium is enthalpy or entropically stabilized can be achieved by thermodynamic analysis. Studies show that enthalpy stabilization is usually associated with the formation of new bonds (e.g, hydrogen bonds and van der Waals interactions) in the ligand-receptor-membrane matrix, whereas entropy stabilization is typically characterized by displacement of ordered water molecules associated with the formation of new hydrophobic interactions [13].

The energy exchange in living systems is organized in such a way that reactions that are possible from a thermodynamic point of view (for example, the breakdown of carbohydrates to water and carbon dioxide) and impossible (biosynthesis of complex molecules, active transport through cell membranes, etc.) are simultaneously running in it. This is achieved through energy coupling, the transition of the process into a multi-stage mode and the functioning of multi-enzyme systems. An energy coupling mechanism occurs when, in terms of the entropy criterion, the reaction is combined with the reaction, thermodynamically impossible, and gives it energy. The free energy of the former must exceed the energy consumed by the latter. Conjugating reactions should have a common component, a coupling factor, which is usually a phosphate ion. The conversion of the biochemical process into a multistage mode allows the living organism to easily regulate the synthesis of certain substances in the required quantities. This is because the difference in the free energies of the initial and final states for each of the individual stages is usually small, and therefore the probability of equilibrium is greater for it than for the process as a whole. Multistage passage of chemical transformations in living systems is ensured by the functioning of multi-enzyme systems operating on

the principle of molecular conveyor - the product of one enzymatic reaction serves as a substrate for subsequent transformation.

In living organisms, the most common conjugated process is active transport, that is, the transfer of a substance from a region of less concentration to a region of greater concentration. Such a process cannot arbitrarily occur because it is accompanied by an increase in the orderliness of the system, i.e. a decrease in entropy. Therefore, active transport occurs only in the case of coupling with another process - the source of energy. In the process of conjugation, some of the energy is converted into heat. The energy conversion efficiency in conjugated processes for biological systems is 0.8-0.9.

In [14], a methodology of linear irreversible thermodynamics is applied to study general systems in nonequilibrium states, which take into account both internal and external entropy contributions to analyze the efficiency of two conjugated processes. The results show that there are optimization criteria that can be used specifically for biological systems, where the optimal design of biological parameters created by nature at maximum effective power results in more efficient tools than those created at maximum power or in the best environmental conditions.

The study of the state of a living organism, as an open thermodynamic system, underlies the method of calorimetry (Latin calor - heat + Greek metreo - measure) - the measurement of the amount of heat released during various physical, chemical or biological processes. Calorimetry of biological and biochemical processes (biocalorimetry) allows quantifying the energy and thermal effects of individual biochemical reactions, the activity of cellular organelles and cells, tissues and organs, the body as a whole. Calorimetric studies measure the values of heat fluxes from a living object into the environment and calculate the amount of heat produced and the heat capacity of the organism; the measurement of heat capacity is based on the mass, heat capacity and temperature change of the object.

The direct detection of small thermal changes accompanying biological reactions provides for a universal method for the detection of molecular interactions and offers a significant advantage over biochemical analyses requiring specific development and optimization for each investigated target. Another advantage of calorimetry is that it is carried out in the liquid state of a substance and does not necessitate chemical modification, marking or immobilization.

Microcalorimetric methods in medicine, biology and pharmacy

The principle of calorimetry is based on the statement that in all chemical reactions there are changes in energy, which are usually accompanied by the release of heat (exothermic) or its absorption (endothermic). Microcalorimetry is a highly sensitive method that detects even the smallest temperature changes in small volume samples, which makes it possible to use it when developing biomaterials.

Microcalorimetry is used to study reactions involving biomolecules, including molecule interactions and conformational changes, such as protein folding. Areas of application range from confirmation of target binding in the development of low molecular weight drugs to the development of stable biotherapeutic drugs.

Consider microcalorimetry methods that have been widely used in biomedical and pharmaceutical research.

Isothermal microcalorimetry

Isothermal microcalorimetry (IMC) is a laboratory method of real-time monitoring and dynamic analysis of chemical, physical and biological processes. Within hours or days, the IMC determines the

onset, rate, degree, and energy of these processes for samples in small ampoules (e.g, 3-20 ml) at a constant set temperature (in the range of 15 ° C to 150 ° C).

IMC carries out this dynamic analysis by measuring and recording, compared with the previous time, the heat flow rate ($\mu J/s = \mu W$) to the ampoule with or from the sample, as well as the total amount of heat consumed or produced.

IMC is a powerful and versatile analytical tool for the following closely related reasons:

- all chemical and physical processes are either exothermic or endothermic - produce or consume heat;
- heat flow rate is proportional to the speed of the process;
- IMC is sensitive for detecting and monitoring very slow processes in a few grams of material or processes that generate a small amount of heat (for example, the metabolism of several thousand living cells);
- IMC instruments typically have a wide dynamic range - heat fluxes of approximately 1 μW up to 50,000 μW can be measured with the same instrument.

The IMC method for studying the speed of processes is widely used in practice, provides constant data in real time, and is sensitive. Measurements are quite simple, do not require supervision and fluorescent or radioactive markers.

However, there are cautions that should be kept in mind when using IMC:

- if the ampoules prepared from the outside are used, approximately 40 minutes are required to slowly insert the ampoule into the instrument without significantly disturbing the set temperature in the measuring module. However, arbitrary processes occurring during this time are not controlled;
- IMC records the total net heat flow produced or consumed by all processes occurring in the ampoule. Therefore, to be sure which process or processes produce the measured heat flux, one must be very careful, both in the experimental design and in the initial use of appropriate chemical, physical and biological analyzes.

It is believed that the possible use of IMC is limited only by the imagination of the person who chooses to use it as an analytical tool and the physical limitations of the method. In addition to the basic warnings described above, the limitations also include sample size and ampoules, as well as the temperatures at which measurements can be taken. IMC is generally best suited for evaluating processes that occur over the course of hours or days. Next, we will focus on the use of IMC in medicine, biology, and pharmacy, highlighted in recent publications.

The term metabolism is used to describe studies of the quantitative measurement of the rate at which heat is produced or consumed by whole small organisms, tissue specimens, or cells (including microbial) in culture. Metabolism can be useful as a diagnostic tool, especially for identifying the nature of a sample by its heat flux under specified conditions, or for determining metabolic processes.

To determine the metabolism using IMC, there should be enough cells, tissues or organisms that were initially present (or added later if replication occurs during the measurement of IMC) to generate a heat flux signal above a given detection limit of the device.

[15] describes the relationship of metabolic rate to the mass of an object and how it scales throughout the range from molecules and mitochondria to cells. The authors note that although the rate of metabolism of this type of mammalian cells in vivo is significantly reduced with increasing size (mass) of animals, the size of the donor animal does not affect the rate of cell metabolism when cultured in vitro. Extending theoretical and empirical analyzes of scaling to sub-organism levels can potentially be important for the cellular structure and its functions, as well as for the metabolic basis of aging.

Mammalian cells in culture have a metabolic rate of approximately 30 × 10−12 W/cell. IMC instruments have a sensitivity of at least 1×10^{-6} W (ie 1 μW). Therefore, the metabolic heat of approximately 33.000 cells is practically detected. Based on this sensitivity, the IMC was used to conduct a large number of pioneering studies of the metabolism of cultured mammalian cells in the 1970s and 1980s in Sweden. There are known IMC studies of heat flux from cultured human red blood cells, platelets, lymphocytes, lymphoma cells, granulocytes, adipocytes, etc., skeletal muscles and myocardial tissues. Studies were conducted to determine the possibility of using IMC as a method of clinical diagnosis and establishing metabolic differences between the cells of healthy people and people with various diseases or health problems [16].

IMC was used to evaluate antigen-induced proliferation of lymphocytes [17] and found aspects of proliferation that were not observed with the conventional method of analysis of a continuous radioactive marker. IMCs have also been used in the field of tissue engineering. Studies [18] showed that IMC can be used to measure the growth rate (i.e. proliferation) in a culture of human chondrocytes harvested for tissue engineering.

IMC is used in toxicology to monitor the metabolism of cultured cells in real time and to quantify the rate of metabolic decline as a function of the concentration of a possibly toxic agent. In the study of implant materials [19], both fast-growing fungal cultures and human chondrocyte cultures were exposed to calcium hydroxyapatite particles (<50 μm in diameter) and bioactive silicate glass particles. Glass particles slowed or reduced the growth of fungi as a function of increasing the concentration of particles. Hydroxyapatite particles had a much smaller effect and never completely reduced fungal growth at the same concentrations. The effect of both types of particles on chondrocyte growth was minimal when using the same concentration. The authors concluded that the cytotoxicity of solid particles such as bioactive glass and hydroxyapatite particles can be estimated using the microcalorimetry method. This is a modern method of studying in vitro biocompatibility and cytotoxicity of biomaterials, which can be used along with conventional analyses.

In the 1980s, publications appeared indicating the use of IMC in microbiology. Although some microbiological studies of IMC were aimed at viruses [20] and fungi [21], the entire research concerned bacteria. In [22], methods of using IMC in medical and environmental microbiology are considered. The article reports how accurate are the data on heat flow and fluctuations in the metabolic activity of microorganisms and the rate of replication in this environment.

In [23], the use of the microcalorimetric method for the evaluation of E. coli and S. aureus metabolism is highlighted. Measurements were taken in sealed 24-ml glass ampoules in the temperature range from 5 ° C to 90 ° C. The temperature measurement error was ± 0.02 °C. The detection limit was estimated to be 2 μ*W* and the baseline stability was 2 × 106 μ*W* for 24 hours. By registering heat transfer in real time, the metabolic activity of bacteria was evaluated and the effect of the extracts was investigated. Using kinetic and thermodynamic information from the microcalorimetric method, a number of important kinetic parameters were obtained: the growth rate constant, when reaching a maximum, the inhibition coefficient and the drag coefficient. Escherichia coli growth rate constant showed slight changes with increasing concentration of Aconitum alkaloids. However, the growth rate constant of S. aureus increased and then decreased as the concentration of Aconitum alkaloids increased. This indicated that treatment with Aconitum alkaloid slowed the growth and metabolism of S. aureus. Based on the study of the effect of various concentrations of Aconitum alkaloids on the growth of E. coli and S. aureus, it was concluded that Aconitum alkaloids do not affect the growth of E. coli, but potentially inhibit the action of S. aureus.

Modern isothermal microcalorimeters (IMC) are able to detect the metabolic heat of bacteria with the accuracy sufficient to recognize even the smallest bacterial infection of water, food and medical samples. IMC methods are superior to conventional detection methods in terms of detection time, reliability and technical efforts. In [24], a linear relationship was observed between the calorimetric detection time and the initial concentration of bacteria. This can be used to quantify bacterial infection. A study of the relationship between the level of filling (in mm) of the calorimetric capacity and the specific maximum heat flux (in mW.g-1) illustrated two completely different results for liquid and solid media. The time to detect the presence of bacteria by IMK depends on the initial amount of bacteria present, the sensitivity of the instrument and the level of heat flux above the initial level, which is chosen as an indicator of bacterial growth. In general, bacteria are about 1/10 the size of mammalian cells and possibly produce only 1/10 of the metabolic heat of the cell. However, some bacteria grow faster than mammalian cells, often their number increases within minutes. Therefore, a small initial bacterial count in a culture that does not initially detect IBC quickly yields a detectable amount. For example, 100 bacteria that double every 20 minutes in less than 4 hours will give more heat than 330,000 bacteria, and heat flow will be determined by IMC. Therefore, IMC can be used for easy, rapid detection of bacteria, in particular for the detection of tuberculosis mycobacteria [25]. The metabolic evolution of mycobacterial heat during cell proliferation is measured by the IMC and is considered as a possible alternative to conventional diagnostic agents.

Staphylococcus aureus biofilm plays a major role in implant-associated infections. The sensitivity of S. aureus biofilm to daptomycin, phosphomycin, vancomycin, trimethoprim/ sulfamethoxazole, linezolid and rifampicin has been investigated by isothermal microcalorimetry [26]. In addition, the permanent status of cells isolated from S. aureus biofilm after vancomycin treatment was also analyzed. S. aureus biofilm was resistant to all tested antibiotics except daptomycin. Step-by-step treatment with vancomycin to destroy all metabolically active cells and with daptomycin to destroy persistent cells has destroyed the entire bacterial population. These results support the use in clinical practice of a therapeutic regimen based on the use of two antibiotics to kill persistent cells and eradicate S. aureus biofilm. IMC is an appropriate technique for characterizing real-time reversion from resistant to metabolically active cells.

Candida auris has emerged worldwide as a multi-resistant fungal pathogen. Using IMC, the heat production profiles of C. auris and other Candida spp. strains were compared and evaluated their antifungal susceptibility [27]. C. auris showed a peculiar heat production profile that distinguished it from other species. The thermogenic parameters of C. auris offer slower growth rates compared to C. lusitaniae and another clear thermal profile compared to complex strains of C. haemulonii species. Amphotericin B-based treatment has been identified as a potential therapeutic option for C. auris infection.

The IMC for thermally viable microorganisms in pure cultures and stable formulations was investigated in [28]. Quantifying viable microorganisms is an important step in microbiological research as well as in the formation of microbial products for the development of biological control products or probiotics. Thermal viability methods are new and effective methods for rapidly quantifying different species of bacteria and fungi and for increasing the speed, sensitivity and accuracy of routine viability estimates for pure cultures and controlled microbiomes such as plant seed coatings.

Despite significant advances in diagnostic and therapeutic approaches, fungal infections caused by C. albicans continue to be a serious problem in intensive care units worldwide. The economic cost of fungal blood infections and associated mortality, especially in debilitated patients, remains high. C. albicans is a highly adapted microorganism capable of developing resistance after prolonged exposure

to antifungal agents. The formation of a biofilm that reduces the availability of an antifungal drug, the release of spontaneous mutations that increase expression or reduce the susceptibility of targets, altered chromosomal abnormalities, overexpression of waste from several drugs, and the ability to avoid the body's immune defenses are some of the factors that can contribute to antifungal tolerance and resistance. Knowledge of the mechanisms of antifungal resistance may allow the development of alternative therapeutic options to modulate or restore resistance. The review [29] focuses on the factors involved in antifungal resistance and tolerance in patients with C. albicans blood infections.

In a study [30], the effects of fluconazole, caspofungin, anidulafungin, and amphotericin B are investigated against Candida species in planktonic form and biofilms using an IMC that measures the growth of heat production. An isothermal microcalorimeter equipped with 48 calorimeters and a sensitivity threshold of 0.2 μW was used. The heat flow was recorded for 48 hours. The study demonstrated the potential of microcalorimetry to test real-time antifungal sensitivity and evaluate antifungal activity against planktonic film and Candida biofilm.

Antibiotic abuse has led to increased bacterial resistance, which significantly limits the use of antibiotics for the treatment of bacterial infections. Therefore, it became necessary to develop new antibacterial drugs. Work [31] gives an idea of the effect of traditional Chinese medicine on drug-resistant bacteria. Dracotomelon tao is a traditional medicinal material derived from Anacardiaceae with a long history of treating various infectious diseases such as decubitus and skin ulcers. Recent studies have shown that various extracts from D. tao leaves containing flavonoids and phenolic acids exhibit potent antibacterial activity. In this study, the combination of bacteria-resistant action of these active ingredients was studied. Microcalorimetric measurements and principal component analysis were performed on samples from D. tao leaves in vitro. The results showed that all six samples had significant antibacterial activity, so the drug from the leaves of D. tao can be used as a potential antimicrobial resource in the treatment of infectious diseases.

With the addition of an IMC, which made it particularly valuable for biomedical and pharmaceutical applications, P. mirabilis was found to increase in the Luria broth environment between 2 and 9 h. research. The culture emitted 2.1 J with a maximum thermal output of 76 μW. The growth rate, calculated using calorimetric and spectrophotometric data, was 0.60 and 0.57 h – 1, respectively. Additional information gathered on the protease activity of P. mirabilis, which corresponds to the last peak in heat production. Tumor microtissues growth was also monitored, which exhibit a maximum thermal power of 2.1 μW, which corresponds to an increase in microtissue diameter from about 100 to 428 μm. This opened up new areas of research in oncology, diagnosis and the development of new antitumor drugs. For parasitic worms, the technique allows one to evaluate the survival of parasites using motor and metabolic activity of even one individual [32].

Isothermal titration calorimetry

Isothermal titration calorimetry (ITC) is one of the most powerful methods for obtaining accurate information about the energy of biomolecules, which are associated with other biological macromolecules. ITC is a thermodynamic technique that directly measures the release or absorption of heat in intermolecular interactions such as ligand-protein, protein-protein [8]. An ITC experiment consists of calorimetric titration of a specific volume of one of the reagents, usually a macromolecule, with a controlled amount of another reagent, usually a ligand, at a constant temperature and pressure. Thus, the measured heat during titration corresponds to the enthalpy of such interactions [10]. This relatively simple experiment allows for a complete and accurate thermodynamic characterization of

the binding event (binding constant, enthalpy change, reaction stoichiometry, process heat change) that are important for understanding and optimizing molecular interactions [33].

Most biological phenomena affect intermolecular recognition and interaction. It is the main tool for the development and study of drugs and the regulation of protein interactions.

Over the last thirty years, ITC has become a powerful tool for studying a wide variety of molecular interactions. This technique is able to provide a complete thermodynamic profile of the interaction process in one experiment, with several advantages over other comparable methods, such as a smaller sample size or no chemical modification or labeling. Therefore, it is not surprising that ITC is used to study various types of interactions of natural products to gain new insights into the key molecular factors involved in the complexation of this type of compounds. A review article [34] describes the methodology of ITC and discusses some applications of ITC for studying protein-ligand interactions, protein-protein interactions, self-association, and drug development processes. The use of ITC to determine the kinetic parameters of enzyme catalyzed reactions as well as thermodynamic parameters is discussed. The review [35] confirms the use of ITC as a powerful tool for investigating the interaction of natural products with proteins, nucleic acids, oligosaccharides, and other types of receptors.

The enthalpy and entropy of binding in the creation of complexes that provide the release of therapeutic substances was investigated in [36] by the method of ITC. The information obtained is very important for drug developers, as it warns against taking into account the particularities of drug behavior in different environments.

Calorimetry of isothermal titration is a tool capable of determining thermodynamic as well as kinetic parameters associated with protein-ligand recognition and plays an important role in drug design. Further efforts to investigate the protein-ligand binding characteristics of ITC with a large amount of thermodynamic and kinetic data will lead to new discoveries that will extend our ability to understand the full range of protein-ligand recognition and treatment and to use these results appropriately for medical applications [37].

Differential scanning calorimetry

Differential scanning calorimetry (DSC) is a thermoanalytical technique in which the difference in the amount of heat required to increase the temperature of a sample and a reference is measured as a function of temperature. Both the samples and the reference are maintained at almost the same temperature throughout the experiment. As a rule, the temperature program for DSC analysis is designed in such a way that the temperature of the sample holder increases linearly as a function of time. The control sample should have a well-defined heat capacity in the temperature range to be scanned.

The DSC is based on the principle that during the physical transformation of the sample such as phase transitions, it will receive more or less heat than the reference, to maintain both samples at the same temperature. More or less heat will be supplied to the sample depends on whether the process is exothermic or endothermic. For example, if a solid sample is melted to a liquid state, it needs more heat entering the sample in order to increase its temperature at the same speed as the reference. This is due to the absorption of heat by the sample, since it experiences an endothermic phase transition from solid to liquid. If the sample is subjected to exothermic processes (such as crystallization), less heat is required to increase the sample temperature. By controlling the heat flux difference between the sample and the standard, the DSC is able to measure the amount of heat absorbed or released during such transitions. DSC can also be used to observe subtle physical changes such as glass transition.

The result of the DSC experiment is a heat flux curve depending on temperature or time. This curve can be used to calculate the enthalpy of transitions:

$$\Delta H = K S,$$

where ΔH is the enthalpy of the transition, K is the calorimetric constant, and S is the area under the curve. The calorimetric constant varies depending on the device, so it is determined using samples with known transition enthalpies.

DSC can be used for thermodynamic analysis of proteins, namely to reveal important information about the global structure of proteins and the interaction between proteins and ligands. In particular, mutations reduce protein stability, whereas ligand binding usually increases protein stability [38]. With DSC, stability can be measured by obtaining the Gibbs free energy value at any given temperature. This allows researchers to compare the free unfolding energy between a protein without a ligand and a protein-ligand complex, or between wild-type proteins and mutants. DSC can also be used to study the interaction between proteins and lipids, nucleotides, between drugs and lipids [39].

DSC provides a complete thermodynamic profile for unfolding of system energy. The determination of binding energy is then determined by considering the unfolding of energy of the biomolecules in the presence and absence of the binding component. The DSC method is widely used in the pharmaceutical industry to determine drug treatment parameters. Therefore, if the drug is to be delivered in an amorphous form, it is recommended to treat the drug at a temperature below crystallization temperature.

The solubility of gemfibrozil, a drug that lowers cholesterol and is poorly soluble in water, was studied by DSC. The solvents used in the pharmacy were tested: water, methanol, ethanol, isopropanol, 1-butanol, 2-butanol, ethylene glycol, propylene glycol, polyethylene glycol-400, ethyl acetate, dimethyl sulfoxide and transcutol in the temperature range from 298.2 K to 318.2 K at atmospheric pressure P = 0.1 MPa. It was found that the maximum solubility characteristic of transcutol is minimal for water. Thermodynamic analysis on experimental solutions showed endothermic and entropy dissolution of gemfibrozil in each pharmaceutically used solvent [40].

Micro DSC is capable of both isothermal and non-isothermal calorimetric studies. Due to the increase in cell size and sensitivity requirements, the scanning speed is usually low (up to about 1 °C/min). Temperature ranges from approximately - 40 °C to 100-200 °C. The device allows you to control a very slow scan speed, such as 0.001 °C/min.

Micro DSC in combination with x-ray diffraction is also used to study phase transitions in biological samples, degradation of medical preparations, study of antiviral drugs, to determine their thermodynamically stable forms [41 – 43].

Conclusions

An analysis of the practical application of isothermal calorimetry, isothermal titration calorimetry and differential scanning calorimetry in biology, medicine and pharmacy shows that these methods have been widely used to determine the thermodynamic parameters of the system, in particular, Gibbs free energy, enthalpy, entropy, which are important for understanding and optimizing molecular interactions, phase transitions in solid and liquid states, studying solubility and crystallization processes, which is important for better use of pharmaceuticals. Microcalorimetry methods are used to study the processes of metabolism, in tissue engineering and toxicology and for the practical needs of microbiology: the study of viruses, bacteria, fungi. The main purpose is to eliminate their resistance to

the action of drugs. The results of microcalorimetric studies are used to create new drugs, including anticancer therapies.

References

1. L.I. Anatychuk (1979). Termoelementy i termoelektricheskiie ustroistva [*Thermoelements and thermoelectric devices*]. Kyiv: Naukova dumka [in Russian].
2. L.I. Anatychuk, O.J. Luste (1981). Mikrokalorimetriia [*Microcalorimetry*]. Lviv, Vyshcha shkola [in Russian].
3. J.A. Zimmerman (2020). Laws of thermodynamics. *ThoughtCo*, thoughtco.com/laws-of-thermodynamics-p3-2699420.
4. Application of thermodynamics to biological and materials science (2011) T. Mizutani (Ed). Published by InTech.
5. L.I. Hryhorieva, Yu.A. Tomilin (2011) Osnovy biofizyky i biomekhaniky [*Fundamentals of biophysics and biomechanics*]. Mykolaiv: ChDU im. Petra Mohyly [in Russian].
6. V.S. Antoniuk, M.O. Bondarenko, V.A. Vashchenko, H.V. Kanashevych, H.S. Tymchuk, I.V. Yatsenko (2012) Biofizyka i biomekhanika: pidruchnyk [*Biophysics and biomechanics: Textbook*]. Kyiv: NTUU «KPI» [in Ukranian].
7. Anatychuk L.I., Luste O.J., Kobylianskyi R.R. (2017) Information-energy theory of medical purpose thermoelectric temperature and heat flux sensors. *J.Thermoelectricity,* 3, 5-20.
8. N.C. Garbett., J.B. Chaires (2012) Thermodynamic studies for drug design and screening. *Expert Opin Drug Discov*, 7(4): 299–314.
9. J. Udgaonkar (2001) Entropy in biology. *Resonance*, 6(9), 61-66.
10. M. Sacchetti (2014) Thermodynamics of water–solid interactions in crystalline and amorphous pharmaceutical materials. *Journal of Pharmaceutical Sciences*, 103(9), 2772-2783.
11. N.F. Zolkiflee, M.M.R Meor Mohd Affandi, A.B.A Majeed. (2020) Thermodynamics and solute-solvent interactions of lovastatin in an aqueous arginine solution. *European Journal of Pharmaceutical Sciences*, 141(1), 105111.
12. Maksay G. (2011) Allostery in pharmacology: thermodynamics, evolution and design. *Prog Biophys Mol Biol*., 106(3), 463-73.
13. S.P. Mitra (2009) Drug-receptor Interaction: pharmacology, binding and thermodynamics – A Review. *Journal of Surface Science and Technology*, 25(3-4), 103-152.
14. J.C Chimal., N. Sanchez, P.R. Ramírez (2017). Thermodynamic optimality criteria for biological systems in linear irreversible thermodynamics. *J. Phys.: Conf. Ser*, 792, 012082.
15. G.B. West, W.H. Woodruff, J.H. Brown (2002) Allometric scaling of metabolic rate from molecules and mitochondria to cells and mammals. *PNAS*, 99, 2473–2478.
16. M. Monti (1990). Application of microcalorimetry to the study of living cells in the medical field. *Thermochimica Acta*, 172, 53–60.
17. C. Murigande, S. Regenass, D. Wirz, A.U. Daniels, A. Tyndall (2009).A comparison between (3H)-thymidine incorporation and isothermal microcalorimetry for the assessment of antigen-induced lymphocyte proliferation. *Immunological Investigations*, 38 (1), 67–75.
18. R. Santoro, O. Braissant, B. Müller, D. Wirz, A.U. Daniels, I. Martin, D. Wendt (2011). Real-time measurements of human chondrocyte heat production during in vitro proliferation. *Biotechnology and Bioengineering*, 108 (12), 3019–3024.
19. A. Doostmohammadi, A. Monshi, M.H. Fathi, S. Karbasi, O. Braissant, A.U. Daniels (2011) Direct cytotoxicity evaluation of 63S bioactive glass and bone-derived hydroxyapatite particles

using yeast model and human chondrocyte cells by microcalorimetry. *Journal of Materials Science: Materials in Medicine*, 22 (10), 2293–2300.

20. Z. Heng, Z. Congyi, W. Cunxin, W. Jibin, G. Chaojiang, L. Jie, L. Yuwen (2005). Microcalorimetric study of virus infection; The effects of hyperthermia and 1b recombinant homo interferon on the infection process of BHK-21 cells by foot and mouth disease virus. *Journal of Thermal Analysis and Calorimetry*, 79 (1), 45–50..
21. O.A. Antoce, V. Antocie, K. Takahashi, N. Pomohaci, I. Namolosanu (1997) Calorimetric determination of the inhibitory effect of C1-C4 n-alcohols on growth of some yeast species". *Thermochimica Acta*, 297 (1–2), 33–42.
22. Braissant O., Wirz D., Gopfert B., Daniels A. U. (2010) Use of isothermal microcalorimetry to monitor microbial activities. *FEMS Microbiol. Lett*, 303 (1), 1–8.
23. Y. Shi, L. Liu, W. Shao, T. Wei, G. Lin (2015) Microcalorimetry studies of the antimicrobial actions of Aconitum alkaloids *J. Zhejiang Univ Sci B*., 16(8), 690–695.
24. C. Fricke, H. Harms, T. Maskow (2019) Rapid calorimetric detection of bacterial contamination: influence of the cultivation technique. *Front Microbiol*, 10, 2530.
25. O. Braissant, G. Theron, S.O. Friedrich, A.H. Diacon, G. Bonkat (2020). Comparison of isothermal microcalorimetry and BACTEC MGIT960 for the detection of the metabolic activity of Mycobacterium tuberculosis in sputum samples. *J Appl Microbiol*. doi:10.1111/jam.14549.
26. M. Butini, G. Abbandonato, C. Di Rienzo, A. Trampuz, M. Di_luca (2019). Isothermal microcalorimetry detects the presence of persister cells in a Staphylococcus aureus biofilm after vancomycin treatment. *Front. Microbiol*. 10, 332.
27. M. Di Luca, A. Koliszak, S. Karbysheva, A. Chowdhary, J.F. Meis, A. Trampuz (2019). Thermogenic characterization and antifungal susceptibility of candida auris by microcalorimetry. *J. Fungi*. 5(4):103.
28. J. Nykyri, A.M. Herrmann, S. Håkansson (2019). Isothermal microcalorimetry for thermal viable count of microorganisms in pure cultures and stabilized formulations. *BMC Microbiol*.19, 65, 10.
29. S. Costa-de-Oliveira, A.G. Rodrigues (2020) Candida albicans antifungal resistance and tolerance in bloodstream infections: The triad yeast-host-antifungal. *Microorganisms*, 8(2), 154.
30. E. M. Maiolo, U. F. Tafin, O. Borens, A. Trampuz (2014)Activities of Fluconazole, Caspofungin, Anidulafungin, and Amphotericin B on Planktonic and Biofilm Candida Species Determined by Microcalorimetry. *Antimicrobial Agents and Chemotherapy*, 58(5), 2709–2717.
31. Z. Xu, H. Li, X. Qin, T. Wang, J. Hao, J. Zhao, J. Wang, R. Wang, D. Wang, S. Wei, H. Cai, Y. Zhao (2019). Antibacterial evaluation of plants extracts against ampicillin-resistant Escherichia coli (E. coli) by microcalorimetry and principal component analysis. *AMB Expr,* 9,101.
32. O. Braissant, J. Keiser, I. Meister, A. Bachmann, D. Wirz, B. Göpfert, G. Bonkat, I. Wadsö (2015). Isothermal microcalorimetry accurately detects bacteria, tumorous microtissues, and parasitic worms in a label-free well-plate assay. *Biotechnol J.,* 10(3), 460–468.
33. Applications of calorimetry in a wide context – differential scanning calorimetry, isothermal titration calorimetry and microcalorimetry (2013). Amal Ali Elkordy (Ed.). InTech.
34. M.S. Atria, A.A. Sabouryb, F. Ahmad (2015). Biological applications of isothermal titration *Calorimetry. Phys. Chem. Res*., 3(4), 319-330.
35. O. Callies, A. Hernández Daranas (2016). Application of isothermal titration calorimetry as a tool to study natural product interactions. *Nat. Prod. Rep*, 33, 881-904.
36. A-M. Totea, J. Sabin, I. Dorin, K. Hemming, P. Laity, B. Conway, L. Waters, K. Asare-Addo (2019). Thermodynamics of clay – Drug complex dispersions: Isothermal titration calorimetry

and high-performance liquid chromatography. *Journal of Pharmaceutical Analysis*. https://doi.org/10.1016/j.jpha.2019.12.001

37. H. Su, Y. Xu (2018). Application of ITC-based characterization of thermodynamic and kinetic association of ligands with proteins in drug design. *Front. Pharmacol*, 9, 1133.
38. A. Schön, R.K. Brown, B.M. Hutchins, E. Freire (2013). Ligand binding analysis and screening by chemical denaturation shift *Analytical Biochemistry,* 443 (1), 52–7.
39. M.H. Chiu, E.J. Prenner (2011). Differential scanning calorimetry: An invaluable tool for a detailed thermodynamic characterization of macromolecules and their interactions *Journal of Pharmacy & Bioallied Sciences*. 3 (1), 39–59.
40. M.A. Kalam, S. Alshehri, A. Alshamsan, M. Alkholief, R. Ali, F. Shakeel (2019). Solubility measurement, Hansen solubility parameters and solution thermodynamics of gemfibrozil in different pharmaceutically used solvents. *Drug Dev Ind Pharm*, 45(8), 1258-1264.
41. K. Lohner, E. J. Prenner (2000). Differential scanning calorimetry and X-ray diffraction studies of the specificity of the interaction of antimicrobial peptides with membrane-mimetic systems *Biochimica et Biophysica Acta (BBA),* 1462 (1–2), 141-56.
42. Y. Pang, A. Buanz, R. Telford, O.V. Magdysyuk, S. Gaisforda, Ga.R. Williamsa (2019). A simultaneous X-ray diffraction–differential scanning calorimetry study into the phase transitions of mefenamic acid. *Journal of Applied Crystallography,* 52(6), 1264-1270.
43. R.L. Roque-Flores, J.R. Matos (2019). Simultaneous measurements of X-ray diffraction–differential scanning calorimetry. *J Therm Anal Calorim,* 137, 1347–1358.

Submitted 29.01.2020

В.І. Федів, *докт. фіз.– мат. наук, проф.*
О.Ю. Микитюк, *канд. фіз.– мат. наук, доц.*
О.І. Олар, *канд. фіз.– мат. наук, доц.*
В.В. Кульчинський, *канд. фіз.– мат. наук, асист.*
Т.В. Бірюкова, *канд. техн. наук, доц.*
О.П.Микитюк, *канд. мед. наук, доц.*

Вищий державний навчальний заклад України
«Буковинський державний медичний університет»
Театральна площа, 2,Чернівці, 58002, Україна
e-mail: fediv.volodymyr@bsmu.edu.ua

РОЛЬ МІКРОКАЛОРИМЕТРИЧНИХ ДОСЛІДЖЕНЬ У МЕДИЦИНІ І ФАРМАЦІЇ

Стаття присвячена огляду деяких практичних застосувань мікрокалориметричних методів дослідження для потреб медичної і фармацевтичної науки та практики. Основним регулятором хімічних процесів – процесів обміну речовин у біологічних системах - є закони

термодинаміки. Кількісним вивченням енергетичних перетворень, що відбуваються в живих організмах, структурах і клітинах, чи природи та функції хімічних процесів, що лежать в основі цих перетворень, займається біологічна термодинаміка. Мікрокалориметрія є незамінним інструментом для визначення термодинамічних параметрів системи, що необхідно як при дослідженні структури біологічної системи, так і процесів, які відбуваються в системі. Дія ліків на біологічну систему та процеси створення нових лікарських засобів також характеризуються зміною термодинамічних показників. Бібл. 43.
Ключові слова: мікрокалориметрія, термодинаміка, фазові переходи, медицина, фармація

В.И. Федив, *докт. физ.– мат. наук, проф.*
О.Ю. Микитюк, *канд. физ.– мат. наук, доц.*
О.И. Олар, *канд. физ.– мат. наук, доц.*
В.В. Кульчинский, *канд. физ.– мат. наук, ассист.*
Т.В. Бирюкова, *канд. тех. наук, доц.*
О.П.Микитюк, *канд. мед. наук, доц.*

Высшее государственное учебное заведение Украины
«Буковинский государственный медицинский университет»
Театральна площадь, 2,Черновцы, 58002, Украина
e-mail: fediv.volodymyr@bsmu.edu.ua

РОЛЬ МИКРОКАЛОРИМЕТРИЧЕСКИХ ИССЛЕДОВАНИЙ В МЕДИЦИНЕ И ФАРМАЦИИ

Статья посвящена обзору некоторых практических применений микрокалориметрических методов исследования для целей медицинской и фармацевтической науки и практики. Основным регулятором химических процессов – процессов обмена веществ в биологических системах - являются законы термодинамики. Количественным изучением энергетических преобразований, происходящих в живых организмах, структурах и клетках, или природы и функции химических процессов, лежащих в основе этих преобразований, занимается биологическая термодинамика. Микрокалориметрия является незаменимым инструментом для определения термодинамических параметров системы, что необходимо как при исследовании структуры биологической системы, так и процессов, происходящих в ней. Действие лекарств на биологическую систему и процессы создания новых лекарственных средств также характеризуются изменением термодинамических показателей. Библ. 43.
Ключевые слова: микрокалориметрия, термодинамика, фазовые переходы, медицина, фармация

References

1. L.I. Anatychuk (1979). Termoelementy i termoelektricheskiie ustroistva [*Thermoelements and thermoelectric devices*]. Kyiv: Naukova dumka [in Russian].
2. L.I. Anatychuk, O.J. Luste (1981). Mikrokalorimetriia [*Microcalorimetry*]. Lviv, Vyshcha shkola [in Russian].
3. J.A. Zimmerman (2020). Laws of thermodynamics. *ThoughtCo*, thoughtco.com/laws-of-thermodynamics-p3-2699420.
4. Application of thermodynamics to biological and materials science (2011) T. Mizutani (Ed). Published by InTech.
5. L.I. Hryhorieva, Yu.A. Tomilin (2011) Osnovy biofizyky i biomekhaniky [*Fundamentals of biophysics and biomechanics*]. Mykolaiv: ChDU im. Petra Mohyly [in Russian].
6. V.S. Antoniuk, M.O. Bondarenko, V.A. Vashchenko, H.V. Kanashevych, H.S. Tymchuk, I.V. Yatsenko (2012) Biofizyka i biomekhanika: pidruchnyk [*Biophysics and biomechanics: Textbook*]. Kyiv: NTUU «KPI» [in Ukranian].
7. Anatychuk L.I., Luste O.J., Kobylianskyi R.R. (2017) Information-energy theory of medical purpose thermoelectric temperature and heat flux sensors. *J.Thermoelectricity,* 3, 5-20.
8. N.C. Garbett., J.B. Chaires (2012) Thermodynamic studies for drug design and screening. *Expert Opin Drug Discov*, 7(4): 299–314.
9. J. Udgaonkar (2001) Entropy in biology. *Resonance*, 6(9), 61-66.
10. M. Sacchetti (2014) Thermodynamics of water–solid interactions in crystalline and amorphous pharmaceutical materials. *Journal of Pharmaceutical Sciences*, 103(9), 2772-2783.
11. N.F. Zolkiflee, M.M.R Meor Mohd Affandi, A.B.A Majeed. (2020) Thermodynamics and solute-solvent interactions of lovastatin in an aqueous arginine solution. *European Journal of Pharmaceutical Sciences*, 141(1), 105111.
12. Maksay G. (2011) Allostery in pharmacology: thermodynamics, evolution and design. *Prog Biophys Mol Biol*., 106(3), 463-73.
13. S.P. Mitra (2009) Drug-receptor Interaction: pharmacology, binding and thermodynamics – A Review. *Journal of Surface Science and Technology*, 25(3-4), 103-152.
14. J.C Chimal., N. Sanchez, P.R. Ramírez (2017). Thermodynamic optimality criteria for biological systems in linear irreversible thermodynamics. *J. Phys.: Conf. Ser*, 792, 012082.
15. G.B. West, W.H. Woodruff, J.H. Brown (2002) Allometric scaling of metabolic rate from molecules and mitochondria to cells and mammals. *PNAS*, 99, 2473–2478.
16. M. Monti (1990). Application of microcalorimetry to the study of living cells in the medical field. *Thermochimica Acta*, 172, 53–60.
17. C. Murigande, S. Regenass, D. Wirz, A.U. Daniels, A. Tyndall (2009).A comparison between (3H)-thymidine incorporation and isothermal microcalorimetry for the assessment of antigen-induced lymphocyte proliferation. *Immunological Investigations*, 38 (1), 67–75.
18. R. Santoro, O. Braissant, B. Müller, D. Wirz, A.U. Daniels, I. Martin, D. Wendt (2011). Real-time measurements of human chondrocyte heat production during in vitro proliferation. *Biotechnology and Bioengineering*, 108 (12), 3019–3024.
19. A. Doostmohammadi, A. Monshi, M.H. Fathi, S. Karbasi, O. Braissant, A.U. Daniels (2011) Direct cytotoxicity evaluation of 63S bioactive glass and bone-derived hydroxyapatite particles using yeast model and human chondrocyte cells by microcalorimetry. *Journal of Materials Science: Materials in Medicine*, 22 (10), 2293–2300.

20. Z. Heng, Z. Congyi, W. Cunxin, W. Jibin, G. Chaojiang, L. Jie, L. Yuwen (2005). Microcalorimetric study of virus infection; The effects of hyperthermia and 1b recombinant homo interferon on the infection process of BHK-21 cells by foot and mouth disease virus. *Journal of Thermal Analysis and Calorimetry*, 79 (1), 45–50..
21. O.A. Antoce, V. Antocie, K. Takahashi, N. Pomohaci, I. Namolosanu (1997) Calorimetric determination of the inhibitory effect of C1-C4 n-alcohols on growth of some yeast species". *Thermochimica Acta*, 297 (1–2), 33–42.
22. Braissant O., Wirz D., Gopfert B., Daniels A. U. (2010) Use of isothermal microcalorimetry to monitor microbial activities. *FEMS Microbiol. Lett*, 303 (1), 1–8.
23. Y. Shi, L. Liu, W. Shao, T. Wei, G. Lin (2015) Microcalorimetry studies of the antimicrobial actions of Aconitum alkaloids *J. Zhejiang Univ Sci B*., 16(8), 690–695.
24. C. Fricke, H. Harms, T. Maskow (2019) Rapid calorimetric detection of bacterial contamination: influence of the cultivation technique. *Front Microbiol*, 10, 2530.
25. O. Braissant, G. Theron, S.O. Friedrich, A.H. Diacon, G. Bonkat (2020). Comparison of isothermal microcalorimetry and BACTEC MGIT960 for the detection of the metabolic activity of Mycobacterium tuberculosis in sputum samples. *J Appl Microbiol*. doi:10.1111/jam.14549.
26. M. Butini, G. Abbandonato, C. Di Rienzo, A. Trampuz, M. Di_luca (2019). Isothermal microcalorimetry detects the presence of persister cells in a Staphylococcus aureus biofilm after vancomycin treatment. *Front. Microbiol*. 10, 332.
27. M. Di Luca, A. Koliszak, S. Karbysheva, A. Chowdhary, J.F. Meis, A. Trampuz (2019). Thermogenic characterization and antifungal susceptibility of candida auris by microcalorimetry. *J. Fungi*. 5(4):103.
28. J. Nykyri, A.M. Herrmann, S. Håkansson (2019). Isothermal microcalorimetry for thermal viable count of microorganisms in pure cultures and stabilized formulations. *BMC Microbiol*.19, 65, 10.
29. S. Costa-de-Oliveira, A.G. Rodrigues (2020) Candida albicans antifungal resistance and tolerance in bloodstream infections: The triad yeast-host-antifungal. *Microorganisms*, 8(2), 154.
30. E. M. Maiolo, U. F. Tafin, O. Borens, A. Trampuz (2014)Activities of Fluconazole, Caspofungin, Anidulafungin, and Amphotericin B on Planktonic and Biofilm Candida Species Determined by Microcalorimetry. *Antimicrobial Agents and Chemotherapy*, 58(5), 2709–2717.
31. Z. Xu, H. Li, X. Qin, T. Wang, J. Hao, J. Zhao, J. Wang, R. Wang, D. Wang, S. Wei, H. Cai, Y. Zhao (2019). Antibacterial evaluation of plants extracts against ampicillin-resistant Escherichia coli (E. coli) by microcalorimetry and principal component analysis. *AMB Expr,* 9,101.
32. O. Braissant, J. Keiser, I. Meister, A. Bachmann, D. Wirz, B. Göpfert, G. Bonkat, I. Wadsö (2015). Isothermal microcalorimetry accurately detects bacteria, tumorous microtissues, and parasitic worms in a label-free well-plate assay. *Biotechnol J.,* 10(3), 460–468.
33. Applications of calorimetry in a wide context – differential scanning calorimetry, isothermal titration calorimetry and microcalorimetry (2013). Amal Ali Elkordy (Ed.). InTech.
34. M.S. Atria, A.A. Sabouryb, F. Ahmad (2015). Biological applications of isothermal titration *Calorimetry. Phys. Chem. Res*., 3(4), 319-330.

35. O. Callies, A. Hernández Daranas (2016). Application of isothermal titration calorimetry as a tool to study natural product interactions. *Nat. Prod. Rep*, 33, 881-904.
36. A-M. Totea, J. Sabin, I. Dorin, K. Hemming, P. Laity, B. Conway, L. Waters, K. Asare-Addo (2019). Thermodynamics of clay – Drug complex dispersions: Isothermal titration calorimetry and high-performance liquid chromatography. *Journal of Pharmaceutical Analysis*. https://doi.org/10.1016/j.jpha.2019.12.001
37. H. Su, Y. Xu (2018). Application of ITC-based characterization of thermodynamic and kinetic association of ligands with proteins in drug design. *Front. Pharmacol*, 9, 1133.
38. A. Schön, R.K. Brown, B.M. Hutchins, E. Freire (2013). Ligand binding analysis and screening by chemical denaturation shift *Analytical Biochemistry,* 443 (1), 52–7.
39. M.H. Chiu, E.J. Prenner (2011). Differential scanning calorimetry: An invaluable tool for a detailed thermodynamic characterization of macromolecules and their interactions *Journal of Pharmacy & Bioallied Sciences*. 3 (1), 39–59.
40. M.A. Kalam, S. Alshehri, A. Alshamsan, M. Alkholief, R. Ali, F. Shakeel (2019). Solubility measurement, Hansen solubility parameters and solution thermodynamics of gemfibrozil in different pharmaceutically used solvents. *Drug Dev Ind Pharm*, 45(8), 1258-1264.
41. K. Lohner, E. J. Prenner (2000). Differential scanning calorimetry and X-ray diffraction studies of the specificity of the interaction of antimicrobial peptides with membrane-mimetic systems *Biochimica et Biophysica Acta (BBA),* 1462 (1–2), 141-56.
42. Y. Pang, A. Buanz, R. Telford, O.V. Magdysyuk, S. Gaisforda, Ga.R. Williamsa (2019). A simultaneous X-ray diffraction–differential scanning calorimetry study into the phase transitions of mefenamic acid. *Journal of Applied Crystallography,* 52(6), 1264-1270.
43. R.L. Roque-Flores, J.R. Matos (2019). Simultaneous measurements of X-ray diffraction–differential scanning calorimetry. *J Therm Anal Calorim,* 137, 1347–1358.

Submitted 29.01.2020

P.V. Gorskiy

Gorskyi P.V.[1,2] *dok. phys.– mat. sciences*

[1]Institute of Thermoelectricity of the NAS and MES of Ukraine,
1, Nauky str., Chernivtsi, 58029, Ukraine,
e-mail: anatych@gmail.com;
[2]Yu.Fedkovych Chernivtsi National University,
2, Kotsiubynskyi str., Chernivtsi, 58012, Ukraine

ON THE FUNDAMENTAL DIFFERENCE BETWEEN THERMOELECTRIC COMPOSITES AND DOPED THERMOELECTRIC MATERIALS AND THE CONSEQUENCES IT IMPLIES

It is shown that if the effect of doping impurities on a thermoelectric material is reduced only to a change in the concentration of free charge carriers in it, then, for example, for a material based on bismuth telluride even at a temperature of 400 K, it is impossible to obtain a value of the dimensionless thermoelectric figure of merit, which would be far in excess of 1. On the other hand, the dimensionless thermoelectric figure of merit of thermoelectric composites based on semiconductor materials with metal nanoclusters or nanoparticles can significantly exceed 1, if they are indeed composites, that is, materials, each component of which, having entered the composition of the composite, retains its inherent macroscopic values of kinetic coefficients and their temperature dependences. In this case, the increase in the figure of merit of such a thermoelectric composite is reduced to optimizing its composition and solving the problem of the technological possibilities of manufacturing this particular composite. However, it should be borne in mind that the answer to the question about the practical application of such composites, even if they are created and their parameters are stably reproducible, depends on the possibility of creating devices in which they are used, that should have not only high consumer characteristics, but also the corresponding stability, reliability, durability and service life. Bibl. 6, Fig. 6.

Key words: thermoelectric material, doping, dimensionless thermoelectric figure of merit, percolation threshold, composite, nanoparticles, optimal composition of the composite.

Introduction

Today, significant efforts of specialists in the field of thermoelectric materials science are aimed at solving both theoretical and practical problems related to finding ways to increase the dimensionless thermoelectric figure of merit of both doped thermoelectric materials and composites. However, despite these efforts, significant progress in this direction has either not been achieved, or some high results are not consistently reproducible. From this point of view, efforts aimed, for example, at creating superlattices or quantum well materials, deserve a separate analysis. But the purpose of this paper is an unbiased analysis of the situation in the field of creation and application of TEM based on "traditional" alloys of *Bi* (*Sb*) - *Te* (*Se*) system.

About the limited potential of doped TEM

To prove this limitation by calculation, we investigate the effect of the concentration of doping impurities on the dimensionless thermoelectric figure of merit of TEM under the following model assumptions:

1) the band spectrum of charge carriers in TEM is parabolic and isotropic with the temperature-independent effective mass;
2) quasi-elastic scattering of charge carriers in the relevant temperature area occurs on a deformation potential of acoustic phonons with the energy-independent cross-section and mean free path inversely proportional to temperature;
3) the lattice thermal conductivity of semiconductor is determined by phonon-phonon scattering with Umklapp and is inversely proportional to temperature, obeying the Leibfried-Schlemann law [1, 2];
4) doping impurities do not affect anything except the concentration of free charge carriers in material.

Given the validity of these assumptions, the scattering index of charge carriers r = - 0.5.

For further calculations, we assume that at a certain temperature T_0 we know the thermoelectric parameters of the undoped TEM, namely its thermoEMF α_{s0}, electrical conductivity σ_{s0} and thermal conductivity κ_{s0}. Assume also that the relative increase in the concentration of free charge carriers in the TEM after the introduction of a doping impurity is equal to x.

The construction of the necessary temperature dependences and concentration dependences of the characteristics of the doped TEM on the basis of known general relations [1] is carried out in the following order.

From the relation for thermoEMF

$$\alpha_{s0} = \frac{k}{e}\left[\frac{2F_1(\eta_0)}{F_0(\eta_0)} - \eta_0\right] \tag{1}$$

we find a reduced chemical potential η_0 of charge carrier gas in the undoped material at a temperature of T_0.

Then from equation

$$\frac{T^{1.5}F_{0.5}(\eta)}{(1+x)T_0^{1.5}F_{0.5}(\eta_0)} = 1 \tag{2}$$

we determine the temperature dependence of reduced chemical potential η of charge carrier gas on temperature T in given temperature range at an arbitrary concentration of doping impurities.

From the relation

$$\alpha_s = \frac{k}{e}\left[\frac{2F_1(\eta)}{F_0(\eta)} - \eta\right] \tag{3}$$

we determine the temperature dependence of the thermoEMF of doped TEM.

From the relation

$$L_s(\eta)=\left(\frac{k}{e}\right)^2\left[\frac{3F_2(\eta)}{F_0(\eta)}-\frac{4F_1^2(\eta)}{F_0^2(\eta)}\right] \tag{4}$$

we determine the temperature dependence of the Lorentz number of doped TEM.

The temperature dependence of the electrical conductivity of doped TEM under the above model assumptions is determined as follows:

$$\sigma_s=\sigma_{s0}\cdot(1+x)\left(\frac{T_0}{T}\right)^{1.5}\frac{F_0(\eta)F_{0.5}(\eta_0)}{F_{0.5}(\eta)F_0(\eta_0)}\,. \tag{5}$$

The temperature dependence of the electrical conductivity of doped TEM with regard to everything said above is determined as:

$$\kappa_s=\sigma_s L_s(\eta)T+\left[\kappa_{s0}-\sigma_{s0}L_s(\eta_0)T_0\right]\frac{T_0}{T}\,. \tag{6}$$

In formulae (1) – (5), $F_m(\eta)$ denote the Fermi integrals which are determined by the following relation:

$$F_m(\eta)=\int_0^\infty x^m\left[\exp(x-\eta)+1\right]^{-1}dx\,. \tag{7}$$

Relations (1) – (7) fully determine the temperature dependences of the thermoEMF, electrical conductivity and thermal conductivity of doped TEM.

The calculated concentration dependences of the dimensional thermoelectric figure of merit of doped TEM at temperatures 200 and 400 K are shown in Fig. 1.

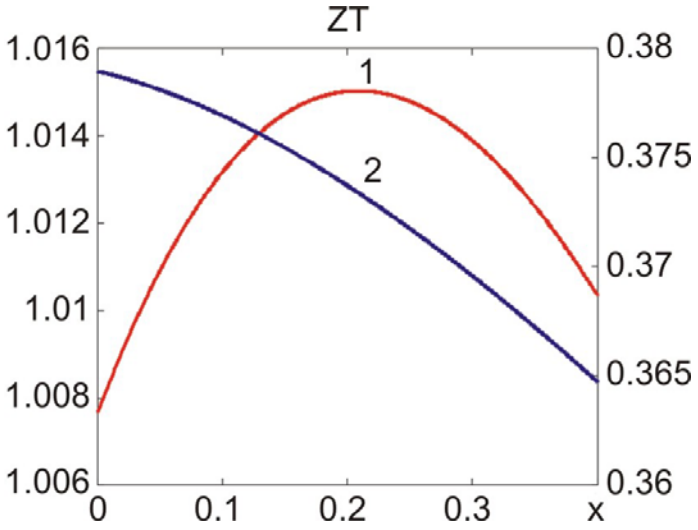

Fig. 1.Concentration dependences of the dimensional thermoelectric figure of merit of doped TEM at temperatures:1 – 400 K (left axis), 2 – 200 K (right axis)

When constructing plots, the following parameters of TEM were taken: $\alpha_{s0} = 200$ μ V/K, $\sigma_{s0} = 800$ S/cm, $\kappa_{s0} = 1.4$ W/(m·K) [1].

The plots show that at a temperature of 400 K even the highest value of the dimensionless thermoelectric figure of merit of the doped material, which corresponds to its "optimal" composition near $x = 0.2$, is only about 0.01, i.e. less than 1 % higher than the value of the thermoelectric figure of merit of the source material. The existence of the optimum in this case is explained by two competing factors: an increase in electrical conductivity and a decrease in thermoEMF with increasing concentration of charge carriers. At lower temperature, when the gas of free charge carriers is quite degenerate, the concentration dependence of the dimensionless thermoelectric figure of merit is also weak (the highest value differs from the lowest in the considered range of concentrations of charge carrier by about 5.5%), but this dependence is entirely determined by the decrease in thermoEMF.

Thus, we clearly see the limited potential of doped TEM. The best results are achieved when doping simultaneously reduces the lattice thermal conductivity. Moreover, doping of TEM by isovalent impurities is effective, because in this case the electrical conductivity, the electron (hole) part of thermal conductivity and thermoEMF of the material change relatively little, and the lattice thermal conductivity changes to a greater extent, quite often in the direction of decrease.

On the fundamental difference between thermoelectric composites and doped TEM and their potential

Thus, we have seen that the fundamental role of doping impurities in the traditional sense of the term is that they, changing their state, either "supply" free charge carriers of this or other sign, or do not supply carriers, but affect the scattering or spectrum of phonons in TEM, changing in this or other direction the lattice thermal conductivity and even the nature of its temperature dependence, on which we will also dwell later. It is clear that in this case the characteristics of the doped material cannot be described in any way due to the macroscopic characteristics of its components. The principal feature of the composite, in contrast to the doped material, is the ability to determine at least its kinetic coefficients, namely electrical conductivity, thermal conductivity and thermoEMF due to the relevant characteristics of individual components (phases) and the composition of the composite without going deep into the microscopic mechanisms of these characteristics. That is why the theory of composites is quite often identified with the theory of the "effective medium", which is understood as a purely macroscopic object. It is clear that in this case only that material can be called a composite whose components (phases), when incorporated into the composite, regardless of its composition, retain their inherent macroscopic properties and their temperature dependences. The "rules of mixing" macroscopic characteristics, according to which the characteristics of the composite as a whole are determined, depend on the concept of "effective environment" followed by the researcher. For example, if we follow the concept, according to which the percolation effect is insignificant, then for a two-phase system the TEM - metal kinetic coefficients are defined as follows [2]:

$$\sigma_c = \sigma_m \nu_m + \sigma_s (1 - \nu_m), \tag{8}$$

$$\kappa_c = \kappa_m \nu_m + \kappa_s (1 - \nu_m). \tag{9}$$

The indices "*s*" and "*m*" refer to TEM and metal, respectively, ν_m – the volume fraction of metal. The thermoEMF of composite is determined as [3]:

$$\alpha_c = \frac{(\alpha_m/\kappa_m)\nu_m + (\alpha_s/\kappa_s)(1-\nu_m)}{\kappa_m^{-1}\nu_m + \kappa_s^{-1}(1-\nu_m)}. \tag{10}$$

However, if percolation effect is essential, formulae (8) and (9), respectively, acquire the form [3, 4]:

$$\sigma_c = 0.25\left\{\sigma_s(2-3\nu_m) + \sigma_m(3\nu_m-1) + \sqrt{[\sigma_s(2-3\nu_m) + \sigma_m(3\nu_m-1)]^2 + 8\sigma_m\sigma_s}\right\}, \tag{11}$$

$$\kappa_c = 0.25\left\{\kappa_s(2-3\nu_m) + \kappa_m(3\nu_m-1) + \sqrt{[\kappa_s(2-3\nu_m) + \kappa_m(3\nu_m-1)]^2 + 8\kappa_m\kappa_s}\right\}, \tag{12}$$

and formula (10) remains unchanged.

Consider the difference between these two concepts using an example of composite, even though hypothetical, which consists of bismuth telluride and nickel. The plot of the electrical conductivity of the composite depending on the volume fraction of the metal $\nu_m \equiv \nu$ in accordance with formulae (8) and (11) is shown in Fig. 2. In this case, the electrical conductivity of nickel is taken equal to $1.3 \cdot 10^5$ S/cm.

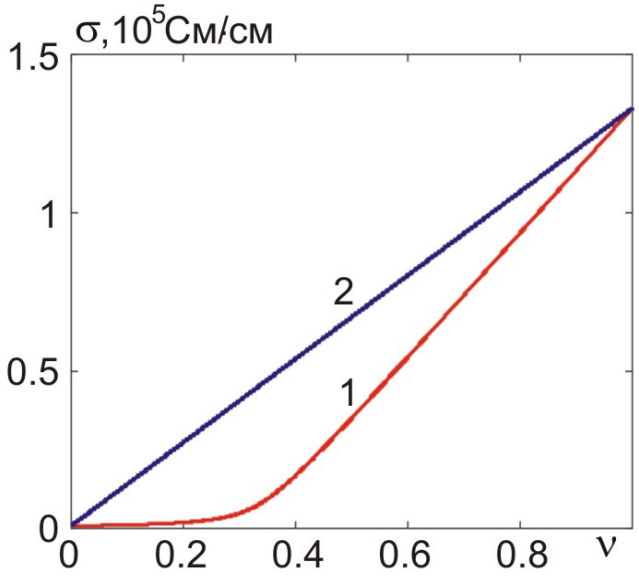

Fig. 2.Dependence of the electrical conductivity of "bismuth telluride-nickel" composite on the volume fraction of nickel: 1 – in the presence of percolation; 2 – in the absence of percolation

The figure shows that in the presence of percolation, as the content of nickel particles in the composite increases, the electrical conductivity of the composite increases first more slowly and then faster than in its absence.

Let us consider the question of what size of the nickel fraction can be considered macroscopic. If we consider, for example, a cluster with a radius of 35 nm, then taking into account that the nickel lattice constant is equal to 0.5 nm [5] and this lattice is body-centered, we obtain that such a cluster can accommodate approximately 2.9×10^6 atoms, which means that the relative deviation of the macroscopic parameters of the cluster from their average values is less than 0.1%, that is, this or larger clusters can be considered macroscopic and one can ascribe to them the conductivity of nickel. Based on the conductivity of nickel and the concentration of electrons in it [5], we can find that the free path of electrons in nickel at 300 K is 4.18 nm. Then at an arbitrary temperature the electrical conductivity of the metal cluster is approximately equal to:

$$\sigma_{cl} = \sigma_0(T_0/T)\frac{r_c}{r_c + l_0(T_0/T)}. \qquad (13)$$

In this formula, σ_0 – electrical conductivity of the bulk nickel sample at a temperature of T_0, r_c – cluster radius, l_0 – mean free path of electron in the bulk nickel sample at 300 K.

Fig.3 shows the dependences of the thermoelectric figure of merit of TEM-nickel clusters composite on its composition with regard to the percolation effect at temperatures 200 and 400 K.

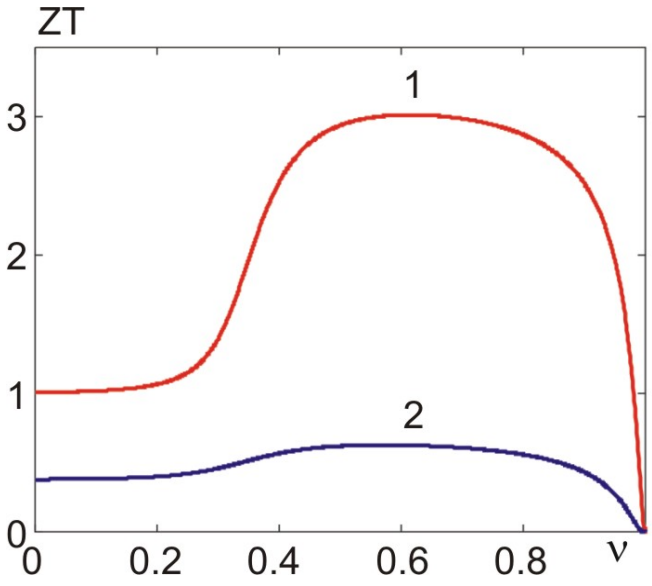

Fig. 3. Thermoelectric figure of merit of composite with regard to the percolation effect at temperatures:1 – 400 K, 2 – 200 K.

It was assumed that the thermal conductivity of nickel is 90 W/(m·K) and by virtue of the Wiedemann-Franz law does not depend on temperature. The thermoEMF of nickel was considered to be equal to 23 μV/K and temperature independent.

From the figure it is seen that up to nickel content almost 30% by volume, i.e. within the percolation threshold, the thermoelectric figure of merit of the composite at 400 K retains a value equal to 1, but after this threshold increases rapidly, reaching a value of almost 3 at about 60 volume % of nickel, goes to the "plateau", and then rapidly decreases to the value inherent in pure nickel.

Fig.4 shows the same dependences as in Fig.3, but without regard to percolation effect.

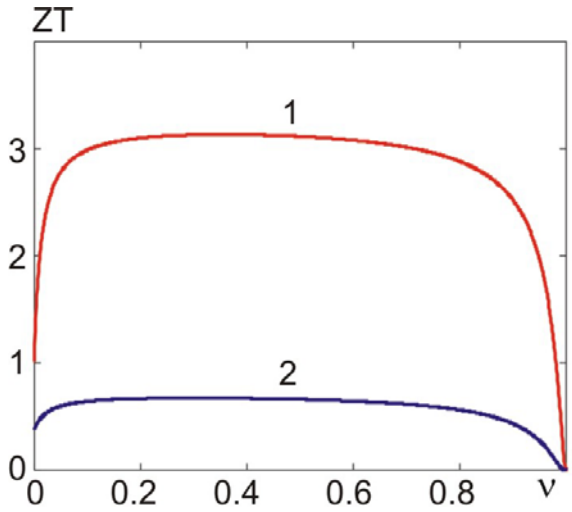

Fig. 4. Thermoelectric figure of merit of the composite without regard to the percolation effect at temperatures:1 – 400 K, 2 – 200 K.

The figure shows that neglect of the percolation has little effect on the maximum thermoelectric figure of merit of the composite, although it significantly affects the rate of reaching this maximum, the length of the "plateau" and the rate of further decline to a small value inherent in pure nickel. Note that Figs. 3 and 4 correctly reflect the physical situation if the temperature dependence of the lattice thermal conductivity of TEM is subject to the Leibfried-Schlemman formula. Instead, the following plots in Figs. 5 and 6 are constructed for the case when this formula is violated in such a way that the lattice thermal conductivity increases approximately linearly with temperature [6].

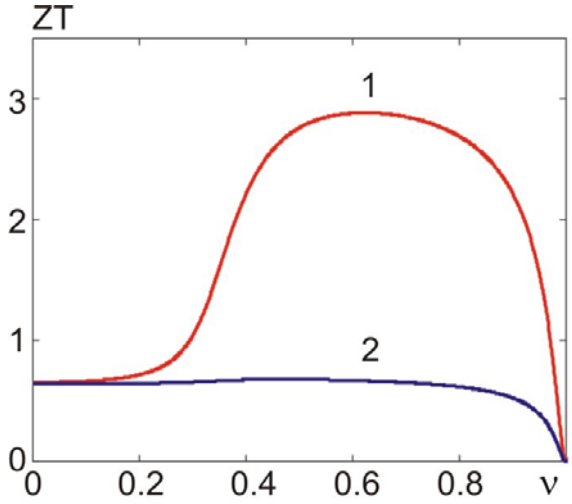

Fig. 5. Thermoelectric figure of merit of the composite with regard to the percolation effect and a deviation of TEM lattice thermal conductivity from the Leibfried-Schlemann formula at temperatures: 1 – 400 K, 2 – 400 K.

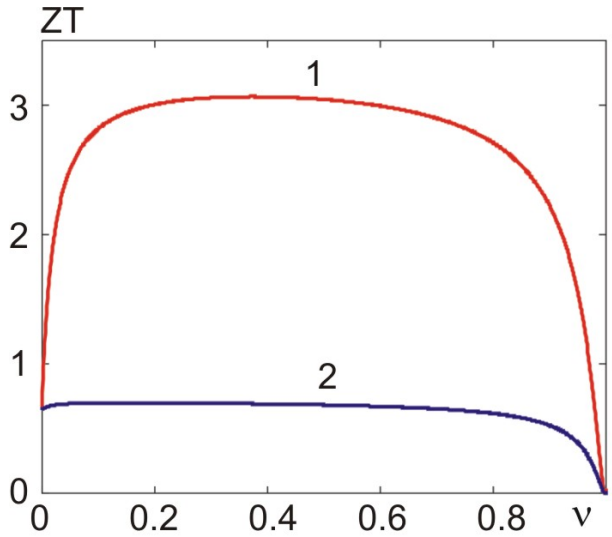

Fig. 6. Thermoelectric figure of merit of the composite without regard to the percolation effect, but with regard to a deviation of TEM lattice thermal conductivity from the Leibfried-Schlemann formula at temperatures: 1 – 400 K, 2 – 200 K.

The figures show that even the linear increase in the lattice thermal conductivity of TEM with temperature does not affect the maximum value of the thermoelectric figure of merit of the composite. From this we conclude that such a significant advantage of composites over doped materials, at least in principle, is achievable precisely because the components that make up the composites retain their macroscopic characteristics. If this does not happen, then such an advantage will not be obtained. Therefore, those materials that have a relatively low thermoelectric efficiency should be considered as specially doped materials rather than the composites, despite the fact that the authors consider them to be the composites. Consider from this point of view, for example, the results of [6]. Its authors report that they obtained for the graphite/ $Bi_{0.5}Sb_{1.5}Te_3$ composite an increase in thermoelectric figure of merit to 1.05 or 35 % compared to the "pure" TEM with a graphite content of 0.05 mol.%. And such an increase in the composite is impossible if the percolation effect occurs (Fig. 5), but it is possible if the percolation effect is absent (Fig. 6). However, since this effect occurs, and according to [6] the electrical conductivity of the material with the addition of graphite generally decreases, although insignificantly, thermoEMF increases slightly, and the lattice thermal conductivity decreases by more than 1.5 times, it should be assumed that we are dealing not with a composite, and with a specially doped material, the main role of graphite in which is the rearrangement of the phonon spectrum of TEM and phonon scattering mechanisms in it, which leads to a significant decrease in lattice thermal conductivity and changes in the nature of its temperature dependence.

However, it should be noted that we do not consider in this paper either the technological aspects of the manufacture of the composite thermoelectric materials, taking into account the above requirements for them, or their strength characteristics and service life. And these aspects are no less, if not more important than the actual thermoelectric figure of merit. Therefore, the trend in the development of thermoelectric materials and devices, albeit very slowly, is shifting towards the development of a kind of "compromise" materials and structures, in which, with given consumer characteristics, minimum mechanical stresses, and, consequently, maximum reliability, durability and service life of both materials and devices would be achieved.

Conclusions

1. It is shown that the dimensionless thermoelectric figure of merit of materials based on bismuth telluride cannot increase by more than 1%, if the role of the doping impurity is only to increase the concentration of charge carriers.
2. Unlike doped thermoelectric materials, the composites that contain highly conductive, such as metal, clusters with a diameter of 70 nm or more, have significantly greater thermoelectric capabilities making it possible to obtain at 400 K the dimensionless thermoelectric figure of merit about 3. This value is not affected by the percolation or possible increase of lattice thermal conductivity of TEM with temperature. This is possible primarily because in the composites, in contrast to doped materials, their components retain the thermoelectric characteristics, including their temperature dependences, which were inherent in these components before entering the composite. This feature for the composite is fundamental. If the preservation of the characteristics of the components does not take place, then we are not dealing with a composite, but with a special doped material, which cannot offer such significant advantages.
3. From this point of view, it is important to dope TEM primarily with such impurities and in such quantities that little change the electrical conductivity and thermoEMF of TEM, but significantly reduce its lattice thermal conductivity, even if changing the nature of its temperature dependence.

References

1. Goltsman B.M., Kudinov I.A., Smirnov I.A. (1972). *Poluprovodnikovyie termoelektricheskiie materialy na osnove Bi_2Te_3 [Semiconductor thermoelectric materials based on Bi_2Te_3]*. Moscow: Nauka [in Russian].
2. Klemens P.D. Lattice thermal conductivity (1958). In: *Solid State Physics. Advances in Research and Applications. Vol.7*, pp. 1-98. New York: Academic Press. Inc. Publishers, New York.
3. Snarskii A.A., Sarychev A.K., Bezsudnov I.V., Lagar'kov V.N. (2012). Termoelektricheskaia dobrotnost' obiomnykh nanostructurirovannykh kompositov s raspredelionnymi parametrami [Thermoelectric figure of merit of the bulk nanostructured composites with distributed parameters]. *Semiconductors*, 46, 677-683 [in Russian].
4. Gorskyi P.V., Mitskaniuk N.V. (2019). On the temperature dependences of thermoelectric characteristics of bismuth telluride-metal transient layer with regard to percolation effect. *J.Thermoelectricity*. 3, 5-22.
5. Kittel Ch. (1978). Introduction to solid state physics. Moscow: Nauka [Russian transl.]
6. Hu W., Zhou H., Mu X., et al. (2017). Preparation and thermoelectric properties of graphite/$Bi_{0.5}Sb_{1.5}Te$ composites. *J. Electronic Materials*. – DOI: 10.1007/s11664-017-5908-8.

Submitted 13.02.2020

Горський П.В. *док. фіз.-мат. наук*[1,2]

[1]Інститут термоелектрики НАН і МОН України, вул. Науки, 1,
Чернівці, 58029, Україна; *e-mail: anatych@gmail.com*;
[2]Чернівецький національний університет
ім. Юрія Федьковича, вул. Коцюбинського 2,
Чернівці, 58000, Україна

ПРО ПРИНЦИПОВУ ВІДМІННІСТЬ ТЕРМОЕЛЕКТРИЧНИХ КОМПОЗИТІВ ВІД ЛЕГОВАНИХ ТЕРМОЕЛЕКТРИЧНИХ МАТЕРІАЛІВ ТА НАСЛІДКИ З НЕЇ

Показано, що якщо вплив легуючих домішок на термоелектричний матеріал зводиться лише до зміни концентрації вільних носіїв заряду у ньому, то, наприклад, для матеріалу на основі телуриду вісмуту навіть за температури 400 К неможливо отримати значення безрозмірної термоелектричної ефективності, яке б істотно перевищувало 1. З іншого боку безрозмірна термоелектрична ефективність термоелектричних композитів на основі напівпровідникових матеріалів з металевими нанокластерами або наночастинками може істотно перевищувати 1, якщо вони справді є композитами, тобто матеріалами, кожна складова яких, увійшовши до складу композиту, зберігає притаманні їй макроскопічні значення кінетичних коефіцієнтів та їх температурні залежності . В цьому разі підвищення добротності такого термоелектричного композиту зводиться до оптимізації його складу і вирішення питання про технологічні можливості виготовлення саме цього композиту. Однак слід мати на увазі, що відповідь на питання про практичне застосування таких композитів, якщо вони навіть будуть створені і їх параметри будуть стабільно відтворюваними, залежить від можливості створення з їх застосуванням пристроїв, які б мали не лише високі споживчі характеристики, а й відповідну стабільність,надійність, довговічність та ресурсну стійкість. Бібл. 6, рис. 6.

Ключові слова: термоелектричний матеріал, легування, безрозмірна термоелектрична ефективність, поріг перколяції, композит, наночастинки, оптимальний склад композиту.

Горский П.В., *док. физ.-мат. наук*[1,2]

[1]Институт термоэлектричества НАН и МОН Украины,
ул. Науки, 1, Черновцы, 58029, Украина,
e–mail: anatych@gmail.com;
[2]Черновицкий национальный университет
им. Юрия Федьковича, ул. Коцюбинского, 2,
Черновцы, 58012, Украина

О ПРИНЦИПИАЛЬНОМ ОТЛИЧИИ ТЕРМОЭЛЕКТРИЧЕСКИХ КОМПОЗИТОВ ОТ ЛЕГИРОВАННЫХ ТЕРМОЭЛЕКТРИЧЕСКИХ МАТЕРИАЛОВ И СЛЕДСТВИЯХ ИЗ НЕГО

Показано, что если влияние легирующих примесей на термоэлектрический материал (ТЭМ) сводится только к изменению концентрации свободных носителей заряда в нем, то, например, для материала на основе теллурида висмута даже при температуре 400 К невозможно получить значение безразмерной термоэлектрической эффективности, которое бы существенно превышало 1. С другой стороны, безразмерная термоэлектрическая эффективность термоэлектрических композитов на основе полупроводниковых материалов с металлическими нанокластерами либо наночастицами может существенно превышать 1, если они действительно являются композитами, т.е. материалами, каждая составляющая которых, войдя в состав композита, сохраняет присущие ей макроскопические значения кинетических коэффициентов и их температурные зависимости. В этом случае повышение добротности такого термоэлектрического композита сводится к оптимизации его состава и решении вопроса о технологических возможностях изготовления именно этого композита. Однако следует иметь в виду, что ответ на вопрос о практическом применении таких композитов, если они даже будут созданы и их параметры будут стабильно воспроизводимыми, зависит от возможности создания с их применением устройств, которые должны иметь не только высокие потребительские характеристики, но и соответствующую стабильность, надежность, долговечность и ресурсную устойчивость. Библ. 6, рис. 6.

Ключевые слова: термоэлектрический материал, легирование, безразмерная термоэлектрическая эффективность, порог перколяции, композит, наночастицы, оптимальный состав композита.

References

1. Goltsman B.M., Kudinov I.A., Smirnov I.A. (1972). *Poluprovodnikovyie termoelektricheskiie materialy na osnove Bi_2Te_3 [Semiconductor thermoelectric materials based on Bi_2Te_3]*. Moscow: Nauka [in Russian].
2. Klemens P.D. Lattice thermal conductivity (1958). In: *Solid State Physics. Advances in Research and Applications. Vol.7*, pp. 1-98. New York: Academic Press. Inc. Publishers, New York.
3. Snarskii A.A., Sarychev A.K., Bezsudnov I.V., Lagar'kov V.N. (2012). Termoelektricheskaia dobrotnost' obiomnykh nanostructurirovannykh kompositov s raspredelionnymi parametrami [Thermoelectric figure of merit of the bulk nanostructured composites with distributed parameters]. *Semiconductors*, 46, 677-683 [in Russian].
4. Gorskyi P.V., Mitskaniuk N.V. (2019). On the temperature dependences of thermoelectric characteristics of bismuth telluride-metal transient layer with regard to percolation effect. *J.Thermoelectricity*. 3, 5-22.
5. Kittel Ch. (1978). Introduction to solid state physics. Moscow: Nauka [Russian transl.]
6. Hu W., Zhou H., Mu X., et al. (2017). Preparation and thermoelectric properties of graphite/$Bi_{0.5}Sb_{1.5}Te$ composites. *J. Electronic Materials*. – DOI: 10.1007/s11664-017-5908-8.

Submitted 13.02.2020

V.G. Kolobrodov, *doc. techn. sciens, professor*
V.I. Mykytenko, *doc. techn. sciences, assist professor*
G.S. Tymchyk, *doc. techn. sciens, professor*

National Technical University of Ukraine
"Igor Sikorsky Kyiv Polytechnic Institute"
37 Peremohy Ave., Kyiv, 03056, Ukraine
e-mail: deanpb@kpi.ua

POLARIZATION MODEL OF THERMAL CONTRAST OBSERVATION OBJECTS

This paper proposes a polarization model of a thermal imager for the purpose of its application in the study of thermoelectric phenomena and devices, which allows increasing the efficiency of such devices. To study and design such thermal imagers, a physico-mathematical model of polarization of radiation from observation objects is considered, which takes into account the polarization properties of the intrinsic thermal radiation and the reflected external radiation. The developed model was used to determine the polarization properties of the radiation from a flat iron plate. The analysis of the obtained results shows that for thermal radiation at observation angles ψ <40 ° the components of the radiation coefficient are almost identical $\varepsilon_{\parallel} \approx \varepsilon_{\perp} \approx 0.16$, but $\varepsilon_{\parallel} < \varepsilon_{\perp}$. As the observation angle ψ <40 ° increases, the perpendicular polarization component $\varepsilon_{\perp}$ decreases monotonically to zero, and the parallel component $\varepsilon_{\parallel}$ increases and reaches its maximum value at an angle ψ = 84 °, and then decreases to zero. The degree of polarization of radiation increases with increasing angle ψ and at an angle ψ = 84 ° is equal to 0.96. The obtained research results are worthwhile to be used in the development of a model of thermoelectrics which can be employed in the design of a polarization thermal imager. Bibl. 8, Tabl. 1, Fig. 7.

Key words: polarization thermal imager, temperature distribution, partially polarized radiation, degree of polarization.

Introduction

Thermal imagers are widely used in various fields of science, technology and military art, as well as in the study of thermoelectric phenomena and devices [1–3]. Thermal imagers observe the contrast of brightness (intensity) of the object of observation, located in the background, and make it possible to measure the temperature distribution on the surface of the thermoelectric sensor in static or dynamic modes. To increase the temperature and spatial separation, promising thermal imagers use the polarization characteristics of the radiation from the observation object and the background.

Infrared (IR) radiation generated by the observation objects contains information about the objects and their location. The perception of this information by means of a thermal imager and its corresponding processing enable one to define and control many parameters which are difficult or impossible to measure directly.

The object of research in this paper is the polarization characteristics of thermal radiation from the objects and the possibility of their use to build a polarization thermal imager.

Modeling of thermal radiation polarization

At present, modeling methods are widespread in almost all fields of science and technology. This is due to the fact that modeling simplifies and speeds up the search for the right solutions, is cost-effective and easy to use. In the field of determining the affiliation of an object to a narrow class (for example, a car or a tank), we can distinguish two directions in modeling methods:

1. Mathematical – used to process finished images using a complex mathematical apparatus (e.g, spatial spectral analysis) in order to improve image quality and further processing to solve a specific problem.

2. Physical and mathematical – used to process images directly in the process of obtaining them, the result of which is an algorithm for solving the problem (detection, recognition, classification, identification).

In the general case, polarization of the intrinsic radiation of materials arises due to the phenomena of reflection and refraction at the "medium - air" interface, which are described by the theory of reflection for metals and dielectrics [4]. In this case, the degree of polarization of the intrinsic surface radiation increases with increasing the angle between the direction of radiation and the normal to the radiation surface.

Objects with temperatures above the absolute zero Kelvin emit light energy by changing the energy state of electronic, oscillating and rotational transitions of atoms and molecules. The thermal radiation of objects is based on Planck's formula, which determines the spectral luminosity of the surface of nonblack body [5, 6]

$$M_{bb}(\lambda, T) = \frac{c_1}{\lambda^5 \left[\exp\left(\frac{c_2}{\lambda T} \right) - 1 \right]}, \quad \frac{\text{Вт}}{\text{см}^2 \cdot \text{мкм}} \tag{1}$$

where c_1 = 37415 W·cm^{-2}·μm^4, c_2 = 14388 μm·K are constant coefficients; λ is wavelength, μm.

The spectral luminosity of the surface of nonblack body is determined as

$$M(\lambda, T) = \varepsilon(\lambda, T) M_{bb}(\lambda, T), \tag{2}$$

where $\varepsilon(\lambda, T)$ is the spectral coefficient of radiation the value of which is less than unity.

If the surface of the object radiates according to Lambert's law, the spectral energy brightness is determined by the formula

$$L(\lambda, T) = \frac{1}{\pi} \varepsilon(\lambda, T) M_{bb}(\lambda, T) \cos\psi, \tag{3}$$

where $\psi = \theta_v = \theta_t$ is the observation angle of the object surface element (Fig. 1).

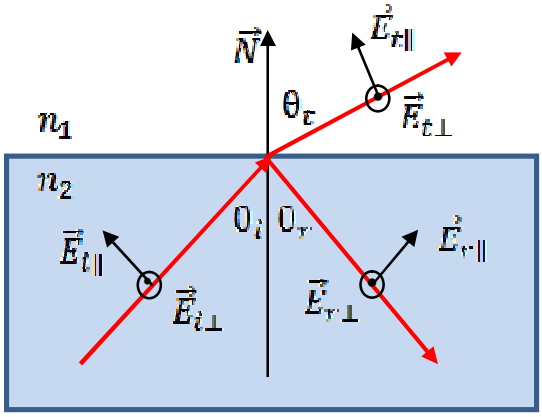

Fig. 1. Schematic for explaining the polarization of the intrinsic thermal radiation of the object: n_1 and n_2 are refractive indices of air and metal, respectively; $\vec{N}$ is normal to the element surface; θ_i, θ_r, and θ_t are the angles of incidence, reflection and refraction (observation angle θ_v), respectively.

According to formula (3), the brightness of the intrinsic radiation of the observation object is formed by two processes:

1. Direct radiation by the bulk of the object, which is described by the Planck function, and depends on the object temperature.

2. The contribution of the object surface, which is determined by the radiation coefficient of the surface and the state of its roughness. The radiation coefficient $\varepsilon(\lambda, T)$ depends on the complex refractive index $n_c = n+j\kappa$ of the medium.

Under the condition of thermodynamic stability for opaque media the absorption coefficient $\alpha(\lambda, T)$ is equal to the radiation coefficient $\varepsilon(\lambda, T)$ [7,8], and the spectral energy coefficients of reflection $R(\lambda, T)$ and radiation $\varepsilon(\lambda, T)$ are interrelated by the ratio

$$\varepsilon(\lambda, T) = 1 - R(\lambda, T)\,. \tag{4}$$

The degree of polarization of the intrinsic radiation is determined by the difference between the radiation coefficients of the object surface $\varepsilon_\parallel$ and $\varepsilon_\perp$ for the components of this radiation, polarized in the plane of refraction and perpendicular plane, respectively. The magnitude of the degree of polarization of the object intrinsic radiation is determined by the formula

$$P(\psi)=\frac{L_\parallel(\lambda,T;x,y)-L_\perp(\lambda,T;x,y)}{L_\parallel(\lambda,T;x,y)+L_\perp(\lambda,T;x,y)}=\frac{\varepsilon_\parallel-\varepsilon_\perp}{\varepsilon_\parallel+\varepsilon_\perp}\,. \tag{5}$$

The values of $\varepsilon_\parallel$ and $\varepsilon_\perp$ for opaque media are determined by the Fresnel formulae [6,9], which characterize the dependence of the polarization components of the radiation coefficient on the real and imaginary part of the complex refractive index $n_c = n+j\kappa$:

$$\varepsilon_\parallel = \frac{4n\cos\psi}{(n\cos\psi+1)^2+\kappa^2\cos^2\psi}; \tag{6}$$

$$\varepsilon_{\perp} = \frac{4n\cos\psi}{(n\cos\psi)^2 + \kappa^2}. \tag{7}$$

The total radiation coefficient is the average value of the parallel and perpendicular components:

$$\varepsilon(\psi) = \frac{\varepsilon_{\parallel} + \varepsilon_{\perp}}{2}. \tag{8}$$

The degree of polarization of the intrinsic radiation from the object surface is obtained by substituting (6) and (7) to the formula (5):

$$P(\psi) = DOP(\psi) = \frac{(n^2 + \kappa^2 - 1)\sin\psi}{(n^2 + \kappa^2 + 1)(1 + \cos^2\psi) + 4n\cos\psi}. \tag{9}$$

The degree of polarization of the intrinsic radiation of materials is determined by the state of the surface, as well as the real and imaginary components of the complex refractive index. For example, for glass ($1 < n < 2$, $\kappa << 1$) the radiation is less polarized than for metals $\left(\sqrt{n^2 + \kappa^2} > 3.3\right)$

Along with the intrinsic radiation, external IR radiation falls on the object surface, which is reflected and refracted. Let us consider the features of the reflected radiation, which is perceived by the thermal imager. Since partial polarization of light occurs during reflection and refraction, it is rather difficult to solve the problem posed directly for natural light. To simplify the solution of this problem, consider a model of natural light, in which its vector $\vec{E}_n$ is represented as the sum of two waves which are linearly polarized in two mutually perpendicular planes, have the same intensity and propagate in the direction of natural light (Fig. 2). Mathematically, this can be represented in the form of relations

$$\vec{E}_n = \vec{E}_{\parallel} + \vec{E}_{\perp};\ I_n = I_{\parallel} + I_{\perp};\ I_{\parallel} = I_{\perp} = 0.5I_n, \tag{10}$$

where $\vec{E}_{\parallel} = \vec{E}_p$ is vector of a linearly polarized wave, the plane of polarization of which is parallel to the plane of incidence of the beam; $\vec{E}_{\perp} = \vec{E}_s$ is vector of a linearly polarized wave, the plane of polarization of which is perpendicular to the plane of incidence of the beam; I_n, $I_{||}$, $I_{\perp}$ – are intensities of light waves $\vec{E}_n$, $\vec{E}_{||}$, $\vec{E}_{\perp}$, respectively.

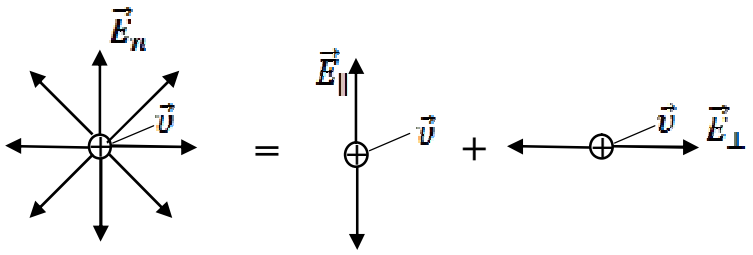

Fig. 2. Model of natural light

Let the natural radiation fall on the "air - metal" interface at an angle θ_i, which is reflected and refracted into the metal (Fig. 3). Let us determine the parameters of the reflected radiation using the model of natural light in the form of two linearly polarized in mutually perpendicular planes components $E_{||} \perp E_{\perp}$.

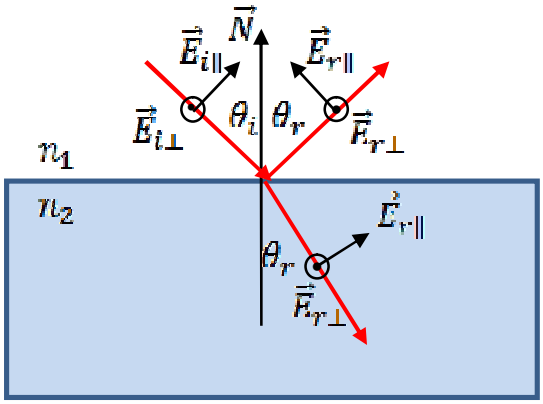

Fig. 3. Schematic for explaining the polarization of reflected radiation

The energy reflection coefficients for the parallel $R_{\|}$ and perpendicular $R_{\perp}$ components are determined by the Fresnel formulae [4]

$$R_{\|} = \left|\frac{E_{R0\|}}{E_{n0\|}}\right|^2 = \left|\frac{n_2 \cos\theta_i - n_1 \cos\theta_t}{n_2 \cos\theta_i + n_1 \cos\theta_t}\right|^2, \tag{11}$$

$$R_{\perp} = \left|\frac{E_{R0\perp}}{E_{n0\perp}}\right|^2 = \left|\frac{n_1 \cos\theta_i - n_2 \cos\theta_t}{n_1 \cos\theta_i + n_2 \cos\theta_t}\right|^2. \tag{12}$$

The angle of incidence θ_i and the angle of refraction θ_i are interrelated by the Snell's law.

$$n_1 \sin\theta_i = n_2 \sin\theta_t. \tag{13}$$

With a normal incidence of radiation on the surface of metal when θ_i=0°, formulae (11) and (12) are given by

$$R_{\|} = R_{\perp} = \frac{(n_2 - 1)^2 + \kappa^2}{(n_2 - 1)^2 + \kappa^2}. \tag{14}$$

Partial energy reflection coefficients can be calculated on the basis of relation (4) as

$$R_{\|} = 1 - \varepsilon_{\|} \text{ and } R_{\perp} = 1 - \varepsilon_{\perp}. \tag{15}$$

The degree of polarization of the reflected radiation is determined as

$$P(\theta_r) = \frac{R_{\parallel}(\theta_r) - R_{\perp}(\theta_r)}{R_{\parallel}(\theta_r) + R_{\perp}(\theta_r)}. \quad (16)$$

The magnitude of the radiation reflected from the object depends on the intensity of the external radiation, and, as a rule, in most cases it will be less than the intrinsic radiation. In this case, its effect on the polarization model can be neglected. In some cases, if there are high-temperature obstacles near the object, it is necessary to take into account the reflected radiation.

Polarization ellipse

Consider the propagation of a plane electromagnetic wave along the *Z* axis (Fig. 4). In the general case, the monochromatic wave is described by the equation

$$\vec{E}(\vec{r}, t) = \vec{E}_0(\vec{r})\cos(\vec{kr} + \delta), \quad (17)$$

where $\vec{E}_0(\vec{r})$ is constant amplitude at point $P(x, y, z)$; ω and δ are the frequency and the initial phase of the wave, respectively; $\vec{k}$ is a wave vector that is directed along the propagation of the wave; $\vec{r}$ is radius vector that determines the coordinates of point $P(x, y, z)$. In so doing, the scalar product of two vectors $\vec{k}$ and $\vec{r}$ is determined by the equation

$$\vec{kr} = \frac{2\pi}{\lambda}\left(x\cos\alpha + y\cos\beta + z\cos\gamma\right), \quad (18)$$

where λ is the wavelength; $\cos\alpha, \cos\beta, \cos\gamma$ are guiding cosines that determine the direction of wave propagation. In a light wave, the electrical field intensity vector $\vec{E}$ is always perpendicular to the direction of wave propagation, i.e. $\vec{E} \perp \vec{k}$.

Consider the components of the vector $\vec{E}$ in the plane *xy* (Fig. 4):

$$E_x(x, y, t) = E_{0x}(x, y)\cos(\omega t - \vec{kr} + \delta_x), \quad (19)$$

$$E_y(x, y, t) = E_{0y}(x, y)\cos(\omega t - \vec{kr} + \delta_y), , \quad (20)$$

$$E_z(x, y, t) = 0. \quad (21)$$

Let us establish the relationship between the components E_x and E_y by excluding the time variable *t* from equations (19) and (20):

$$\left(\frac{E_x}{E_{0x}}\right)^2 + \left(\frac{E_y}{E_{0y}}\right)^2 - 2\frac{E_x}{E_{0x}}\frac{E_y}{E_{0y}}\cos\delta = \sin^2\delta, \quad (22)$$

where $\delta = \delta_x - \delta_y$.

Equation (22) is called the equation of the polarization ellipse with the angle of polarization (orientation) θ, which is determined by equation (Fig. 5)

$$\mathrm{tg}2\theta = \frac{2E_{0x}E_{0y}}{E_{0x}^2 - E_{0y}^2}\cos\delta\,. \tag{23}$$

The shape of the ellipse is determined by the ellipticity angle χ as the ratio of the smaller axis of the ellipse a to the larger axis b:

$$\mathrm{tg}\chi = \pm\frac{b}{a}. \tag{24}$$

Through the electric field components E_{0x} and E_{0x} the ellipticity angle can be expressed as

$$\sin 2\chi = \frac{2E_{0x}E_{0y}\sin\delta}{E_{0x}^2 + E_{0y}^2}. \tag{25}$$

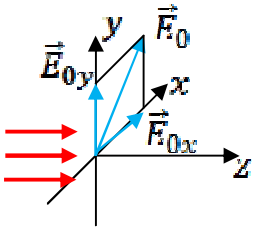

Fig. 4. Vector model of natural light

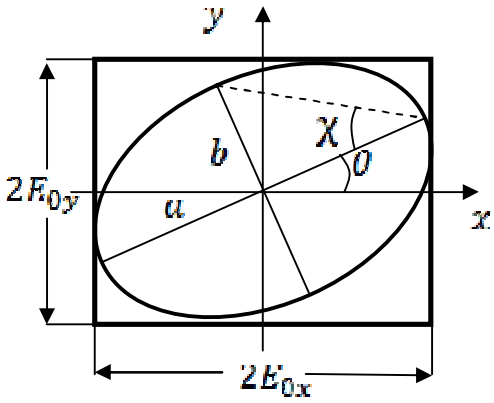

Fig. 5. Polarization ellipse

In the general case, the ellipse (22) is located inside a rectangle of size $2E_{0x} \times 2E_{0y}$ 2 and touches its contour at four points (Fig. 5). If the third term in equation (22) is zero, then the axes of the ellipse are parallel to the x and y axes.

The shape of the ellipse can be represented as linear and circular polarization. Linear polarization occurs when the phase difference δ is 0º or 180º.

If $\theta = \pi$, then Eq.(22) is transformed into equation of the line

$$E_y = \pm\frac{E_{0y}}{E_{0x}}E_x\,. \tag{26}$$

Eq.(26) characterizes a linearly polarized light for which the angle of polarization θ is determined by the formula $\mathrm{tg}\theta = \frac{E_{0y}}{E_{0x}}$. The ellipticity angle χ for the linearly polarized light is equal to zero.

The resulting vector $\vec{E} = \vec{E}_x + \vec{E}_y$ rotates clockwise, when $\sin\delta > 0$ (R-polarization). If $\sin\delta < 0$, then the vector $\vec{E}$ rotates counterclockwise (L-polarization). The state of polarization is

determined by the ratio of the axes of the ellipse, the angle of orientation 0 and *R*- *L*-polarizations.

If $E_{0x} = E_{0y} = E_{0c}$, and $\delta = 2\pi$, then Eq.(22) is given by

$$E_x^2 + E_y^2 = E_{0c}^2 . \tag{27}$$

Equation (27) characterizes circularly polarized light.

Stokes vector

The polarization state of the reflected or emitted IR light (energy brightness, luminosity, illuminance), which determines the background-target environment (BTE), is calculated using the Stokes parameters. The BTE polarization model is characterized by the image intensity, the degree of polarization and the polarization angle which are determined by the Stokes parameters. Parameters S_0, S_1, S_2, S_3 can be written as one column vector or matrix.

The Stokes vector is a column vector composed of four Stokes parameters that describe the state of polarization of light. The Stokes parameters were introduced in 1852 by Gabriel Stokes as a mathematically convenient alternative for describing the state of partially polarized light in terms of the total intensityS_0, the degree of polarization *P*, and the parameters azimuth θ and ellipticity χ.

Table 1 shows the Stokes parameters calculated for several states of polarization. In this case, the light intensity was normalized to S_0=1. The results clearly show the meaning of the Stokes parameters: for S_1 the extreme values ±1 are achieved with horizontal and vertical linear polarization; for S_2 – with linear polarization and the orientation of polarization plane at an angle of ±45º; for S_3 – with circular polarization. The parameter S_0=1 determines the intensity of light, and other parameters – the state of polarization of the electromagnetic wave. For the case of unpolarized light, *a* = *b*, $S_0 = 1$, and $S_1 = 0$. Since δ has arbitrary values, on the average sinδ = cosδ = 0. Also in this case $S_2 = S_1 = 0$.

The Stokes parameters can be determined through the electric field components E_{0x} and E_{0x} and the phase difference δ between two orthogonal electric field strengths $\vec{E}_x \perp \vec{E}_y$:

$$S_0 = I_{0x} + I_{0y}; \tag{28}$$

$$S_1 = I_{0x} - I_{0y}; \tag{29}$$

$$S_2 = 2\sqrt{I_{0x} I_{0y}} \cos\delta; \tag{30}$$

$$S_3 = 2\sqrt{I_{0x} I_{0y}} \sin\delta. \tag{31}$$

The first three Stokes parameters can be determined from the intensity of radiation polarized in a plane oriented at angles of 0º, 90º and 45º relative to the horizon

$$S_0 = I_{0^\circ} + I_{90^\circ}; \tag{28'}$$

$$S_1 = I_{0^\circ} - I_{90^\circ}; \tag{29'}$$

$$S_2 = 2I_{45^\circ} - I_{0^\circ} - I_{90^\circ}. \tag{30'}$$

Table

Stokes vectors for some polarization states

	Linear polarization				Circular polarization	
	horizontal	vertical	+45º	–45º	right	left
θ	0	+90º	+45º	–45º	–	–
cos2θ	1	-1	0	0	–	–
sin2θ	0	0	1	-1	–	–
χ	0	0	0	0	+45º	–45º
cos2χ	1	1	1	1	0	0
sin2χ	0	0	0	0	1	–1
S_0 S_1 S_0 S_3	$\begin{bmatrix}1\\1\\0\\0\end{bmatrix}$	$\begin{bmatrix}1\\-1\\0\\0\end{bmatrix}$	$\begin{bmatrix}1\\0\\1\\0\end{bmatrix}$	$\begin{bmatrix}1\\0\\-1\\0\end{bmatrix}$	$\begin{bmatrix}1\\0\\0\\1\end{bmatrix}$	$\begin{bmatrix}1\\0\\0\\-1\end{bmatrix}$

For a *polarimetric thermal imager*, *the Stokes parameters are calculated for each pixel*. The image intensity *I*, the degree of polarization *P* and the polarization angle θ are determined from the Stokes parameters by the formulae:

$$I = S_0;\ P = DOP = \frac{\sqrt{S_1^2 + S_2^2}}{S_0};\ \theta = \frac{1}{2}\text{arctg}\left(\frac{S_2}{S_1}\right). \tag{30}$$

Examples of calculation of polarization characteristics of radiation from thermal objects

Fig. 6 shows the dependences of the partial radiation coefficients $\varepsilon_{\parallel}$ and $\varepsilon_{\perp}$ and the degree of polarization of the natural radiation on the observation angle ψ for an iron plate having a complex refractive index $n_c = 5.81 - j30.4$ or a wavelength of 10 μm [6]. For thermal radiation at observation angles ψ <40 °, the components of the radiation coefficient are almost the same $\varepsilon_{\parallel} \approx \varepsilon_{\perp} \approx 0.16$, but $\varepsilon_{\parallel} < \varepsilon_{\perp}$. At an angle $\psi = 33°$ $\varepsilon_{\parallel} = \varepsilon_{\perp} = 0.175$. As the angle ψ < 40° increases, the perpendicular polarization component $\varepsilon_{\perp}$ decreases monotonically to zero, and the parallel component $\varepsilon_{\parallel}$ increases and reaches a maximum value at an angle of 84º, and then decreases to zero. The degree of polarization of radiation increases with increasing angle ψ, but at an angle ψ = 33 ° it is zero, and at an angle ψ = 84 ° - 0.96.

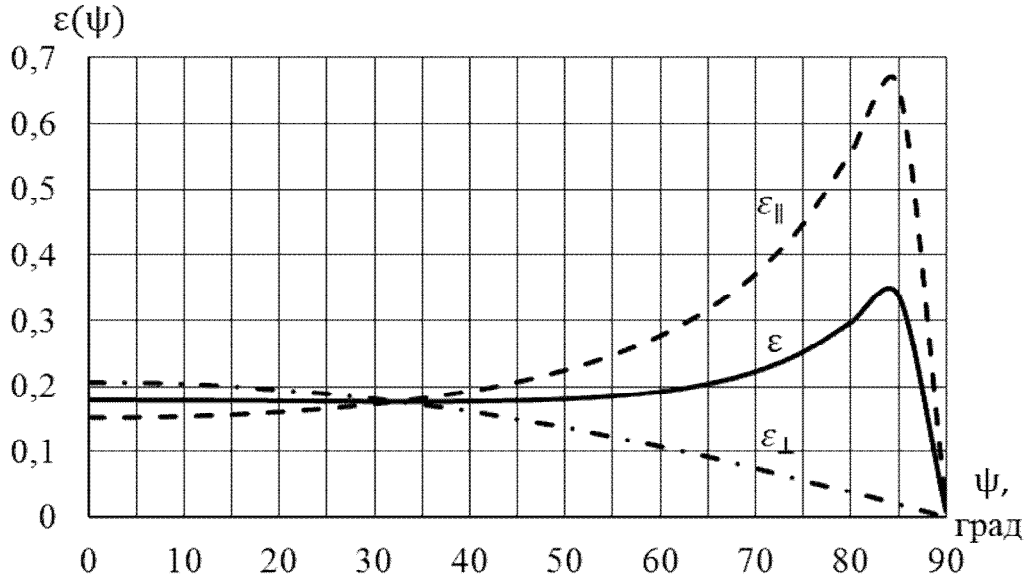

a)

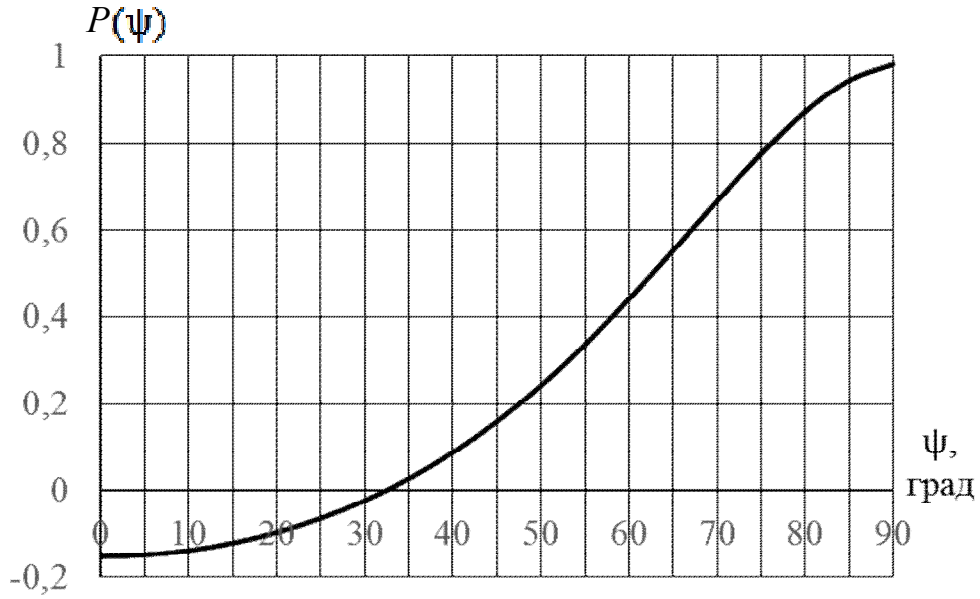

b)

Fig. 6. The dependence of the components of the radiation coefficients ε∥ and ε⊥ (a) and the degree of polarization P (b) of the intrinsic radiation from the iron surface with a complex refractive index $n_c = 5.81 - j30.4$ *the angle of observation ψ*

Fig. 7 shows the dependences of partial energy reflection coefficients $R_{\|}$ and $R_{\perp}$ and the degree of polarization P of reflected radiation at the "air – iron" interface on the incidence angle θ_i. The reflection coefficient with a normal incidence according to formula (14) is about 0.848.

For any angle, the perpendicularly polarized component is larger than the parallel component. The parallel component has a minimum of 0.32, at an angle of incidence of about 84º. For this angle, the degree of polarization of the reflected radiation is equal to 0.49.

For the "air-dielectric" interface the coefficient of reflection for the parallel component is equal to zero with a Brewster angle, and the perpendicular component is equal to unity.

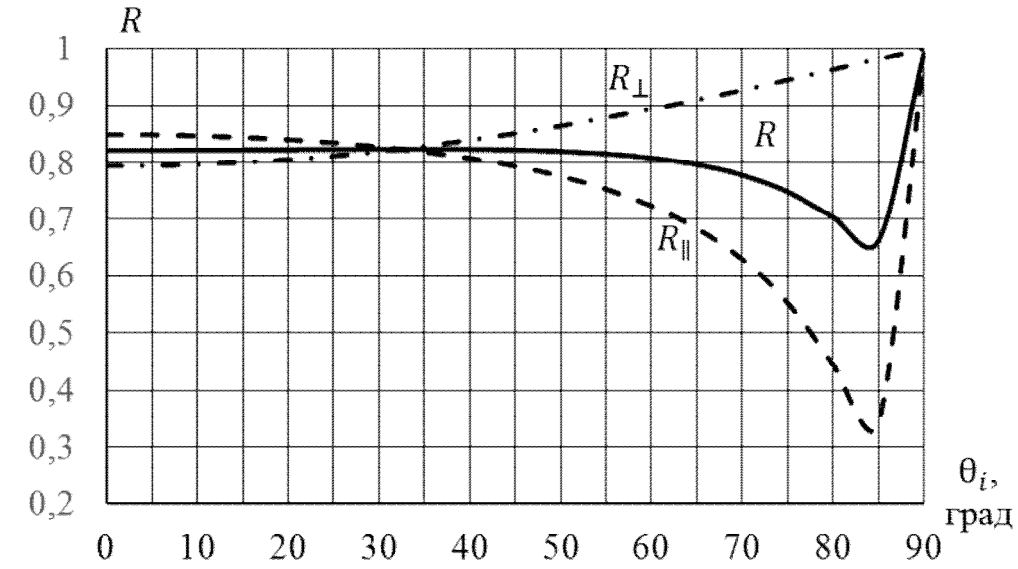

a)

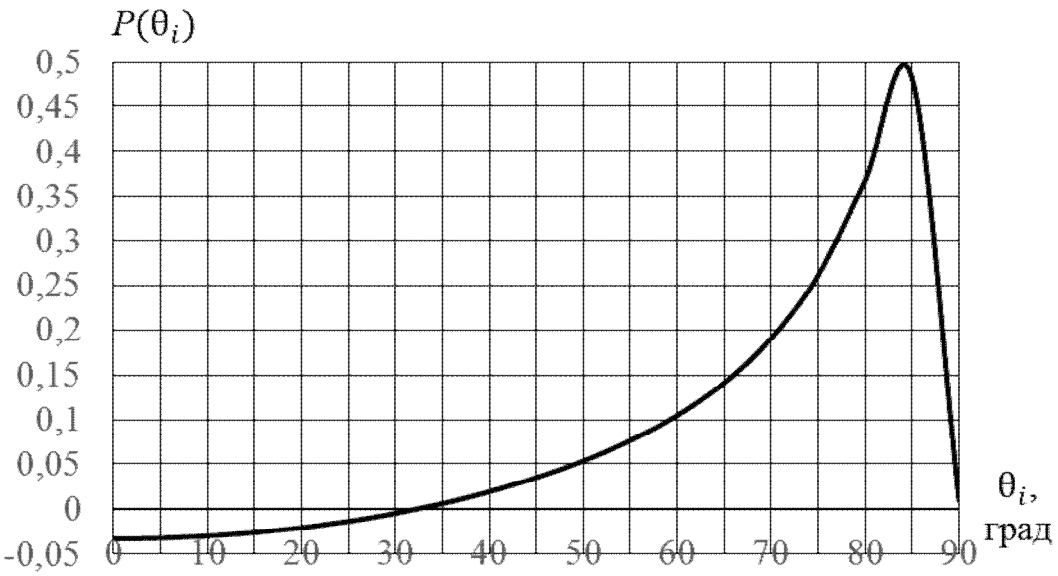

b)

Fig. 7. Dependence of the components of reflection coefficient $R_\parallel$ and $R_\perp$ at the "air-iron" interface and the degree of polarization P of the reflected radiation on the incidence angle θ_i

Conclusions

The use of thermal imagers for the study of thermoelectric phenomena and devices can increase the efficiency of such devices. Using the polarization properties of the infrared radiation to visualize thermal contrast objects enables one to create a new class of high-precision optoelectronic devices, i.e. polarization thermal imagers. To study and design such thermal imagers, a physico-mathematical model of polarization of radiation from observation objects is considered, which takes into account the polarization properties of the intrinsic thermal radiation and the reflected external radiation. As a result of research of this model it is established that

1. The intrinsic radiation is partially polarized due to the difference in the radiation coefficients of the object surface for two linearly polarized waves in mutually perpendicular planes. The study of the components of the radiation coefficients showed that the component for the wave that is polarized in the plane of incidence is greater than the component that is polarized in the perpendicular plane.

2. The reflected external radiation is also partially polarized due to the difference in the reflection coefficients of the object surface for two linearly polarized waves in mutually perpendicular planes. Moreover, the component that is polarized in the plane of incidence is always less than the component that is polarized in the perpendicular plane.

3. To simulate the polarization state of the radiation from the observation object, it is advisable to choose the image intensity, the degree of polarization and the polarization angle determined by the Stokes parameters.

4. The developed model was used to study the polarization properties of the radiation from a flat iron plate, which had a complex refractive index. Analysis of the results shows that

4.1. For thermal radiation at observation angles ψ <40°, the components of the radiation coefficient are almost the same $\varepsilon_{\parallel} \approx \varepsilon_{\perp} \approx 0.16$, but $\varepsilon_{\parallel} < \varepsilon_{\perp}$. As the observation angle ψ <40 ° increases, the perpendicular polarization component $\varepsilon_{\perp}$ decreases monotonically to zero, and the parallel component $\varepsilon_{\parallel}$ increases and reaches its maximum value at an angle of 84º, and then decreases to zero. The degree of polarization of radiation increases with increasing angle ψ and at an angle ψ = 84 ° is equal to 0.96.

4.2. The reflection coefficient at normal incidence is equal to 0.85. For any angle, the perpendicularly polarized component is larger than the parallel component. The parallel component has a minimum of 0.32 at an angle of incidence of 84º. For this angle, the degree of polarization of the reflected radiation is equal to 0.49.

5. It is advisable to use the obtained research results when developing a model of thermoelectrics which is necessary when designing a polarization thermal imager.

References

1. Zhao Yonqiang, Yi Chen, Kog Seong G., Pan Quan, Cheng Yongmei (2016). *Multi-band polarization imaging and applications*. Berlin Heidelberg: National Defense Industry Press, Beijing and Springer-Verlag.
2. Yang Bin, Wu Taixia, Chen Wei, Li Yanfei, Knjazhikhin Yuri, et.al. (2017). Polarization remote sensing physical mechanism, key methods and application. *The International Archives of the Photogrammetry, Remote Sensing and Spatial Information Sciences*, XLII-2/W7, 956-960.
3. Anatychuk L.I., Vikhor L.M., Kotsur M.P., Kobylianskyi R.R., Kadeniuk T.Ya. (2016).Optimal control of time dependence of cooling temperature in thermoelectric devices. *J.Thermoelectricity*, 5, 5-11.
4. Born M., Wolf E. (2002). *Principles of optics, 7th ed.*, Cambridge University Press.
5. Vollmer Michael and Mollman Klaus-Peter (2018). *Infrared thermal imaging. Fundamentals, research and applications*. 2nd ed. Weinheim: Wiley – VCH.
6. Kolobrodov V.G., Lykholit M.I. (2007). *Design of thermal imaging and television surveillance systems*. Kyiv: NTUU “ KPI” [in Ukrainian].
7. Siegel R., Howell J.R. (1981). *Thermal radiation heat transfer, 2nd ed*. Hemisphere Publishing Corp.
8. Vollmer M., Karstadt S., Mollman K-P., Pinno F. (2001). Identification and suppression of thermal imaging. *InfraMation Proceedings*. University of Applied Sciences: Brandenburg (Germany).

Submitted 26.02.2020

Колобродов В.Г., *докт. техн. наук, професор*
Микитенко В.І., *докт. техн. наук, доцент*
Тимчик Г.С. *докт. техн. наук, професор*

Національний технічний університет України
«Київський політехнічний інститут імені Ігоря Сікорського»
проспект Перемоги, 37, Київ, 03056, Україна
e-mail: deanpb@kpi.ua

ПОЛЯРИЗАЦІЙНА МОДЕЛЬ ТЕПЛОКОНТРАСТНИХ ОБ'ЄКТІВ СПОСТЕРЕЖЕННЯ

У статті запропоновано поляризаційну модель тепловізора з метою його застосування при дослідженні термоелектричних явищ і пристроїв, що дозволяє підвищити ефективність роботи таких пристроїв. Для дослідження і проектування таких тепловізорів розглянута фізико-математична модель поляризації випромінювання від об'єктів спостереження, яка враховує поляризаційні властивості власного теплового випромінювання і відбитого зовнішнього випромінювання. Розроблена модель була застосована для визначення поляризаційних властивостей випромінювання плоскої залізної пластини. Аналіз отриманих результатів свідчить про те, що для теплового випромінювання при кутах спостереження $\psi < 40°$ складові коефіцієнта випромінювання є майже однаковими $\varepsilon_{\parallel} \approx \varepsilon_{\perp} \approx 0.16$, але $\varepsilon_{\parallel} < \varepsilon_{\perp}$. Із збільшенням кута спостереження $\psi<40°$ перпендикулярна поляризаційна компонента $\varepsilon_{\perp}$ монотонно зменшується до нуля, а паралельна компонента $\varepsilon_{\parallel}$ збільшується і досягає максимального значення при куті $\psi=84°$, а потім зменшується до нуля. Ступінь поляризації випромінювання зростає із збільшенням кута ψ і при куті $\psi = 84°$ дорівнює 0.96.

Отримані результати досліджень доцільно використовувати при розробці моделі термоелектриків, яка може використовуватись при проектуванні поляризаційного тепловізора. Бібл. 8, рис. 7, табл. 1.

Ключові слова: поляризаційний тепловізор, температурне розділення, частково поляризоване випромінювання, ступінь поляризації.

Колобродов В.Г., *докт. техн. наук, професор*
Микитенко В.І., *докт. техн. наук, доцент*
Тимчик Г.С. *докт. техн. наук, професор*

Національний технічний університет України
«Київський політехнічний інститут імені Ігоря Сікорського»
проспект Перемоги, 37, Київ, 03056, Україна
e-mail: deanpb@kpi.ua

ПОЛЯРИЗАЦІЙНА МОДЕЛЬ ТЕПЛОКОНТРАСТНИХ ОБ'ЄКТІВ СПОСТЕРЕЖЕННЯ

У статті запропоновано поляризаційну модель тепловізора з метою його застосування при дослідженні термоелектричних явищ і пристроїв, що дозволяє підвищити ефективність роботи таких пристроїв. Для дослідження і проектування таких тепловізорів розглянута фізико-математична модель поляризації випромінювання від об'єктів спостереження, яка враховує поляризаційні властивості власного теплового випромінювання і відбитого зовнішнього випромінювання. Розроблена модель була застосована для визначення поляризаційних властивостей випромінювання плоскої залізної пластини. Аналіз отриманих результатів свідчить про те, що для теплового випромінювання при кутах спостереження $\psi < 40°$ складові коефіцієнта випромінювання є майже однаковими $\varepsilon_{\parallel} \approx \varepsilon_{\perp} \approx 0.16$, але $\varepsilon_{\parallel} < \varepsilon_{\perp}$. Із збільшенням кута спостереження $\psi<40°$ перпендикулярна поляризаційна компонента $\varepsilon_{\perp}$ монотонно зменшується до нуля, а паралельна компонента $\varepsilon_{\parallel}$ збільшується і досягає максимального значення при куті $\psi=84°$, а потім зменшується до нуля. Ступінь поляризації випромінювання зростає із збільшенням кута ψ і при куті $\psi = 84°$ дорівнює 0.96. Отримані результати досліджень доцільно використовувати при розробці моделі термоелектриків, яка може використовуватись при проектуванні поляризаційного тепловізора. Бібл. 8, рис. 7, табл. 1.

Ключові слова: поляризаційний тепловізор, температурне розділення, частково поляризоване випромінювання, ступінь поляризації.

References

1. Zhao Yonqiang, Yi Chen, Kog Seong G., Pan Quan, Cheng Yongmei (2016). *Multi-band polarization imaging and applications*. Berlin Heidelberg: National Defense Industry Press, Beijing and Springer-Verlag.
2. Yang Bin, Wu Taixia, Chen Wei, Li Yanfei, Knjazhikhin Yuri, et.al. (2017). Polarization remote sensing physical mechanism, key methods and application. *The International Archives of the Photogrammetry, Remote Sensing and Spatial Information Sciences*, XLII-2/W7, 956-960.
3. Anatychuk L.I., Vikhor L.M., Kotsur M.P., Kobylianskyi R.R., Kadeniuk T.Ya. (2016).Optimal control of time dependence of cooling temperature in thermoelectric devices. *J.Thermoelectricity*, 5, 5-11.
4. Born M., Wolf E. (2002). *Principles of optics, 7th ed.*, Cambridge University Press.
5. Vollmer Michael and Mollman Klaus-Peter (2018). *Infrared thermal imaging. Fundamentals, research and applications*. 2nd ed. Weinheim: Wiley – VCH.
6. Kolobrodov V.G., Lykholit M.I. (2007). *Design of thermal imaging and television surveillance systems*. Kyiv: NTUU " KPI" [in Ukrainian].
7. Siegel R., Howell J.R. (1981). *Thermal radiation heat transfer, 2nd ed*. Hemisphere Publishing Corp.
8. Vollmer M., Karstadt S., Mollman K-P., Pinno F. (2001). Identification and suppression of thermal imaging. *InfraMation Proceedings*. University of Applied Sciences: Brandenburg (Germany).

Submitted 26.02.2020

R.G. Cherkez

R.G. Cherkez, *dok. phys.– mat. sciences, acting professor*[1,2]
I.A. Konstantynovych, *cand. phys.– mat. sciences, assistant professor*[1,2]

[1]Institute of Thermoelectricity of the NAS and MES of Ukraine, 1, Nauky str., Chernivtsi, 58029, Ukraine
[2]Yuriy Fedkovych Chernivtsi National University, 2, Kotsiubynsky str., Chernivtsi, 58012, Ukraine

I.A. Konstantynovych

GENERALIZED THEORY OF THERMOELECTRIC ENERGY CONVERSION FOR PERMEABLE THERMOELEMENTS

A generalized theory of calculation of permeable thermoelements is presented, taking into account the dependences of the parameters of legs material on the temperature and current carrier concentration and changes in the conditions of heat transfer along the height of the leg. Methods for simulating the distributions of temperatures and heat flows in 1-D and 3-D dimensional models of a permeable thermoelement are described. The theory of calculating permeable thermoelements has been improved for the case of solving a multifactor optimization problem in order to achieve the maximum energy efficiency of thermoelectric energy conversion. Bibl. 12, Fig. 2.

Key words: generalized theory of permeable thermoelements, methods of designing a permeable thermoelement.

Introduction

Permeable thermoelements are thermocouples in which heat exchange with a heat source (sink) occurs not only on the surfaces of the junctions but also inside the thermoelement legs (Fig. 1).

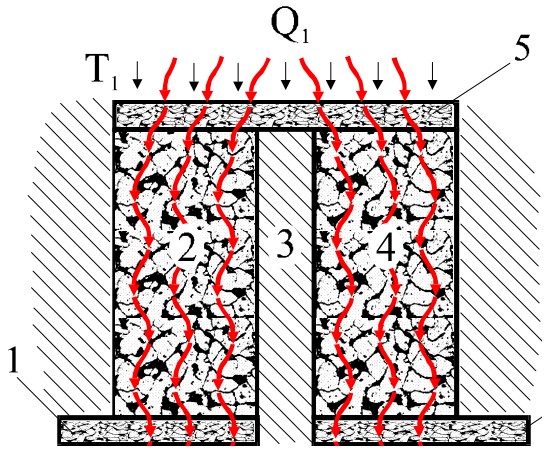

Fig. 1. A model of a permeable thermoelement in which heat carrier is passed from the hot to cold junctions ($T_1 > T_2$). 1,5,6 – connecting plates, 3 – adiabatic insulation, 2,4 – legs that have channels (pores), ↓ – heat flows;

↯ – heat carrier flows.

In this case, the legs material is made permeable (has channels or pores) for pumping a heat carrier (liquid or gas) therethrough.

Since, thanks to the use of materials of high permeability, the inner surface of heat exchange can be sufficiently developed, the intensity of heat exchange increases, and the temperature difference between the media that exchange heat decreases. This leads to an increase in the useful temperature difference across the thermoelement, which makes it possible to increase the efficiency of energy conversion [1 – 3].

By changing the heat transfer conditions along the leg height, it is possible to influence the volumetric distribution of heat sources (sinks) in the legs of a permeable thermoelement. Thus, it becomes possible to influence the energy characteristics of the thermoelement – the efficiency or power of the generator or the coefficient of performance of coolers or air conditioners.

The parameters of porous structures were also studied in [4-6]. The estimation of the output power of a porous annular thermoelectric generator for waste heat harvesting was carried out in [4]. This article points out the fact that the porous TEGs have better performance than the bulk TEGs. However, in these works, the multiparameter optimization of permeable thermoelements was not carried out taking into account the change in heat transfer conditions along the height of the leg, the effect of contact resistances and connecting heat spreaders.

To do this, it is necessary to generalize the theory of calculation of permeable thermoelements taking into account the change of heat exchange conditions for 1D and 3D model of a permeable thermoelement, which is the purpose of this work.

Physical model and its mathematical description

The presence of heat exchange between the thermoelectric material and the heat carrier (Fig. 2) makes it necessary to solve the problem of finding the distributions of temperatures, electric potential and heat flows in the material conjugate with the equations of motion and heat transfer for the heat carrier.

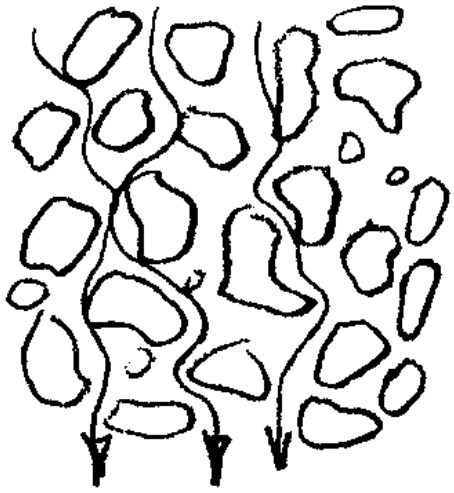

Fig.2. Pattern of heat carrier flow in a permeable material.

The system of the Navier-Stokes equation and the continuity equation is used to describe the motion of the heat carrier in the channel, and the heat conduction equation is used to describe the temperature distribution in the heat carrier.

The Navier-Stokes equation and the continuity equation can be written as [7]

$$\left.\begin{aligned} \rho\frac{d\vec{\vartheta}}{dt} &= \rho\vec{F} - \vec{\nabla}P + \mu\vec{\nabla}^2\vec{\vartheta} + \frac{1}{3}\mu\vec{\nabla}(div\vec{\vartheta}), \\ div\ \rho\vec{\vartheta} &= 0. \end{aligned}\right\} \quad (1)$$

The left-hand side of the first equation (1) is the inertial force. The first term on the right-hand side of this equation is the mass force, the second is the action of surface pressure forces (normal stresses), and the last two terms are the action of the tangential components of surface forces (internal friction forces).

Heat exchange in liquid is described by thermal conductivity equation

$$\rho C_p\left(\frac{\partial T}{\partial t} + (\vec{\vartheta}\vec{\nabla})T\right) = -(\vec{\nabla}\vec{q}) + \sum_{i,j}\tau_{ij}S_{ij} - \frac{T}{\rho}\frac{\partial\rho}{\partial T}\bigg|_P\left(\frac{\partial\rho}{\partial t} + (\vec{\vartheta}\vec{\nabla})P\right) + Q \quad (2)$$

where ρ is density, C_p is heat capacity, T is temperature, $\vec{\vartheta}$ is liquid velocity vector, q is heat flow density, P is pressure, τ_{ij} is viscous stress tensor, $\vec{S}_{ij}$ is strain rate tensor, Q are internal heat sources.

The generalized mathematical model for a thermoelectric medium is based on the equations of heat balance in solid phases, mass transfer of gas components, continuity equations, filtration hydrodynamics and equations of state. In addition, it is necessary to formulate the appropriate boundary conditions. It is advisable to solve this problem by computer tools using specially developed applications, such as COMSOL Multiphysics.

The results of such studies, carried out for a permeable thermoelement in a 3D model, were first obtained in [8] for cooling liquid and air flows. The influence of the rate of heat carrier pumping and the supply voltage of the thermoelement on the temperature difference and the characteristics of energy conversion is investigated. The optimal values of the water (air) supply rate at the inlet to the channels and the potential difference across the thermoelement, whereby the maximum cooling capacity is realized during cooling, are determined in this paper. Optimization for other parameters in a 3D model was a significant challenge.

Therefore, to carry out multiparameter optimization of a permeable thermoelement, a 1D-dimensional model and the mathematical theory of optimal control are used [9, 10]. In this case, the steady-state one-dimensional heat conductivity equation for the thermoelectric leg material is given by

$$\frac{d}{dx}\left(\kappa\left(T,\xi(x)\right)\frac{dT}{dx}\right) + i^2\rho\left(T,\xi(x)\right) - Ti\frac{d\alpha\left(T,\xi(x)\right)}{dx} - \frac{\alpha_T P_K^1 N_K}{\left(S - S_K\right)}\left(T - t\right) = 0, \quad (3)$$

where P_K^1 is channel perimeter; N_K is the number of channels; S_K is cross-sectional area of all channels; S is cross-section of a leg together with channels; t is heat carrier temperature at point x; T is leg temperature at point x; α_T is heat exchange coefficient; i is current density ($i=\frac{I}{S - S_K}$); $\alpha(T, \xi(x))$, $\kappa(T, \xi(x))$, $\rho(T,\xi(x))$ - the Seebeck coefficient, thermal conductivity and resistivity of leg material are functions of temperature T and parameter of material inhomogeneity $\xi(x)$. In the capacity of $\xi(x)$, we can use the concentration of current carriers in semiconductor, doping impurities, or other value that characterizes thermoelectric structure inhomogeneity along the height of thermoelement legs. It should be noted that the thermoelectric medium parameters α,κ,ρ are interdependent. The system of these relations assigns a certain set $G\xi$ for possible values of the inhomogeneity parameter ξ. Specifying the physical model, one should

assign such relations, for instance, in the form of theoretical or experimental dependences α, κ, ρ on ξ and *T*, and thus determine the set *G*ξ.

In the one-dimensional steady-state case on the leg section *dx* the change in heat carrier temperature *dt* is determined by the law of conservation of energy given by the expression

$$Gc_P dt = \alpha_T P_K^1 N_K \left(t - T\right) dx \ , \tag{4}$$

where G is mass flow rate of heat carrier through the leg of thermoelement; c_p is heat capacity of heat carrier.

Taking into account the relation (4), the equation for temperature distribution of heat carrier *t* can be represented as

$$\frac{dt}{dx} = \frac{\alpha_T P_K^1 N_K}{Gc_P}\left(t - T\right). \tag{5}$$

The solution of the system of differential equations (3) and (5) is temperature distribution in the materials of legs and the heat carrier.

We convert this system of equations to the form convenient for solving the problem. To do this, we introduce new symbols

$$j = il \ , \ \ q = \frac{1}{j}\left(\alpha jT - \kappa\frac{dT}{dx}\right), \quad \mathrm{x} = \frac{x}{l}, \ \alpha_e = \alpha_T P_K^1 N_K l \ , \tag{6}$$

where α_e is effective heat transfer coefficient, l is the height of thermoelement legs, q is specific heat flow.

Let us direct the *x*-axis from the cold to hot junctions. The change in the type of conductivity is carried out simultaneously with the change in the direction of the current, so that the condition $\alpha j<0$ is met in the *n*- and *p*- type thermoelement legs. Then it is possible to make the change $\alpha j = -|\alpha j|$ and then use the absolute values of the parameters α and *j* for the legs of both types of conductivity.

With regard to (6), the system of differential equations will take on the form:

$$\left.\begin{array}{l} \dfrac{dT}{d\mathrm{x}} = -\dfrac{\alpha\ j}{\kappa}\ T - \dfrac{j}{\kappa}q, \\ \dfrac{dq}{d\mathrm{x}} = \dfrac{\alpha^2 j}{\kappa}T + \dfrac{\alpha\ j}{\kappa}q + j\rho + \dfrac{\alpha_e l}{\left(S - S_K\right)j}\left(t - T\right), \\ \dfrac{dt}{d\mathrm{x}} = \dfrac{\alpha_e}{Gc_P}\left(t - T\right). \end{array}\right\}_{n,p} \tag{7}$$

The system of differential equations (7) written for *n*- and *p*- type legs (denoted by indices *n* and *p*, respectively) makes it possible to find the distributions of temperatures in the material of legs and the heat carrier, to determine heat flows. Based on this system of differential equations, one can find the optimal parameters and operating modes of permeable thermoelements, study their energy characteristics.

The values of specific heat flows on the cold and hot thermoelement junctions $q(1)$ and $q(0)$ will be determined with regard to the Joule heat release on the contact r_c and connecting resistances in the following way [10]:

$$\left.\begin{aligned} q(1) &= \sum_{n,p}\left[q^{n,p}(1) + \frac{j^{n,p}}{l} r_c^{n,p} \right] + \frac{2 r_{com} I}{h_{com}}\left(K_{com} - \frac{2}{3} \right) \\ q(0) &= \sum_{n,p}\left[q^{n,p}(0) - \frac{j^{n,p}}{l} r_c^{n,p} \right] - \frac{2 r_{com} I}{h_{com}}\left(K_{com} - \frac{2}{3} \right) \end{aligned}\right\} . \qquad (8)$$

Consider the problem of maximum energy efficiency of thermoelectric cooling at fixed temperatures of heat sources T_h and T_c.

The problem reduces to finding maximum coefficient of performance ε and efficiency η

$$\varepsilon = \frac{Q_c}{Q_h - Q_c} \qquad (9)$$

The efficiency is determined by the relation of the thermoelement power to the change in the enthalpy of the heat carrier as follows:

$$\eta = \frac{W}{\sum_{n,p} G c_p \left(T_m - T_C \right)} \quad . \qquad (9^*)$$

in the case of differential constraints (7) and the boundary conditions

$$T_{n,p}(0) = T_{\mathrm{h}}, \quad T_{n,p}(1) = T_c, \quad t_{n,p}(0) = T_s, \qquad (10)$$

where T_h is the temperature of the hot surface of junctions, T_c is the temperature of the cold surface of junctions, T_s is the initial temperature of heat carrier, Q_h, Q_c are heat flows that

the thermoelement exchanges with external heat sources

$$Q_h = Q_n(0) + Q_p(0),$$

$$Q_c = Q_n(1) + Q_p(1) + Q_L;$$

here Q_L is heat which is supplied due to internal heat transfer from the cooled heat carrier $Q_L = \sum_{n,p} V c_P S_R \left(t(0) - t(1) \right)$.

Hereinafter, instead of maximum ε it is convenient to consider functional minimum $\Im$:

$$\Im = \ln q(0) - \ln q(1), \qquad (11)$$

where

$$q(0) = \frac{Q_h}{I} = q_n(0) + q_p(0),$$

$$q(1) = \frac{Q_c}{I} = q_n(1) + q_p(1) + \frac{Q_L}{j\left(S - S_K \right)} l,$$

here $q_n(1)$, $q_p(1)$, $q_n(0)$, $q_p(0)$ are the values of specific heat flows on the cold and hot thermoelement junctions for *n*- and *p*-type legs that are determined from solving the system of differential equations (7) with regard to (8).

The optimization problem is to select from the set of admissible controls $\xi \in G_\xi$ such concentration functions $\xi^{n,p}(x)$ and simultaneously assign such a specific mass velocity of the heat carrier in the channels $V=V_0$, whereby in the case of constraints (7) - (11) and under the condition

$$q_n(1) + q_p(1) = 0 \tag{12}$$

the functional $\Im$ will take on the lowest value, in which case the coefficient of performance ε will be maximum [10, 11].

Finding the efficiency maximum reduces to a search for the functional minimum

$$\Im = \ln[\sum_{n,p}\left\{Gc_P\left(T_m - T_C\right)\right\}] - \ln[\sum_{n,p}\left\{Gc_P\left(T_m - t(0)\right) + q(0)\frac{j\left(S - S_K\right)}{l} - I\left(\frac{r_0}{S_n} + \frac{r_0}{S_p}\right)\right\}]. \tag{13}$$

For further solutions, the mathematical theory of optimal control developed under the guidance of L.S. Pontryagin is generally used [12].

Method for solving the problem

Next, the problem is reduced to finding control $\xi(x)$, parameter vectors ω and their respective solution $X(x)$ of system (7), (10) such that the functional $\Im$ acquires a minimum value. The problem set in this way is called optimization. Its solution in the most general form was first formulated by Pontryagin in the form of the maximum principle, which yields the necessary optimality condition in the problems of optimal control.

The maximum principle is formulated by the following theorem.

Let $\xi^*(x)$ be optimal control, ω^* - optimal parameter vector, $X^*(x)$ - optimal trajectory. Then there is such a vector of pulses $\psi^*(x)$, that for each x the following conditions are met:

1. The Hamiltonian function which is written as equation

$$H(X_*(x), \xi_*(x), \psi_*(x), \omega_*, x) = (\psi, f\ ) \tag{14}$$

(in our case f_1, f_2, f_3 are the right-hand sides of equation system (7)), with respect to variable ξ reaches its maximum:

$$H(X^*(x), \xi^*(x), \psi^*(x), \omega^*, x) = \max_{\xi \in G_\xi} H\ (X^*(x), \xi, \psi^*(x), \omega^*, x). \tag{14*}$$

2. Parameter vector ω must satisfy a system of integral differential equations

$$-\frac{\partial \Im(x(x), \omega)}{\partial \omega_i} + \int \sum_{j=1}^{n} \psi_j \cdot \frac{\partial f_j^k(x, \xi, \omega)}{\partial \omega_i} dt = 0, \qquad i = 1, .., r. \tag{15}$$

Pulse vector $\psi(x)$ satisfies a system of differential equations of the form

$$\frac{d\psi}{dx} = -\frac{\partial H}{\partial X}, \tag{16}$$

which is canonically conjugate with system (7), where $X(X_1, X_2, X_3)$ is vector function of phase variables (in our case with components $X_1 = T$, $X_2 = q$, $X_3 = t$), with the boundary conditions

$$\psi(x) = -\frac{\partial J}{\partial X}. \tag{17}$$

The solution of optimal problems which is based on the use of the maximum principle can be realized by numerical methods with the development of corresponding computer programs.

With its help it is possible to investigate various problems of optimal control, differing in the way of assigning the functional (Lagrange, Mayer, Boltz problems), constraints, etc.

We specify the previously stated formalism of the mathematical theory of optimal control in relation to our problem.

Introduce the Hamiltonian function

$$H = \psi_1 f_1 + \psi_2 f_2 + \psi_3 f_3 , \tag{18}$$

here f_1, f_2, f_3 are the right-hand sides of the system of equations (7):

$$f_1 = -\frac{\alpha\ j\ T}{\kappa} - \frac{q}{\kappa}, \quad f_2 = \frac{\alpha^2 j}{dx} T + \frac{\alpha\ j}{\kappa} q + i^2 \rho - \frac{\alpha_T P_K^1 N_K l^2}{(S - S_K) j}(T - t),$$

$$f_3 = \frac{\alpha_T P_K^1 N_K l}{V c_P S_R}(T - t).$$

Functions $\psi(x)$ (pulses) must satisfy a system of equations (with regard to (7) and (17)):

$$\begin{cases} \dfrac{d\psi_1}{d\mathrm{x}} = \dfrac{\alpha\ j}{\kappa} R_1 \psi_1 - \left(\dfrac{\alpha\ j}{\kappa} R_2 - \dfrac{\alpha_T P_K^1 N_K l^2}{(S - S_K) j} \right) \psi_2 - \dfrac{\alpha_T P_K^1 N_K l}{V c_P S_R} \psi_3, \\ \dfrac{d\psi_2}{d\mathrm{x}} = \dfrac{j}{\kappa} \psi_1 - \dfrac{\alpha\ j}{\kappa} \psi_2, \\ \dfrac{dt}{d\mathrm{x}} = -\dfrac{\alpha_T P_K^1 N_K l^2}{(S - S_K) j} \psi_2 + \dfrac{\alpha_T P_K^1 N_K l}{V c_P S_R} \psi_3, \end{cases}_{n,p} \tag{19}$$

where

$$\begin{cases} R_1 = 1 + \dfrac{d \ln \alpha}{dT} T - \dfrac{d \ln \kappa}{dT} \left(T + \dfrac{q}{\alpha} \right) \\ R_2 = R_1 + \dfrac{1}{Z_K} \dfrac{d \ln \sigma}{dT} + \dfrac{d \ln \kappa}{dT} \left(T + \dfrac{q}{\alpha} \right) \end{cases}_{n,p}$$

are canonically conjugate with system (7).

With the following boundary conditions (transversality conditions)

$$\psi(0)=\left.\frac{\partial \bar{J}}{\partial y}\right|_{x=0}, \quad \psi(1)=-\left.\frac{\partial \bar{J}}{\partial y}\right|_{x=1}, \tag{20}$$

where $\bar{J}=J+\sum(\nu, g)$ is extended functional; ν , g are vectors of undetermined constant Lagrange multipliers and the boundary conditions (10).

Then the boundary conditions for the conjugate system will acquire the form

$$\psi_2^{n,p}(0)=\frac{1}{q_n(0)+q_p(0)},$$
$$\psi_2^{n,p}(1)=-\frac{(S-S_K)j}{lVc_P S_R\left(2t(0)-t_n(1)-t_p(1)\right)},$$
$$\psi_3^{n,p}(1)=-\frac{1}{2t(0)-t_n(1)-t_p(1)}.$$

Using the systems of differential equations (7), (19) with regard to (10), (20) and numerical solution methods, it is possible to create a program of computer design of optimal inhomogeneity functions of thermoelectric material $\xi(x)$ (or optimally homogeneous material for thermoelement legs from (15)), the optimal velocity of heat carrier V_0, the parameter of electric current density j and others, in order to achieve maximum energy efficiency of permeable cooling thermoelements and electricity generation.

Conclusions

1. Theory of thermoelectric energy conversion is generalized for the case of heat sources and sinks in a permeable thermoelectric medium. Methods for simulation of such thermoelements in 3-D and 1-D space are described. The influence of connecting plates and contact resistances at points of connection of legs is taken into account.

2. Theory of calculation of permeable thermoelements for the case of solving a multifactor optimization problem (optimal inhomogeneity functions of thermoelectric material $\xi(x)$, optimal heat carrier flow rate G, optimal heat carrier velocity V_0, parameter of electric current density j and others) is improved for the purpose of achieving maximum energy efficiency of thermoelectric energy conversion.

References

1. V.N. Kozliuk, G.M. Shchegolev (1973). Termodinamicheskii analiz pronitsayemykh termoelektricheskikh kholodilnikov [Thermodynamic analysis of permeable thermoelectric coolers]. *Teplofizika i teploteknika*, 25, 96-100 [in Russian].
2. G.K. Kotyrlo, V.N. Kozliuk, Lobunets Yu.N. (1975). Termoelektricheskii generator s razvitoi poverkhnostiu teploobmena [Thermoelectric generator with a developed surface of heat exchange]. *Teplotekhnicheskiie problemy priamogo preobrazovaniia energii*, 7, 85-95 [in Russian].
3. Yu.N. Lobunets (1989). *Metody rascheta i proektirovaniia termoelekricheskikh preobrazovatelei energii [Methods for calculation and design of thermoelectric power converters]*. Kyiv:

Naukova dumka [in Russian].

4. Y.J. Cui, B.L. Wanga, K.F. Wang, L. Zheng (2019). Power output evaluation of a porous annular thermoelectric generator for waste heat harvesting. *International Journal of Heat and Mass Transfer*, 137, 979–989.
5. E.S. Reddy, J.G. Noudem, C. Goupil (2007). Open porous foam oxide thermoelectric elements for hot gases and liquid environments. *Energy Convers. Manage*., 48, 1251–1254 .
6. Y.J. Cui, B.L. Wang, K.F. Wang., et al. (2018). Fracture mechanics analysis of delamination buckling of a porous ceramic foam coating from elastic substrates. *Ceram. Int.* 44, 17986–17991.
7. I.M. Kadenko, O.M. Kharitonov, R.V. Yermolemko (2010). *Osnovy teplohydrauliky yadernykh enerhetychnykh ustanovok [Fundamentals of heat hydraulics of nuclear power plants]*. Kyiv: "Kyiv University" Publishing Centre [in Ukrainian].
8. R.G. Cherkez, P.P. Fenyak, D.D. Demyanyuk *(2013). Computer simulation of permeable cooling thermoelement. J.Thermoelectricity*, 5, 64-74.
9. L.I. Anatychuk, R.G. Cherkez (2003). On the properties of permeable thermoelements. *Proc. of XXII Intern. Conf. on Thermoelectrics (France),* 480-483.
10. *L.I. Anatychuk, L.N. Vikhor* (2002). Computer design of cascade modules for generators. *J.Thermoelectricity*, 4, 19-27.
11. R.G. Cherkez (2013). Energy characteristics of permeable thermoelements. *Journal of Electronic Materials*, 42(7), 1558-1563.
12. L.S. Pontryagin, V.G. Boltyanskii, R.V. Gamkrelidze, E.F. Mishchenko (1976). *Matematicheskaia teoriia optimalnykh processov [Mathematical theory of optimal processes]*. Moscow: Nauka [in Russian].

Submitted 03.03.2020

Черкез Р.Г. *док. фіз.– мат. наук, в.о. професора*[1,2]
Константинович И.А., *канд. физ.– мат. наук, доцент*[1, 2]

[1]Інститут термоелектрики НАН України та МОН України,
вул. Науки, 1, Чернівці, 58029, Україна,
e-mail: anatych@gmail.com;
[2]Чернівецький національний університет ім. Юрія Федьковича,
вул. Коцюбинського, 2, Чернівці, 58012, Україна

ОБОБЩЕННАЯ ТЕОРИЯ ТЕРМОЭЛЕКТРИЧЕСКОГО ПРЕОБРАЗОВАНИЯ ЭНЕРГИИ ДЛЯ ПРОНИЦАЕМЫХ ТЕРМОЭЛЕМЕНТОВ

Представлена обобщенная теория расчета проницаемых термоэлементов с учетом зависимостей параметров материала ветвей от температуры и концентрации носителей тока и изменения условий теплообмена вдоль высоты ветви. Описаны методы моделирования

распределений температур и тепловых потоков в 1-D и 3-D мерной модели проницаемого термоэлемента. Усовершенствована теория расчета проницаемых термоэлементов в случае решения многофакторной оптимизационной задачи с целью достижения максимальной энергетической эффективности термоэлектрического преобразования энергии. Бібл. 12, рис. 2.
Ключевые слова: обобщенная теория проницаемых термоэлементов, методы проектирования пропницаемого термоэлемента.

Черкез Р.Г, *док. физ.– мат. наук, и.о. профессора*[1,2]
Константинович И.А., *канд. физ.– мат. наук, доцент*[1, 2]

[1]Институт термоэлектричества НАН и МОН Украины,
ул. Науки, 1, Черновцы, 58029, Украина,
e–mail: anatych@gmail.com;
[2]Черновицкий национальный университет имени Юрия Федьковича,
ул. Коцюбинского, 2, Черновцы, 58012, Украина

ОБОБЩЕННАЯ ТЕОРИЯ ТЕРМОЭЛЕКТРИЧЕСКОГО ПРЕОБРАЗОВАНИЯ ЭНЕРГИИ ДЛЯ ПРОНИЦАЕМЫХ ТЕРМОЭЛЕМЕНТОВ

Представлена обобщенная теория расчета проницаемых термоэлементов с учетом зависимостей параметров материала ветвей от температуры и концентрации носителей тока и изменения условий теплообмена вдоль высоты ветви. Описаны методы моделирования распределений температур и тепловых потоков в 1-D и 3-D мерной модели проницаемого термоэлемента. Усовершенствована теория расчета проницаемых термоэлементов в случае решения многофакторной оптимизационной задачи с целью достижения максимальной энергетической эффективности термоэлектрического преобразования энергии. Библ. 12, рис. 2.
Ключевые слова: обобщенная теория проницаемых термоэлементов, методы проектирования пропницаемого термоэлемента.

References

1. V.N. Kozliuk, G.M. Shchegolev (1973). Termodinamicheskii analiz pronitsayemykh termoelektricheskikh kholodilnikov [Thermodynamic analysis of permeable thermoelectric coolers]. *Teplofizika i teploteknika*, 25, 96-100 [in Russian].
2. G.K. Kotyrlo, V.N. Kozliuk, Lobunets Yu.N. (1975). Termoelektricheskii generator s razvitoi poverkhnostiu teploobmena [Thermoelectric generator with a developed surface of heat exchange]. *Teplotekhnicheskiie problemy priamogo preobrazovaniia energii*, 7, 85-95 [in Russian].
3. Yu.N. Lobunets (1989). *Metody rascheta i proektirovaniia termoelekricheskikh preobrazovatelei energii [Methods for calculation and design of thermoelectric power converters]*. Kyiv: Naukova dumka [in Russian].

4. Y.J. Cui, B.L. Wanga, K.F. Wang, L. Zheng (2019). Power output evaluation of a porous annular thermoelectric generator for waste heat harvesting. *International Journal of Heat and Mass Transfer*, 137, 979–989.
5. E.S. Reddy, J.G. Noudem, C. Goupil (2007). Open porous foam oxide thermoelectric elements for hot gases and liquid environments. *Energy Convers. Manage*., 48, 1251–1254 .
6. Y.J. Cui, B.L. Wang, K.F. Wang., et al. (2018). Fracture mechanics analysis of delamination buckling of a porous ceramic foam coating from elastic substrates. *Ceram. Int.* 44, 17986–17991.
7. I.M. Kadenko, O.M. Kharitonov, R.V. Yermolemko (2010). *Osnovy teplohydrauliky yadernykh enerhetychnykh ustanovok [Fundamentals of heat hydraulics of nuclear power plants]*. Kyiv: "Kyiv University" Publishing Centre [in Ukrainian].
8. R.G. Cherkez, P.P. Fenyak, D.D. Demyanyuk *(2013). Computer simulation of permeable cooling thermoelement. J.Thermoelectricity*, 5, 64-74.
9. L.I. Anatychuk, R.G. Cherkez (2003). On the properties of permeable thermoelements. *Proc. of XXII Intern. Conf. on Thermoelectrics (France),* 480-483.
10. *L.I. Anatychuk, L.N. Vikhor* (2002). Computer design of cascade modules for generators. *J.Thermoelectricity*, 4, 19-27.
11. R.G. Cherkez (2013). Energy characteristics of permeable thermoelements. *Journal of Electronic Materials*, 42(7), 1558-1563.
12. L.S. Pontryagin, V.G. Boltyanskii, R.V. Gamkrelidze, E.F. Mishchenko (1976). *Matematicheskaia teoriia optimalnykh processov [Mathematical theory of optimal processes]*. Moscow: Nauka [in Russian].

Submitted 03.03.2020

Anatychuk L.I., *acad. National Academy of Sciences of Ukraine*[1,2]
Vikhor L.M., *doc. phys.-math. science*[1,2]
Kotsur M.P [1,2]**, Romaniuk I.F.** [2]**,**
Soroka A.V. [21]

Institute of Thermoelectricity of the NAS and MES of Ukraine,
1, Nauky str., Chernivtsi, 58029, Ukraine;
e-mail: anatych@gmail.com
[2]Yu.Fedkovych Chernivtsi National University,
2, Kotsiubynskyi str., Chernivtsi, 58012, Ukraine

OPTIMAL CONTROL OF TRANSIENT THERMOELECTRIC COOLING PROCESS IN THE MODE OF MINIMUM POWER CONSUMPTION

The problem of optimal control of transient thermoelectric cooling process in the mode of minimum power consumption is formulated and a method for its solution is proposed. An algorithm and a computer tool have been developed, which are used to calculate the optimal time dependences of the thermoelement supply current, whereby a given cooling temperature is reached within a given time with minimum power consumption. Examples of computer simulation of such optimal control functions for transient cooling process are given. It has been established that energy saving when supplying thermoelements with an optimally time-dependent current reaches 25 - 50% in comparison with the option of direct current power supply.Bibl. 29, Fig.5, Tabl. 1.
Key words: transient thermoelectric cooling, optimal control, optimal time dependences of thermoelement supply current.

Introduction

Thermoelectric cooling is used in various spheres of human life. But the process of thermoelectric cooling has been studied in detail and optimized mainly for steady-state operating modes of a thermoelectric converter. At the same time, back in the 50s of the 20th century, in the theoretical work of L.S. Stilbans and N.A. Fedorovich [1] it was shown that in transient modes it is possible to achieve deeper cooling than in steady-state ones. This fact was later confirmed by many theoretical and experimental studies [2 – 9] and continues to be intensively studied by modern researchers [10 – 18].

The sphere of practical application of transient modes of thermoelectric coolers concerns cases when object cooling time is of vital importance. These, for example, can be coolers for laser devices, to improve the image quality in night vision devices, thermal imagers and other military devices, as well as to quickly remove heat pulses that are released during the operation of electronic components [19, 20].

It is possible to achieve the advantages of transient cooling modes over steady-state ones if these modes are optimized. The most rational problems of optimization of the process of transient thermoelectric cooling are associated with the search for optimal control functions of this process, in particular, the optimal time dependences of the supply current of thermoelements. For the first time, such theoretical problems were considered in [6, 7, 21, 22] for the simplest models of thermoelectric converter, which did not take into account such important factors as the influence of the Thomson effect, contact resistance at thermoelement junctions, heat release and heat capacity of the cooled object, and the like. Approximate

analytical methods for solving such problems were proposed and, accordingly, approximate results were obtained.

Modern computer methods of searching for optimal time functions of current for thermoelectric coolers in transient modes mainly consist in choosing the best function from a limited set of given time dependences, rather than in solving optimization problems [23, 24].

The problems of transient cooling process optimization are related to the problems of optimal control of objects with distributed parameters [25]. These are complex problems for which there are no generalized solving methods. Therefore, the development of methods for solving the problems of optimal control of the dynamic modes of thermoelectric coolers is an urgent task.

In [26 – 28], approaches were proposed to solve the problem of finding the optimal time dependence of the current to achieve the lowest cooling temperature for a given time. The purpose of this work is to develop, on the basis of optimal control theory, methods and an algorithm for optimizing the process of transient thermoelectric cooling in the mode of minimum power consumption, to calculate the optimal time dependences of thermoelement supply current, whereby the specified cooling temperature is reached with minimum power consumption, and to analyze the efficiency of using such current functions.

Formulation of the problem of optimal control of transient cooling process in the mode of minimum power consumption

The thermoelement model used to optimize transient cooling is shown in Fig. 1. The following important physical factors and rational approximations are taken into account in the mathematical description of the model.

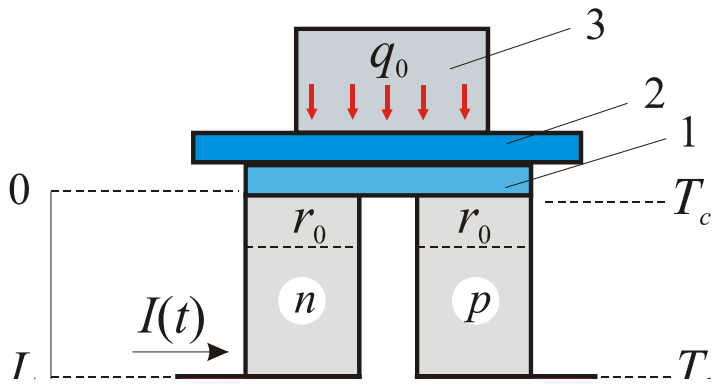

Fig. 1. Model of thermoelement for optimization of transient cooling process.
1 – connecting plate, 2 – insulating plate, 3 – cooled object.

1. The temperature distribution in n- and p-type legs is considered to be one-dimensional, the temperature depends on coordinate x along the height of the legs and changes with time.

2. The material of the legs is homogeneous, the thermoelectric properties – specific heat c, resistivity ρ, the Seebeck coefficient α, thermal conductivity κ can approximately be considered to be temperature-independent and identical for legs of both conduction types.

3. The Thomson heat absorption is taken into account in the bulk of the legs. The Thomson coefficient β can approximately be considered to be a constant value.

4. The Joule heat release on the contact resistance that takes place in the zone of contact with connecting plates on the cold junction of thermoelement legs is taken into account.

5. The process of transient cooling is essentially affected by the heat capacity and heat release of the cooled object, the heat capacity of the insulating and connecting plates, as well as the heat exchange

between the cold surface of module with the environment The cooled object together with the insulating and connecting plate is considered to be a cumulative object with a concentrated heat capacity, the temperature of which is equal to the temperature of the cold junction of the thermoelement and depends on time. Heat exchange of the cold surface of the module with the environment of constant temperature occurs according to Newton's law.

6. The temperature of the hot surface of the module is considered to be fixed.

Under these assumptions, the thermal processes in both thermoelement legs are similar and described by transient thermal conductivity equation in the form

$$c\frac{\partial T}{\partial t}=\kappa\frac{\partial^2 T}{\partial x^2}+\rho\frac{I^2(t)}{s^2}-\beta\frac{I(t)}{s}\frac{\partial T}{\partial x}\ , \tag{1}$$

where $T(t,x)$ is temperature, $I(t)$ is current is the leg which in the general case is a function of time. Time t changes on the interval $t\in[0,t_1]$, and coordinate x is directed along the leg from the cold to the hot junction (Fig.1) and changes on the section $x\in[0,L]$, L is the height, s is the cross-section of the leg.

In this equation, the first term on the right side takes into account the thermal conductivity in the thermoelement leg, the second term – the Joule heat release, the third – the Thomson heat.

The initial condition of the problem of transient thermoelectric cooling is generally given by

$$T(x,0)=T_a\,, \tag{2}$$

where T_a is ambient temperature.

The boundary conditions take into account the heat balance on the heat-absorbing surface and temperature stabilization of the heat-releasing thermoelement and are written as follows:

$$g\frac{\partial T(0,t)}{\partial t}=\left[q_0+Ks(T_a-T)-\alpha I(t)T+I^2(t)\frac{r_0}{s}+\kappa S\frac{\partial T}{\partial x}\right]_{x=0} \tag{3}$$

$$T(L,t)=T_h\,, \tag{4}$$

In condition (3), g is a total volumetric heat capacity of the cooled object, the insulating and connecting plates, calculated for one thermoelement leg. The first term on the right side of (3) takes into account heat release q_0 of the cooled object, the second – heat exchange between the surface and the environment, K is heat exchange coefficient, the third – the Peltier heat, the fourth- the Joule heat release due to contact resistance the value of which is r_0.

The process of transient thermoelectric cooling can be controlled by changing the current I over time within $I\in G_I$, $G_I=\{I_{\min}, I_{\max}\}$. One of the rational optimization problems is to determine the optimal current function $I(t)$ such that for a certain period of time t_1 will assure a given object cooling temperature T_c under the condition of maximum coefficient of performance (COP) of transient process.

By definition, the COP is determined by the relation: $\mathrm{COP}=\dfrac{Q_L}{J}$, where Q_L is thermal load $Q_L=g(T_a-T_c)\equiv\mathrm{const}$, which for the formulated problem is a given value, J is energy consumption. Therefore, the maximum COP corresponds to the minimum energy consumption.

Thus, it is necessary to find the optimal control function $I(t)$ such that satisfies the condition of reaching at a final time moment t_1 of a given temperature T_c,:

$$T\left(0,t_1\right)=T_c\,, \tag{5}$$

and assures minimum power consumption which is determined by the functional

$$J=\int_0^{t_1}\left[\alpha I(t)(T_h-T(0,t))+(\rho+\frac{r_0}{L})\frac{L}{s}I^2(t)\right]dt\,. \tag{6}$$

This problem refers to the problems of optimization of an object with distributed parameters [25], the behavior of which is described by a boundary value problem in parabolic equations (1) - (3).

An efficient way to solve problems of optimization of an object with distributed parameters is its discretization along the coordinate and thus obtaining an object with lumped parameters, which is described by a system of ordinary differential equations [26]. This makes it possible to use the Pontryagin maximum principle [29] for optimization.

Method of solving the problem. Optimality conditions

$T_0(t)$:

$$T_0(t)=\int_0^{t}\left[\alpha I(t)(T_h-T(0,t))+(\rho+\frac{r_0}{L})\frac{L}{s}I^2(t)\right]dt\,. \tag{7}$$

We pass in equations (1) - (4) to the dimensionless coordinate x = x / L, and discretize them by the coordinate. This procedure allows us to write equations (1), (3) as a system of ordinary differential equations, and the boundary value problem (1) - (4) is written as follows:

$$\frac{\partial T_i}{\partial t}=f_i(T(t),I(t)),\quad i=0,1,...N\,, \tag{8}$$

$$T_{N+1}\left(t\right)=T_h\,, \tag{9}$$

where N=1/h is the number of nodes in the coordinate, h is a step in the coordinate, and functions f_i are given by:

$$f_0(t)=\alpha I(t)(T_h-T_1(t))+(\rho+\frac{r_0}{L})\frac{L}{s}I^2(t)\,,$$

$$f_1(t)=\frac{1}{g}\left[q_0+Ks\left(T_a-T_1(t)\right)-\alpha I(t)T_1(t)+I^2(t)\frac{r_0}{s}+\kappa\frac{s}{L}\frac{T_2(t)-T_1(t)}{h}\right], \tag{10}$$

$$f_i(t)=\frac{\kappa}{cL^2h^2}(T_{i+1}(t)-2T_i(t)+T_{i-1}(t))+\rho\frac{I^2\left(t\right)}{cs^2},\quad i=2,...N\,.$$

The initial conditions for the discretized system (8) are as follows:

$$T_0\left(0\right)=0,\quad T_i\left(0\right)=T_a,\quad i=1,...N\,, \tag{11}$$

Condition (5) and functional J (6) take on the form

$$T_1(t_1) = T_c\,, \tag{12}$$

$$J = T_0(t_1). \tag{13}$$

The problem is to find such a function $I(t)$ and the corresponding solution $T_i(t)$ i=0,1, N of the system of equations (8) with the initial conditions (11), whereby condition (12) is satisfied for a certain moment of time t1 and for functional (13) takes its minimum value.

This problem refers to the problems of optimal control of objects, which are described by the equations of motion for phase variables T under the given values of some functions from phase variables at the finite moment of time t_1.

Such a given function is condition (12) which is written as

$$F(T_1(t_1)) \equiv T_c - T_1(t_1) = 0\,, \tag{14}$$

and instead of functional J (13) we consider an expanded functional

$$\Phi = J + \nu F\,, \tag{15}$$

where ν is an unknown parameter that must be chosen so as to satisfy condition (12).

Then the formulated optimization problem becomes a problem for phase variables with a free right end and a fixed time, the solution of which is given by the Pontryagin maximum principle [29].

To solve the problem, the Hamiltonian function is written according to the rule

$$H = \sum_{i=0}^{N} \psi_i f_i(T, I, t)\,, \tag{16}$$

where the unknown functions (pulses) ψ_i are solutions of the auxiliary system of equations

$$\frac{d\psi_i}{dt} = -\frac{\partial H}{\partial T_i}, \quad i = 0,...,N \tag{17}$$

with conditions at point $t = t_1$ (transversality conditions) in the form

$$\psi_i(t_1) = -\frac{\partial \Phi(T(t_1))}{\partial T_i}, \quad i = 0,...,N\,. \tag{18}$$

Optimal control function $I_{opt}(t)$ is found from the Pontryagin maximum condition

$$H(T(t), I_{opt}(t), \psi(t), t) = \max_{I \in G_I} H(T(t), I, \psi(t), t)\,, \tag{19}$$

that is, function $H(T(t),I(t),\psi(t),t)$ of variable I at each $t\in[0,t_1]$ reaches a maximum at point $I=I_{opt}(t)$ for all $I\in G_I$.

For our formulated problem the Hamiltonian function (16) acquires the form

$$H=-f_0(T_1,I,t)+\sum_{i=1}^{N}\psi_i f_i(T,I,t), \tag{20}$$

and the system of equations (17) with transversality conditions (18) for pulses ψ is written as

$$\frac{d\psi_1}{dt}=-\psi_0\frac{\partial f_0}{\partial T_1}-\psi_1\frac{\partial f_1}{\partial T_1}-\psi_2\frac{\partial f_2}{\partial T_1},$$

$$\frac{d\psi_2}{dt}=-\psi_1\frac{\partial f_1}{\partial T_2}-\psi_2\frac{\partial f_2}{\partial T_2}-\psi_3\frac{\partial f_3}{\partial T_2}, \tag{21}$$

$$\frac{d\psi_i}{dt}=-\psi_{i-1}\frac{\partial f_{i-1}}{\partial T_i}-\psi_i\frac{\partial f_i}{\partial T_i}-\psi_{i+1}\frac{\partial f_{i+1}}{\partial T_i},\quad i=3,...,N-1,$$

$$\frac{d\psi_N}{dt}=-\psi_{N-1}\frac{\partial f_{N-1}}{\partial T_N}-\psi_N\frac{\partial f_N}{\partial T_N}.$$

$$\psi_1(t_1)=\nu,\qquad \psi_i(t)=0,\qquad i=2,...,N. \tag{22}$$

Thus, the condition for the maximum (19) of the Hamiltonian function H (20) in conjunction with the basic system of ordinary differential equations (8) with the initial conditions (11) and the associated auxiliary system (21) with conditions at the final moment of time (22), which depend on the parameter ν, and which should provide the specified cooling temperature T_c at the final time moment t_1, set the solution to the problem of optimizing the process of transient thermoelectric cooling in the mode of minimum power consumption. Optimality conditions (19) - (22) make it possible to determine the optimal current function $I_{opt}(t)$ for such a mode.

Obviously, the complexity of such an optimization problem allows it to be solved only by computer methods. To solve it, based on the method of successive approximations, an algorithm was developed and a software tool was created in the MathLab environment.

Results of optimization of transient cooling process

Calculations of optimal current functions $I_{opt}(t)$ and characteristics of transient cooling process were carried out by the example of a thermoelement whose legs are made of Bi_2Te_3 based materials. Used for this purpose, the values of material parameters and other values that characterize transient cooling process are listed in Table.

Table

Parameter values used for calculations

Parameter	Value
Specific heat c, J/cm^3·K	1.4
Seebeck coefficient α, μV/K	200
Resistivity ρ, Ohm·cm	10^{-3}
Thermal conductivity κ, W/cm·K	0.015
Thomson coefficient β, μV/K	75
Contact resistance r_0, Ohm·cm^2	$5\cdot10^{-6}$
Total volumetric heat capacity g, J/ K	$1.25\cdot10^{-3}$
Heat release q_0, W	0.001
Heat exchange coefficient K, W/ cm^2·K	0.001
Ambient temperature T_a, K	300
Leg height L, cm	0.14
Leg cross-section s, cm^2	0.01

Optimal functions $I_{opt}(t)$ were calculated for different time intervals of reaching given cooling temperature under condition of minimum power consumption. Examples of such functions calculated for temperature reduction from 300 K to 260 K for 1 s and for 2.5 s are given in Fig. 2. It is obvious that for different time intervals these functions are different. Fig. 2 also shows the reduction of temperature with time to reach its given value under conditions of using these optimal dependences of current.

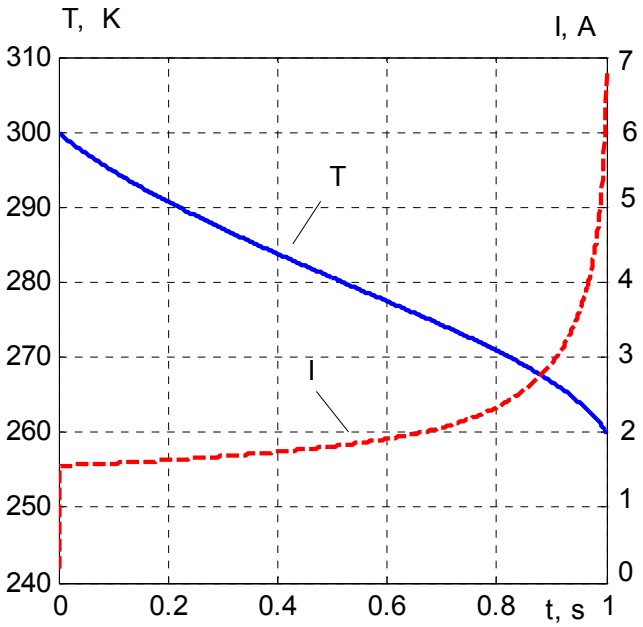

a)

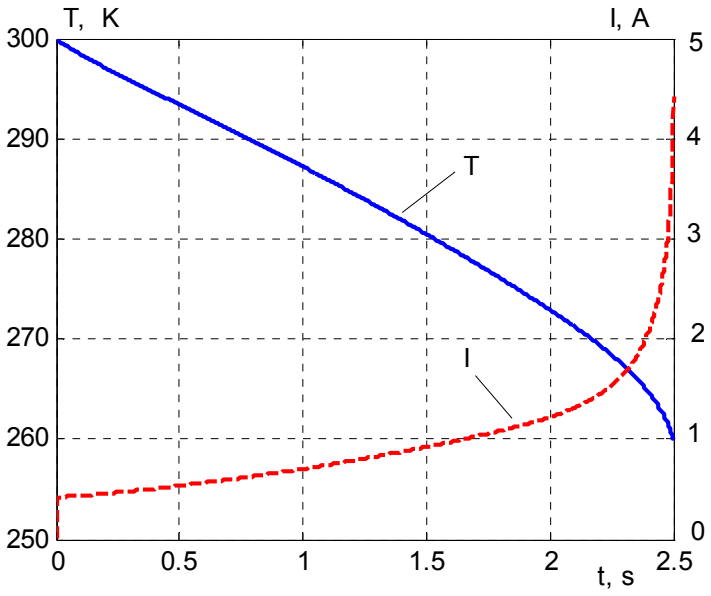

б)

Fig. 2. Optimal functions of current and their respective functions of temperature reduction from 300 K to 260 K for 1 s (a) and 2.5 s (b).

Fig. 3 illustrates the temperature distribution which is set in thermoelement legs for 1 s and 2.5 s.

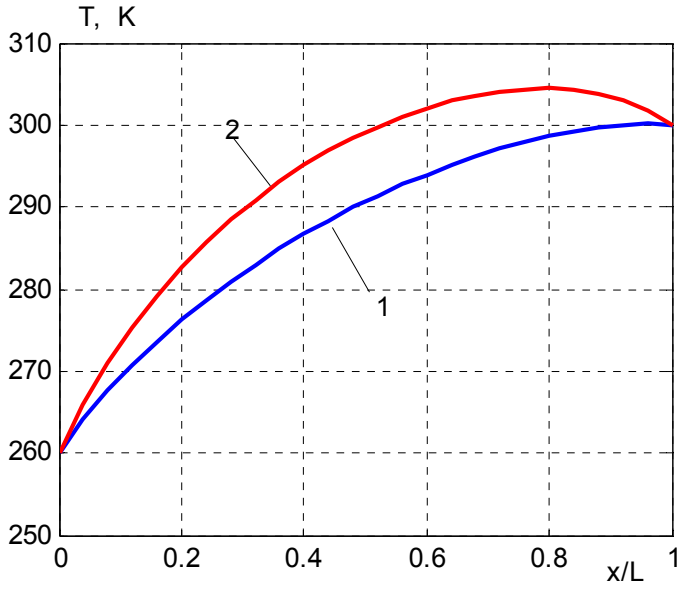

Fig. 3. Temperature distribution in thermoelement legs for 1 s (2) and 2.5 s (1).

Fig. 4 shows the results of calculating the dependence of the power consumed by the thermoelement on the time of reaching the cooling temperature of 260 K under the conditions of application of the optimal current functions. Power consumption significantly depends on the time interval during which the set temperature must be reached. Increasing the time interval leads to a decrease in power consumption. There is an optimal time interval during which cooling to a given temperature is achieved with the lowest power consumption. The results in Fig. 4 show that the specified cooling temperature under the conditions of supplying the thermoelement with a current that varies in time according to the optimal dependence can be

achieved both in a short period of time with a certain power consumption, and for a longer time, but with a significantly lower, namely 2 - 2.5 times, power consumption.

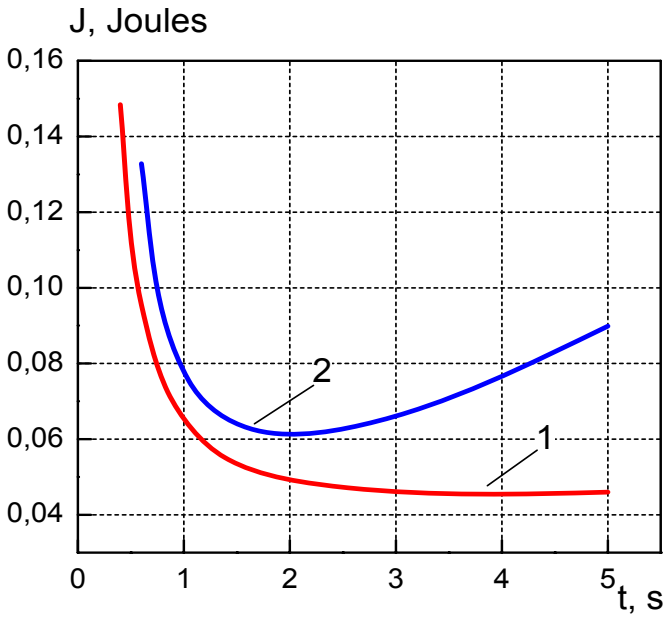

Fig. 4. Time dependences of thermoelement power consumption under the conditions of using optimal functions of current (1) and direct current (2).

Also, the calculations of power consumption were carried out when the thermoelement was supplied with direct current. For different time intervals, the current at which the cooling temperature of 260 K is reached, and, accordingly, the power consumption, were calculated. The results are shown in Fig. 4. For a constant current supplying a thermoelement, there is also a time interval and a corresponding current value at which the specified temperature is reached with the lowest power consumption. Comparison of the results shown in Fig. 4 shows that when using the optimal time functions of current, cooling to a given temperature for a given time occurs with significant power savings. Depending on the time interval, power consumption savings are from 50 to 25% compared to the option of supplying the thermoelement with direct current.

One of the methods for calculating the time dependence of the current, which provides cooling to a given temperature at the maximum coefficient of performance (COP), is to use the quasi-stationary approximation [22]. This approximation is used if the volumetric heat capacity of the thermoelement material is low, which can be neglected in comparison with the heat capacity of the cooled object. If these heat capacities are comparable values, then in the calculations, the heat capacity of the material is added to the heat capacity of the object. In the quasi-stationary approximation, it is assumed that the temperature of the heat-absorbing surface of the thermoelement decreases uniformly step by step to the specified temperature. For each value of the cooling temperature, the current is determined, which provides the maximum COP value for this temperature in the steady-state mode, and the corresponding time during which the heat balance of the heat-absorbing surface of the thermoelement with the cooled object is ensured in the transient mode. The result is a time dependence of the current, for which the value of the consumed power is calculated.

An example of such a calculation of the current function and the corresponding time dependence of cooling temperature is shown in Fig. 5. The time required for cooling from 300 K to 260 K in the quasi-stationary approximation is 11 s, and the power consumption is 0.093 J. These values are significantly

higher than the time of 3 s and the power consumption of 0.046 J (Fig. 4), obtained in the transient mode under the condition of optimal control of the thermoelement supply current.

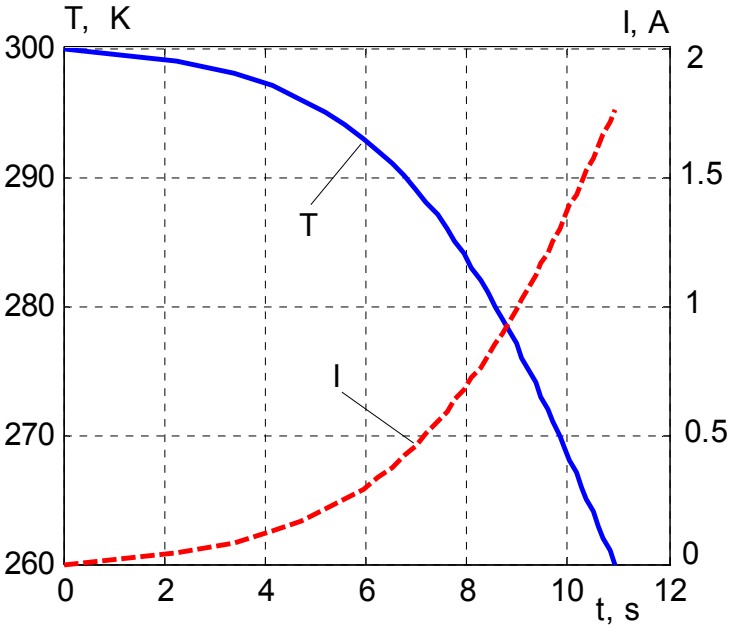

Fig. 5. The current function and the respective function of temperature reduction from 300 K to 260 K, calculated in the quasi-stationary approximation.

Thus, the comparison of the results shows that the quasi-stationary approximation is not correct enough to find the optimal time dependence of the current, which provides thermoelectric cooling with minimum power consumption.

Note that simulation of the optimal control functions of transient cooling is of great practical importance. These functions are used for the design and auto-calibration of regulators, which are necessary to ensure the operation of automatic control systems for the transient cooling process in thermoelectric devices.

Conclusions

As a result of research:

1. One of the main problems of the optimal control of transient cooling is formulated, which consists in determining the optimal time dependence of the supply current, which assures the achievement of a given cooling temperature for a given time under the condition of minimum power consumption.

2. To solve the formulated problem, a method based on the discretization of the mathematical model of transient cooling by the coordinate is proposed, which makes it possible to use the Pontryagin maximum principle for the calculation of the optimal control functions.

3. A computer simulation technique has been developed which is used to calculate the optimal functions of the supply current of thermoelements for coolers with minimum power consumption.

4. It is shown that energy saving when supplying thermoelements with an optimally time-dependent current reaches 25 – 50 % as compared to the option of direct current supply.

5. It is found that the use of the quasi-stationary approximation for calculating the optimal time dependences of the supply current of a thermoelectric cooler is incorrect.

References

1. L.S. Stilbans, N.A. Fedorovich (1958). O rabote okhlazhdaiuschchikh termoelementov v nestatsionarnom rezhime [On the work of cooling thermoelements in transient mode]. *Zhurnal tekhnicheskoi fiziki – Technical Physics*, 28(3), 12–15 [in Russian].
2. J.E. Parrott (1960). The interpretation of stationary and transient behaviour of refrigerating thermocouples. *Solid-State Electronics*, 1 (2), 135–143.
3. V.P. Babin, E.K. Iordanishvili (1969). O povyshenii effekta termoelektricheskogo okhlazhdeniia pri rabote termoelemntov v nestatsionarnom rezhime [Increasing thermoelectric cooling effect with the work of thermoelements in transient mode]. *Zhurnal tekhnicheskoi fiziki – Technical Physics,* 39(2), 399–406 [in Russian].
4. K. Landecker , A.W. Findley (1961). Study of transient behavior of Peltier junctions. *Solid-State Electronics*, 3(3-4), 239–260.
5. G. E. Hoyos, , K.R. Rao, D. Jerger (1977). Fast transient response of novel Peltier. *Energy Conversion*, 17(1), 45–54.
6. G.A. Grinberg (1968). O nestatshionarnom rezhime raboty okhlazhdaiushchikh termoelementov [On the transient operating mode of cooling thermoelements]. *Zhurnal tekhnicheskoi fiziki – Technical Physics,* 38(3), 418–424 [in Russian].
7. A.S. Rivkin (1973). Optimalnoiie upravleniie nestatsionarnym processom termoelektricheskogo okhlazhdeniia [Optimal control of the transient process of thermoelectric cooling]. *Zhurnal tekhnicheskoi fiziki – Technical Physics,* 43(7), 1563–1570.
8. M. Idnurm, , K. Landecker (1973). Experiments with Peltier junctions pulsed with high transient currents. *Journal of Applied Physics*, 34(6), 1806–1810.
9. R.L. Field, , H.A. Blum (1979). Fast transient behavior of thermoelectric coolers with high current pulse and finite cold junction. *Energy Conversion*, 19(3), 159–165.
10. G.J. Snyder , J.P. Fleurial, T. Caillat, R.G. Yang, G.J. Chen (2002). Supercooling of Peltier cooler using a current pulse. *Journal of Applied Physics*, 92(3), 1564–1569.
11. L.M. Shen , F. Xiao, H.X. Chen, S.W. Wang (2012). Numerical and experimental analysis of transient supercooling effect of voltage pulse on thermoelectric element. *International Journal of Refrigeration*, 35 (4), 1156–1165.
12. M. Ma , J. Yu. (2014). A numerical study on the temperature overshoot characteristic of a realistic thermoelectric module under a current pulse operation. *International Journal of Heat and Mass Transfer,* 72, 234–241.
13. T. Thonhauser , G.D. Mahan, L. Zikatanov, J. Roe (2004). Improved supercooling in transient thermoelectrics. *Applied Physics Letters*, 85(15), 3247–3249.
14. J. N. Mao , H.X. Chen, H. Jia, X.L. Qian (2012). The transient behavior of Peltier junctions pulsed with supercooling. Journal of Applied Physics, 112(1), 014514-1–014514-9.
15. H. Lv, X-D. Wang, T-H. Wang, J-H. Meng (2015). Optimal pulse current shape for transient supercooling of thermoelectric cooler. *Energy*, 83, 788–796.
16. H. Lv, X-D. Wang, T-H. Wang, C-H. Cheng (2016). Improvement of transient supercooling of thermoelectric coolers through variable semiconductor cross-section. *Appl Energy*, 164, 501–508.
17. H. Lv, X-D. Wang, J-H. Meng, T-H. Wang, W-M. Yan (2016). Enhancement of maximum temperature drop across thermoelectric cooler through two-stage design and transient supercooling effect. *Appl Energy*, 175, 285–292.
18. Ma. Ming, Yu. Jianlin (2016). Experimental study on transient cooling characteristics of a realistic thermoelectric module under a current pulse operation. *Energy Conversion and Management*, 126, 210–216.
19. R.G.Yang, , G.J. Chen, A.R. Kumar, G.J. Snyder, J.-P. Fleurial (2005). Transient cooling of

thermoelectric coolers and its applications for microdevices. *Energy Conversion and Management*, 46 (9-10), 1407–1421. http://dx.doi.org/10.1016/j.enconman.2004.07.004

20. L.M. Shen , H.X.Chen, F. Xiao, Y.X. Yang, S.W. Wang (2014).The step-change cooling performance of mi niature thermoelectric module for pulse laser. *Energy Conversion and Management*, 80, 39–45.
21. M.A. Kaganov, M.R. Privin (1970). *Termoelektricheskiie teplovyie nasosy [Thermoelectric heat pumps]*. Leningrad: Energiia [in Russian].
22. A.V. Mikhailenko (1984). *Candidate's Thesis*. Chernivtsi [in Ukrainian].
23. C.-H. Cheng , S.-Y. Huang, T.-C. Cheng (2010). A three-dimensional theoretical model for predicting transient thermal behavior of thermoelectric coolers. *International Journal of Heat and Mass Transfer*, 53 (9-10), 2001–2011.
24. L.V. Hao, X.-D. Wang, T.-H. Wang, J.-H. Meng (2015). Optimal pulse current shape for transient supercooling of thermoelectric cooler. *Energy*, 83, 788–796.
25. N.U. Ahmed (2003). Distributed parameter systems. *Encyclopedia of Physical Science and Technology*. Elsevier BV.
26. M.P. Kotsur, A.G. Nakonechnyi (2015). Optimalnoie upravleniie nestatsionarnym rezhimom kaskadnogo termoelektricheskogo okhkladitelia [Optimal control of transient mode of cascade thermoelectric cooler]. *Kibernetika i vychislitelnaia tekhnika – Cybernetics and Computing,* 180, 66-82 [in Russian].
27. M.P. Kotsur (2016). Matematychne modeliuvannia ta optymizatsiia procesu nestatsionarnogo termoelektrychnogo okholodzhennia [Mathematical simulation and optimization of transient thermoelectric cooling process]. *Tekhnologichnyi audit ta rezervy vyrobnytstva – Technology Audit and Production Reserves,* 1/2(27), 29-34 [in Ukrainian].
28. M. Kotsur (2015). Optimal control of distributed parameter systems with application to transient thermoelectric cooling. *Advances in Electrical and Computer Engineering,* 15 (2), 117-122.
29. L.S. Pontryagin, V.G. Boltianskii, R.V. Gamkrelidze, E.F. Mishchenko (1976). *Matematicheskaia teoriia optimalnogo upravleniia [Mathematical theory of optimal control]*. Moscow: Nauka [in Russian].

Submitted 10.03.2020

Анатичук Л.І. *акад. НАН Украины*[1,2]**,**
Вихор Л.М. *док. фіз.-мат. наук*[1]
Коцур М.П, [1,2] **Романюк І.Ф.** [2]**, Сорока А.В.** [2]

[1]Інститут термоелектрики НАН і МОН України,
вул. Науки, 1, Чернівці, 58029, Україна;
e–mail: anatych@gmail.com
[2]Чернівецький національний університет
ім. Юрія Федьковича, вул. Коцюбинського 2,
Чернівці, 58000, Україна,

ОПТИМАЛЬНЕ КЕРУВАННЯ НЕСТАЦІОНАРНИМ ПРОЦЕСОМ ТЕРМОЕЛЕКТРИЧНОГО ОХОЛОДЖЕННЯ В РЕЖИМІ МІНІМАЛЬНОГО ЕНЕРГОСПОЖИВАННЯ

Сформульовано задачу оптимального керування нестаціонарним процесом термоелектричного охолодження в режимі мінімального енергоспоживання та запропоновано метод її вирішення. Розроблено алгоритм і комп'ютерний засіб, які застосовані для розрахунку оптимальних часових залежностей струму живлення термоелемента, за яких задана температура охолодження досягається за заданий час з мінімальними витратами електричної енергії. Наведено приклади комп'ютерного моделювання таких оптимальних функцій керування процесом нестаціонарного охолодження. Встановлено, що економія електроенергії за умови живлення термоелементів оптимально залежним від часу струмом досягає 25 – 50 % порівняно із варіантом живлення постійним струмом. Бібл.29 , рис. 5, табл. 1 .

Ключові слова: нестаціонарне термоелектричне охолодження, оптимальне керування, оптимальні часові залежності струму живлення термоелемента.

Анатычук Л.И. *акад. НАН Украины*[12]**,**
Вихор Л.Н. *док. физ.-мат. наук*[1]
Коцур М.П, [1,2] **Романюк И.Ф.** [2]**, Сорока А.В.** [2]

[1]Институт термоэлектричества НАН и МОН Украины,
ул. Науки, 1, Черновцы, 58029, Украина,
e–mail: anatych@gmail.com;
[2]Черновицкий национальный университет
им. Юрия Федьковича, ул. Коцюбинского, 2,
Черновцы, 58012, Украина

ОПТИМАЛЬНОЕ УПРАВЛЕНИЕ НЕСТАЦИОНАРНЫМ ПРОЦЕССОМ ТЕРМОЭЛЕКТРИЧЕСКОГО ОХЛАЖДЕНИЯ В РЕЖИМЕ МИНИМАЛЬНОГО ЭНЕРГОПОТРЕБЛЕНИЯ

Сформулирована задача оптимального управления нестационарным процессом термоэлектрического охлаждения в режиме минимального энергопотребления и предложен метод ее решения. Разработан алгоритм и компьютерные средства, примененные для расчета оптимальных временных зависимостей тока питания термоэлемента, при которых заданная температура охлаждения достигается за заданное время с минимальными затратами электроэнергии. Приведены примеры компьютерного моделирования таких оптимальных функций управления процессом нестационарного охлаждения. Установлено, что при питании термоэлементов оптимально зависимым от времени током экономия электроэнергии достигает 25 – 50 % по сравнению с вариантом питания постоянным током. Библ.29 , рис. 5, табл. 1 .

Ключевые слова: нестационарное термоэлектрическое охлаждение, оптимальное управление, оптимальные временные зависимости тока питания термоэлемента.

References

1. L.S. Stilbans, N.A. Fedorovich (1958). O rabote okhlazhdaiuschchikh termoelementov v nestatsionarnom rezhime [On the work of cooling thermoelements in transient mode]. *Zhurnal tekhnicheskoi fiziki – Technical Physics*, 28(3), 12–15 [in Russian].
2. J.E. Parrott (1960). The interpretation of stationary and transient behaviour of refrigerating thermocouples. *Solid-State Electronics*, 1 (2), 135–143.
3. V.P. Babin, E.K. Iordanishvili (1969). O povyshenii effekta termoelektricheskogo okhlazhdeniia pri rabote termoelemntov v nestatsionarnom rezhime [Increasing thermoelectric cooling effect with the work of thermoelements in transient mode]. *Zhurnal tekhnicheskoi fiziki – Technical Physics,* 39(2), 399–406 [in Russian].
4. K. Landecker , A.W. Findley (1961). Study of transient behavior of Peltier junctions. *Solid-State Electronics*, 3(3-4), 239–260.
5. G. E. Hoyos, , K.R. Rao, D. Jerger (1977). Fast transient response of novel Peltier. *Energy Conversion*, 17(1), 45–54.
6. G.A. Grinberg (1968). O nestatshionarnom rezhime raboty okhlazhdaiushchikh termoelementov [On the transient operating mode of cooling thermoelements]. *Zhurnal tekhnicheskoi fiziki – Technical Physics,* 38(3), 418–424 [in Russian].
7. A.S. Rivkin (1973). Optimalnoiie upravleniie nestatsionarnym processom termoelektricheskogo okhlazhdeniia [Optimal control of the transient process of thermoelectric cooling]. *Zhurnal tekhnicheskoi fiziki – Technical Physics,* 43(7), 1563–1570.
8. M. Idnurm, , K. Landecker (1973). Experiments with Peltier junctions pulsed with high transient currents. *Journal of Applied Physics*, 34(6), 1806–1810.
9. R.L. Field, , H.A. Blum (1979). Fast transient behavior of thermoelectric coolers with high current pulse and finite cold junction. *Energy Conversion*, 19(3), 159–165.
10. G.J. Snyder , J.P. Fleurial, T. Caillat, R.G. Yang, G.J. Chen (2002). Supercooling of Peltier cooler using a current pulse. *Journal of Applied Physics*, 92(3), 1564–1569.
11. L.M. Shen , F. Xiao, H.X. Chen, S.W. Wang (2012). Numerical and experimental analysis of transient supercooling effect of voltage pulse on thermoelectric element. *International Journal of Refrigeration*, 35 (4), 1156–1165.
12. M. Ma , J. Yu. (2014). A numerical study on the temperature overshoot characteristic of a realistic thermoelectric module under a current pulse operation. *International Journal of Heat and Mass Transfer,* 72, 234–241.
13. T. Thonhauser , G.D. Mahan, L. Zikatanov, J. Roe (2004). Improved supercooling in transient thermoelectrics. *Applied Physics Letters*, 85(15), 3247–3249.
14. J. N. Mao , H.X. Chen, H. Jia, X.L. Qian (2012). The transient behavior of Peltier junctions pulsed with supercooling. Journal of Applied Physics, 112(1), 014514-1–014514-9.
15. H. Lv, X-D. Wang, T-H. Wang, J-H. Meng (2015). Optimal pulse current shape for transient supercooling of thermoelectric cooler. *Energy*, 83, 788–796.
16. H. Lv, X-D. Wang, T-H. Wang, C-H. Cheng (2016). Improvement of transient supercooling of thermoelectric coolers through variable semiconductor cross-section. *Appl Energy*, 164, 501–508.
17. H. Lv, X-D. Wang, J-H. Meng, T-H. Wang, W-M. Yan (2016). Enhancement of maximum temperature drop across thermoelectric cooler through two-stage design and transient supercooling effect. *Appl Energy*, 175, 285–292.
18. Ma. Ming, Yu. Jianlin (2016). Experimental study on transient cooling characteristics of a realistic thermoelectric module under a current pulse operation. *Energy Conversion and Management*, 126, 210–216.

19. R.G.Yang, , G.J. Chen, A.R. Kumar, G.J. Snyder, J.-P. Fleurial (2005). Transient cooling of thermoelectric coolers and its applications for microdevices. *Energy Conversion and Management*, 46 (9-10), 1407–1421. http://dx.doi.org/10.1016/j.enconman.2004.07.004
20. L.M. Shen , H.X.Chen, F. Xiao, Y.X. Yang, S.W. Wang (2014).The step-change cooling performance of mi niature thermoelectric module for pulse laser. *Energy Conversion and Management*, 80, 39–45.
21. M.A. Kaganov, M.R. Privin (1970). *Termoelektricheskiie teplovyie nasosy [Thermoelectric heat pumps]*. Leningrad: Energiia [in Russian].
22. A.V. Mikhailenko (1984). *Candidate's Thesis*. Chernivtsi [in Ukrainian].
23. C.-H. Cheng , S.-Y. Huang, T.-C. Cheng (2010). A three-dimensional theoretical model for predicting transient thermal behavior of thermoelectric coolers. *International Journal of Heat and Mass Transfer*, 53 (9-10), 2001–2011.
24. L.V. Hao, X.-D. Wang, T.-H. Wang, J.-H. Meng (2015). Optimal pulse current shape for transient supercooling of thermoelectric cooler. *Energy*, 83, 788–796.
25. N.U. Ahmed (2003). Distributed parameter systems. *Encyclopedia of Physical Science and Technology*. Elsevier BV.
26. M.P. Kotsur, A.G. Nakonechnyi (2015). Optimalnoie upravleniie nestatsionarnym rezhimom kaskadnogo termoelektricheskogo okhkladitelia [Optimal control of transient mode of cascade thermoelectric cooler]. *Kibernetika i vychislitelnaia tekhnika – Cybernetics and Computing,* 180, 66-82 [in Russian].
27. M.P. Kotsur (2016). Matematychne modeliuvannia ta optymizatsiia procesu nestatsionarnogo termoelektrychnogo okholodzhennia [Mathematical simulation and optimization of transient thermoelectric cooling process]. *Tekhnologichnyi audit ta rezervy vyrobnytstva – Technology Audit and Production Reserves,* 1/2(27), 29-34 [in Ukrainian].
28. M. Kotsur (2015). Optimal control of distributed parameter systems with application to transient thermoelectric cooling. *Advances in Electrical and Computer Engineering,* 15 (2), 117-122.
29. L.S. Pontryagin, V.G. Boltianskii, R.V. Gamkrelidze, E.F. Mishchenko (1976). *Matematicheskaia teoriia optimalnogo upravleniia [Mathematical theory of optimal control]*. Moscow: Nauka [in Russian].

Submitted 10.03.2020

A.V. Prybyla

A.V. Prybyla, *cand. Phys. - math. Sciences*[1,2]
L.I.Anatychuk *acad. National Academy of sciences of Ukraine*[1]

[1]Institute of Thermoelectricity
of the NAS and MES of Ukraine,
1, Nauky str., Chernivtsi, 58029, Ukraine;
e-mail: anatych@gmail.com
[2]Yu.Fedkovych Chernivtsi National University,
2, Kotsiubynskyi str., Chernivtsi, 58000, Ukraine

L.I.Anatychuk

INFLUENCE OF MINIATURIZATION ON THE EFFICIENCY OF A SPACE-PURPOSE THERMOELECTRIC HEAT PUMP

The paper presents the results of calculating the influence of miniaturization on the boundary possibilities of a thermoelectric liquid-liquid heat pump, in particular for its use as a high-efficiency heater for a space-purpose water purification device. Bibl. 10, Fig. 5.
Key words: thermoelectric heat pump, efficiency, distiller.

Introduction

General characterization of the problem. The use of thermoelectric heat pumps (THPs) in air and liquid conditioning systems, special- purpose evaporators is associated with their unique advantages [1 - 7], in particular environmental friendliness (there are no toxic refrigerants in such equipment); reliability (resistance to mechanical impacts, long service life); independence from the orientation in space (the ability to work in the absence of gravity).

An example of the effective use of thermoelectric heat pumps are devices for water regeneration from liquid waste on board manned spacecraft (urine, condensate, sanitary water) [5 - 7]. Tests of their efficiency at the NASA stand showed that in the most important indicators - specific energy consumption, dimensions, weight and quality of the distillate- water purifiers with thermoelectric heat pump outperform known space-purpose analogues [6].

However, such devices are subject to new, higher requirements related to the possibilities of their new applications (manned missions to explore Mars and other planets). This mainly concerns the reduction of their weight and size while maintaining (or even improving) the achieved level of energy efficiency. In [8, 9] the results of calculations of the influence of miniaturization of thermoelectric modules in the heating mode are given. The influence of the height of thermoelectric material legs on the heating coefficient of thermoelectric modules was determined by computer simulation, and the optimal height of the leg of material was found, which provides minimal losses of energy conversion efficiency. However, the complex task of optimizing the thermoelectric heat pump, providing a reduction of its weight and dimensions, has not yet been solved.

The purpose of our work is to study the energy efficiency of a space-purpose thermoelectric heat pump under conditions of reduction of its overall dimensions.

Physical model of THP

Physical model of a thermoelectric heat pump is shown in Figs. 1 - 3. It consists of heat exchangers 1, providing the passage of heat flux *Qh* through the hot side of thermoelectric modules, thermoelectric modules proper 3, heat exchangers 2, providing the passage of heat flux *Qc* through the cold side of thermoelectric modules and a system of hydraulically coupled channels 4, providing circulation of liquid in the thermoelectric heat pump.

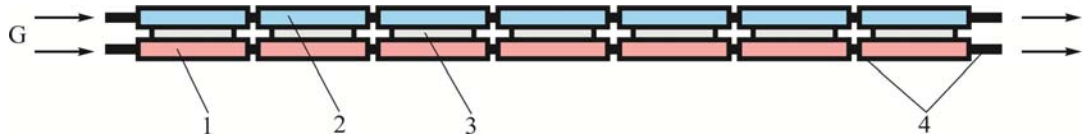

Fig. 1. The simplest physical model of a thermoelectric heat pump.

In the simplest case this model presents series-connected hot heat-exchangers 1 and cold heat-exchangers 2, with thermoelectric modules 3 located between them (Fig. 1). However, practical implementation of such a structure is not always rational. This is due to significant dimensions of such a device.

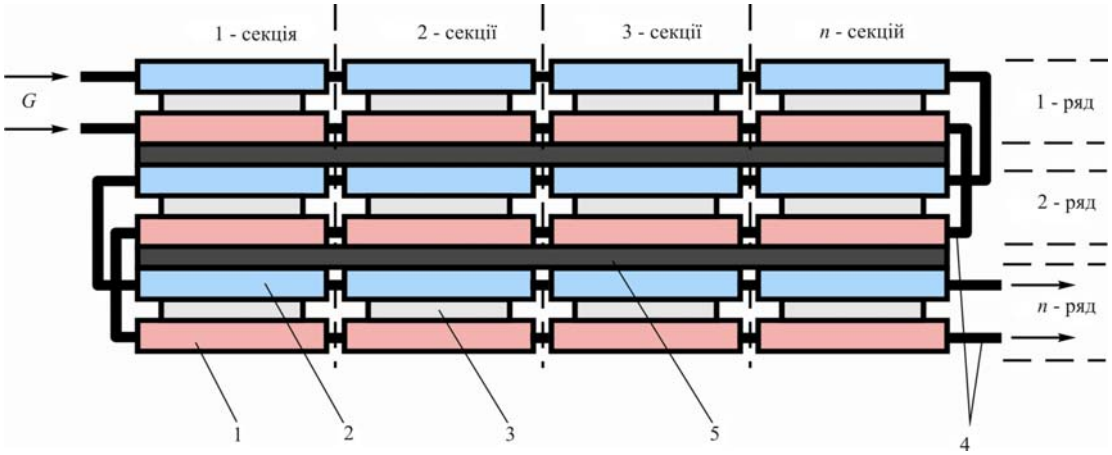

Fig. 2. Physical model of a thermoelectric heat pump with thermal insulation.

In practice, it is more convenient to connect heat exchangers 1, 2 with thermoelectric modules 3 in rows with a different number of sections, between which there is thermal insulation 5.

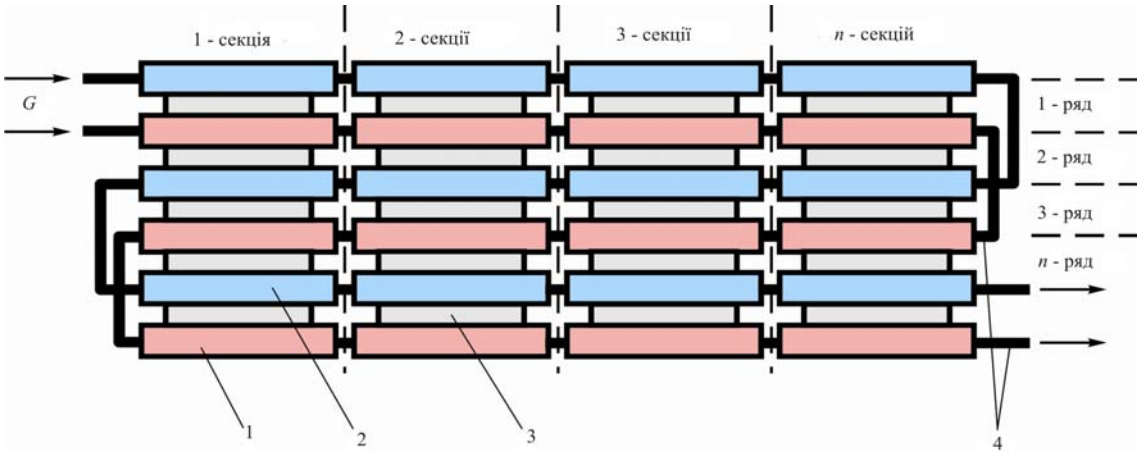

Fig. 3. Physical model of a thermoelectric heat pump.

However, to reduce the weight and dimensions of such equipment, you can simplify the design proposed in Fig. 2. In this case, a number of heat exchangers will provide the operating conditions of two rows of thermoelectric modules (Fig. 3). This makes it possible to significantly reduce the number of heat exchangers, and, consequently, the weight and dimensions of such a device.

Mathematical and computer description of the model

To describe the heat and electricity fluxes, we will use the laws of conservation of energy

$$div\vec{E} = 0 \tag{1}$$

and electrical charge

$$div\vec{j} = 0, \tag{2}$$

where

$$\vec{E} = \vec{q} + U\vec{j}, \tag{3}$$

$$\vec{q} = \kappa\nabla T + \alpha T\vec{j}, \tag{4}$$

$$\vec{j} = -\sigma\nabla U - \sigma\alpha\nabla T. \tag{5}$$

Here, $\vec{E}$ is energy flux density, $\vec{q}$ is heat flux density, $\vec{j}$ is electrical current density, U is electrical potential, T is temperature, α, σ, κ are the Seebeck coefficient, electrical conductivity and thermal conductivity.

With regard to (3) – (5), one can obtain

$$\vec{E} = -(\kappa + \alpha^2\sigma T + \alpha U\sigma)\nabla T - (\alpha\sigma T + U\sigma)\nabla U. \tag{6}$$

Then the laws of conservation (1), (2) will take on the form:

$$-\nabla\left[(\kappa + \alpha^2\sigma T + \alpha U\sigma)\nabla T\right] - \nabla\left[(\alpha\sigma T + U\sigma)\nabla U\right] = 0, \tag{7}$$

$$-\nabla(\sigma\alpha\nabla T) - \nabla(\sigma\nabla U) = 0. \tag{8}$$

The nonlinear differential equations of second order in partial derivatives (7) and (8) determine the distribution of temperature T and potential U in thermoelements.

An equation describing the process of heat transport in the walls of heat exchangers in the steady-state case is written as follows:

$$\nabla(-k_1 \cdot \nabla T_1) = Q_1, \tag{9}$$

where k_1 is thermal conductivity of heat exchanger walls, ∇T_1 is temperature gradient, Q_1 is heat flux.

The processes of heat-and-mass transfer of heat carriers in heat exchanger channels in the steady-state case are described by equations [10]

$$-\Delta p - f_D \frac{\rho}{2d_h} v|\vec{v}| + \vec{F} = 0, \tag{10}$$

$$\nabla(A\rho\vec{v}) = 0, \tag{11}$$

$$\rho \mathrm{AC_p}\vec{v}\cdot\nabla T_2 = \nabla\cdot Ak_2\nabla T_2 + f_D\frac{\rho A}{d_h}|\vec{v}|^3 + Q_2 + Q_{wall}, \tag{12}$$

where p is pressure, ρ is heat carrier density, A is cross-section of the tube, $\vec{F}$ is the sum of all forces, C_p is heat carrier heat capacity, T_2 is temperature, $\vec{v}$ is velocity vector, k_2 is heat carrier thermal conductivity, f_D is the Darcy coefficient, $d = \frac{4A}{Z}$ is effective diameter, Z is perimeter of tube wall, Q_2 is heat which is released due to viscous friction [W/m] (per unit length of heat exchanger), Q_{wall} is heat flux coming from the heat carrier to the tube walls [W/m]

$$Q_{wall} = h\cdot Z\cdot(T_1 - T_2), \tag{13}$$

where h is heat exchange coefficient which is found from equation

$$h = \frac{Nu\cdot k_2}{d}. \tag{14}$$

Here, Nu is the Nusselt number which is found from equation

$$Nu = \frac{\left(\frac{f_d}{8}\right)(Re - 1000)Pr}{1 + 12.7\left(\frac{f_d}{8}\right)^{\frac{1}{2}}\left(Pr^{\frac{2}{3}} - 1\right)}, \tag{15}$$

where $Pr = \frac{C_p\mu}{k_2}$ is the Prandtl number, μ is dynamic viscosity, $Re = \frac{\rho v d}{\mu}$ is the Reynolds number, $3000 < Re < 6\cdot 106$, $0.5 < Pr < 2000$.

The Darcy coefficient f_D is found with the use of the Churchill equation for the entire spectrum of the Reynolds number and all the values of e/d (e is roughness of wall surface)

$$f_D = 8\left[\left(\frac{8}{Re}\right)^{12} + (A+B)^{-1.5}\right]^{1/12}. \tag{16}$$

Here, $A = \left[-2.457\cdot\ln\left(\left(\frac{7}{Re}\right)^{0.9} + 0.27(e/d)\right)\right]^{16}$, $B = \left(\frac{37530}{Re}\right)^{16}$.

From the solution of equations (7) – (12) we obtain the distribution of temperatures, electrical potential (for thermoelements), velocities and pressure (for heat carrier).

To solve the above differential equations with the respective boundary conditions, the Comsol Multiphysics applied software package was used.

Computer simulation results

Below are the results of calculating the parameters of a thermoelectric pump in accordance with the physical model shown in Fig. 3. The influence of energy consumption W_{pump} on the heat carrier pumping through the heat exchange system on the heating coefficient μ of a thermoelectric heat pump was studied for different heights of thermoelectric power converters (*h* from 0.1 to 1 mm) and different temperature differences of the heat carriers at the inlet to the heat exchange circuit of a thermoelectric heat pump (W_{pump}) (Fig. 4).

Thus, from the analysis of Fig.4 it is seen that the heating coefficient of a thermoelectric heat pump weakly depends on the height of the thermoelectric converter up to the height of the thermoelectric converter leg of 0.5 mm and begins to sharply decrease with its further miniaturization. So, when the height of the thermoelectric converter leg decreases by 2 times (from 1 to 0.5 mm), the heating coefficient decreases by only 5 %, but its subsequent decrease (to a height of 0.25 mm) leads to a decrease in μ already by~22 %, and with a leg height of 0.1 mm μ decreases by~45 %. On the other hand, a twofold decrease in the leg height leads to a decrease in the weight of the heat pump by 25 %, the volume by 28 %, and also its cost by 35 %.

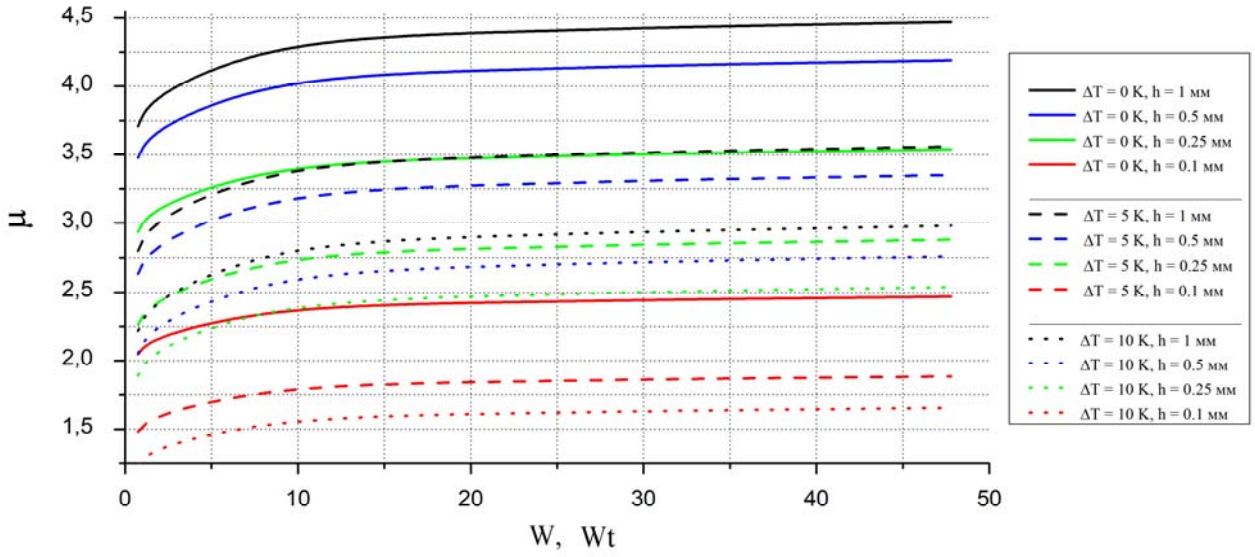

Fig. 4. Dependence of the heating coefficient of a thermoelectric heat pump μ on the supply power of heat exchange system W for different heights of thermoelectric power converters h and different temperature differences of heat carriers at the inlet to heat exchange circuits of a thermoelectric heat pump ΔT.

In addition, we analyzed the losses in the efficiency of the heat pump caused by the need for additional power supply to the heat exchange system (Fig. 5). Analysis of Fig. 5 shows that with an increase in the supply power of the liquid pump, which ensures the circulation of the heat carrier in the heat exchange system, the heating coefficient of the thermoelectric heat pump first increases, which is due to a decrease in the loss of the temperature difference in the heat exchange system due to an increase in the circulation rate of the heat carrier. Taking into account in the expression for the heating coefficient of a thermoelectric heat pump (17) the energy consumption for heat carrier pumping (18) leads to the fact that μ, reaching a maximum, starts gradually decreasing, because energy consumption for heat carrier pumping begin to reach the level of energy consumption for the functioning of thermoelectric modules.

$$\mu = \frac{Q_г}{W_{тн}}, \tag{17}$$

$$\mu_{втр} = \frac{Q_г}{W_{тм} + W_{нас}}, \tag{18}$$

where Q_h is the heat output of the heat pump, W_{TM} is the supply power of thermoelectric modules, W_{pump} is the supply power of the liquid pumps of the heat exchange system.

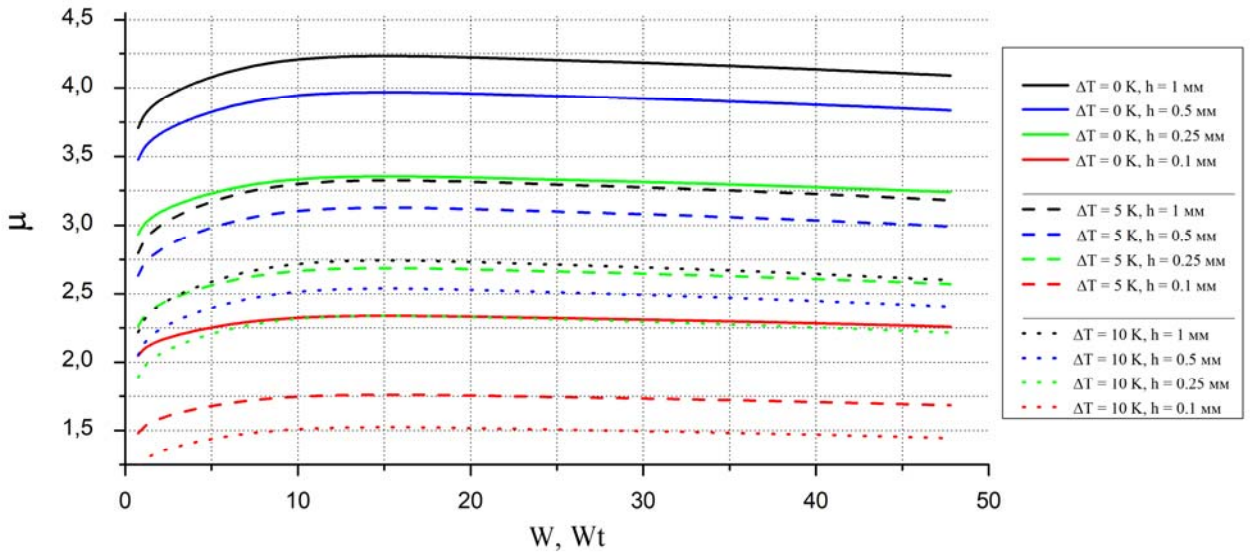

Fig. 5. Dependence of the heating coefficient of a thermoelectric heat pump μ (with regard to energy consumption for heat carrier pumping) on the supply power of heat exchange system W for different heights of thermoelectric power converters h and different temperature differences of heat carriers at the inlet to heat exchange circuits of a thermoelectric heat pump ΔT.

Conclusions

1. The influence of energy consumption for heat carrier pumping through heat exchange system on the heating coefficient μ of a thermoelectric heat pump has been established for different heights of thermoelectric power converters (*h* from 0.1 to 1 mm) and different temperature differences at the inlet to heat exchange circuits of a thermoelectric heat pump (ΔT from 0 to 10 K) (Fig.4).
2. It has been determined that the heating coefficient of a thermoelectric heat pump weakly depends on the height of the thermoelectric converter up to the height of the thermoelectric converter leg of 0.5 mm and begins to sharply decrease with its further miniaturization. So, when the height of the thermal converter leg decreases by 2 times (from 1 to 0.5 mm), the heating coefficient decreases by only 5%, but its subsequent decrease (to a height of 0.25 mm) leads to a decrease in μ already by~ 22%, and with a leg height of 0.1 mm μ decreases by~45%. On the other hand, a twofold decrease in the leg height leads to a decrease in the weight of the heat pump by 25%, the volume by 28%, and also its cost by 35%.
3. It has been established that taking into account in the expression for the heating coefficient of a thermoelectric heat pump of energy consumption for heat carrier pumping leads to the fact that μ, on reaching a maximum, starts gradually decreasing, because energy consumption for heat carrier pumping

begins to reach the level of energy consumption for the functioning of thermoelectric modules.

References

1. Rozver Yu.Yu. (2003). Thermoelectric air-conditioner for transport means. *J.Thermoelectricity*, 2, 52 -56.
2. Anatychuk L.I., Vikhor L.N., Rozver Yu.Yu. (2004). Study of the characteristics of thermoelectric cooler of liquid or gas flows. *J.Thermoelectricity*, 1, 73 – 80.
3. Anatychuk L.I., Suzuki N., Rozver Yu.Yu. (2005). Thermoelectric air-conditioner for rooms. *J.Thermoelectricity*, 3, 53 – 56.
4. Anatychuk L.I., Rozver Yu.Yu., Prybyla A.V. (2017). Experimental study of thermoelectric liquid-liquid heat pump. *J.Thermoelectricity*, 3, 47 – 53. (http://www.scopus.com/inward/record.url?eid=2-s2.0-85059430319&partnerID=MN8TOARS)
5. Anatychuk L.I., Prybyla A.V. (2017). Limiting possibilities of thermoelectric liquid-liquid heat pump. *J.Thermoelectricity*, 4, 49– 54. (http://www.scopus.com/inward/record.url?eid=2-s2.0-85059419349&partnerID=MN8TOARS)
6. Anatychuk L.I., Barabash P.A., Prybyla A.V., Rifert V.G., Solomakha A.S. (2017). Improvement of the system of distillation cascade for long-term space flights. *68-th International Astronautical Congress* (Australia, Adelaide, September 25-29, 2017) (http://www.scopus.com/inward/record.url?eid=2-s2.0-85051361510&partnerID=MN8TOARS).
7. Anatychuk L.I., Rifert V.G., Solomakha A.S., Barabash P.A., Usenko V., Prybyla A.V., Neymark M., Petrenko V. (2019). Upgrade the centrifugal multiple-effect distiller for deep space missions. *70-th International Astronautical Congress* (USA, Washington D.C., October 21-25). (http://www.scopus.com/inward/record.url?eid=2-s2.0 85079143567&partnerID=MN8TOARS).
8. Anatychuk L.I., Vikhor L.M., Prybyla A.V. (2018). Influence of miniaturization on the efficiency of thermoelectric modules in heating mode. *J.Thermoelectricity*, 3, 44-51. (http://www.scopus.com/inward/record.url?eid=2-s2.0-85072013470&partnerID=MN8TOARS)
9. Anatychuk L.I., Vikhor L.N., Prybyla A.V. (2018). The influence of contacts on the efficiency of thermoelectric modules in heating mode under miniaturization conditions. *J.Thermoelectricity*, 4, 45-50. (http://www.scopus.com/inward/record.url?eid=2-s2.0-85072046106&partnerID=MN8TOARS)
10. Michael V. Lurie (2008). Modeling of oil product and gas pipeline transportation. Weinheim, WILEY-VCH Verlag Gmbh & Co. Kgaa.

Submitted 18.03.2020

Анатичук Л.І., *акад. НАН Украини*[1,2]
Прибила А.В., *канд. физ.-мат. наук*[1,2]

[1]Інститут термоелектрики НАН і МОН України,
вул. Науки, 1, Чернівці, 58029, Україна;
e–mail: anatych@gmail.com
[2]Чернівецький національний університет
ім. Юрія Федьковича, вул. Коцюбинського 2,
Чернівці, 58012, Україна

ВПЛИВ МІНІАТЮРИЗАЦІЇ НА ЕФЕКТИВНІСТЬ ТЕРМОЕЛЕКТРИЧНОГО ТЕПЛОВОГО НАСОСА КОСМІЧНОГО ПРИЗНАЧЕННЯ

У роботі наводяться результати розрахунків впливу мініатюризації на граничні можливості термоелектричного теплового насоса рідина-рідина, зокрема для його використання у якості високоефективного нагрівника для приладу очистки води космічного призначення. Бібл. 10, рис. 5.
Ключові слова: термоелектричний тепловий насос, ефективність, дистилятор.

Анатычук Л.И., *акад. НАН Украины*[1,2]
Прибыла А.В., *канд. физ.-мат. наук*[1,2]

[1]Институт термоэлектричества НАН и МОН Украины,
ул. Науки, 1, Черновцы, 58029, Украина, *e–mail: anatych@gmail.com;*
[2]Черновицкий национальный университет
им. Юрия Федьковича, ул. Коцюбинского, 2,
Черновцы, 58012, Украина

ВЛИЯНИЕ МИНИАТЮРИЗАЦИИ НА ЭФФЕКТИВНОСТЬ ТЕРМОЭЛЕКТРИЧЕСКИХ ТЕПЛОВЫХ НАСОСОВ КОСМИЧЕСКОГО НАЗНАЧЕНИЯ

В *работе приводятся результаты расчетов влияния миниатюризации на предельные возможности термоэлектрического теплового насоса жидкость-жидкость, в частности для его использования в качестве высокоэффективного отопителя для прибора очистки воды космического назначения. Библ. 10, рис. 5.*
Ключевые слова: *термоэлектрический тепловой насос, эффективность, дистиллятор.*

References

1. Rozver Yu.Yu. (2003). Thermoelectric air-conditioner for transport means. *J.Thermoelectricity*, 2, 52 -56.
2. Anatychuk L.I., Vikhor L.N., Rozver Yu.Yu. (2004). Study of the characteristics of thermoelectric cooler of liquid or gas flows. *J.Thermoelectricity*, 1, 73 – 80.
3. Anatychuk L.I., Suzuki N., Rozver Yu.Yu. (2005). Thermoelectric air-conditioner for rooms. *J.Thermoelectricity*, 3, 53 – 56.
4. Anatychuk L.I., Rozver Yu.Yu., Prybyla A.V. (2017). Experimental study of thermoelectric liquid-liquid heat pump. *J.Thermoelectricity*, 3, 47 – 53. (http://www.scopus.com/inward/record.url?eid=2-s2.0-85059430319&partnerID=MN8TOARS)
5. Anatychuk L.I., Prybyla A.V. (2017). Limiting possibilities of thermoelectric liquid-liquid heat pump.

J.Thermoelectricity, 4, 49– 54.
(http://www.scopus.com/inward/record.url?eid=2-s2.0-85059419349&partnerID=MN8TOARS)

6. Anatychuk L.I., Barabash P.A., Prybyla A.V., Rifert V.G., Solomakha A.S. (2017). Improvement of the system of distillation cascade for long-term space flights. *68-th International Astronautical Congress* (Australia, Adelaide, September 25-29, 2017) (http://www.scopus.com/inward/record.url?eid=2-s2.0-85051361510&partnerID=MN8TOARS).
7. Anatychuk L.I., Rifert V.G., Solomakha A.S., Barabash P.A., Usenko V., Prybyla A.V., Neymark M., Petrenko V. (2019). Upgrade the centrifugal multiple-effect distiller for deep space missions. *70-th International Astronautical Congress* (USA, Washington D.C., October 21-25). (http://www.scopus.com/inward/record.url?eid=2-s2.0 85079143567&partnerID=MN8TOARS).
8. Anatychuk L.I., Vikhor L.M., Prybyla A.V. (2018). Influence of miniaturization on the efficiency of thermoelectric modules in heating mode. *J.Thermoelectricity*, 3, 44-51. (http://www.scopus.com/inward/record.url?eid=2-s2.0-85072013470&partnerID=MN8TOARS)
9. Anatychuk L.I., Vikhor L.N., Prybyla A.V. (2018). The influence of contacts on the efficiency of thermoelectric modules in heating mode under miniaturization conditions. *J.Thermoelectricity*, 4, 45-50. (http://www.scopus.com/inward/record.url?eid=2-s2.0-85072046106&partnerID=MN8TOARS)
10. Michael V. Lurie (2008). Modeling of oil product and gas pipeline transportation. Weinheim, WILEY-VCH Verlag Gmbh & Co. Kgaa.

Submitted 18.03.2020

NEWS
OF INTERNATIONAL THERMOELECTRIC ACADEMY

ANATOLIY IRRADIONOVICH CASIAN

The International Thermoelectric Academy regrets to inform that **Anatoliy Irradionovich Casian,** a famous scientist, Doctor of Physical and Mathematical Sciences, Professor, academician of the International Thermoelectric Academy died suddenly on May 29, 2020 in the 85th year.

Anatoliy Irradionovich was born on November 17, 1935 in the village of Kolikautsy, Brichany district in Moldova.

In 1957 he graduated with honors from Kishinev State University (now the State University of Moldova) in the specialty “theoretical physics”. Then he entered graduate school in the same educational institution; in 1961 he defended his Ph.D., and in 1988 - his dissertation for the degree of doctor habilitatus. In 1990 A.I. Casian was awarded the title of professor.

During 1960-1969 he held various positions at the Academy of Sciences of Moldova. Until 1976, A.I.Casian headed the Department of Theoretical Mechanics of Kishinev Polytechnic Institute. 1976 - 1982 - years of work in the Moldovan branch of the Institute of Power Sources of Moscow Scientific and Industrial Association "Kvant" as a managerial officer, and eventually director of the branch. From 1982 to September 1, 2016, he headed the Department of Theoretical Mechanics of the Technical University of Moldova. From May 1982 to the day of his death he was Professor of the Department of Theoretical Mechanics of the same university.

Anatoliy Irradionovich Casian was the vice head of the Council for Theoretical Physics of the Academy of Sciences of Moldova, the vice head of the Specialized Council for the defense of candidate and doctoral dissertations in the field of theoretical physics at the Academy of Sciences of Moldova, a member of the international editorial board of the international “Journal of Thermoelectricity" and other periodical scientific publications, the head of the research group of numerous research projects, including six international.

In 1994 A.I. Casian was elected academician of the International Thermoelectric Academy, and in 1999 - corresponding member of the American-Romanian Academy of Arts and Sciences.

The famous physicist was repeatedly invited to read theoretical courses at universities and institutes in France, Israel, and the USA. In 1996 and 2002 prof. Casian was invited for 2 weeks to Ben-Gurion University, Beer-Sheva, Israel. In 1997, 1998 and 2000 he received a one-month invitation to the Henri Poincare University, Nancy, France. In 1999 he visited the Office of Naval Research, Washington, SUA to submit a technical report; paid a visit for a week to the University of California - Riverside in 2002, USA; was at the Observatoire des Nano et Micro Technologies in 2005, Paris, France, where he presented his latest work at the seminar. In 2013 he received an invitation to the University Wűrzburg, Germany; in 2014 - to the Institute of Solid State Physics, Latvia, Riga; in 2015 - to the Institute of Organic Chemistry, Sofia, Bulgaria.

The research interests of the scientist were quite broad. They dealt with fundamental problems of the theory of semiconductors, transfer phenomena and thermoelectric phenomena in low-dimensional structures, quantum wells, thermoelectric properties of quasi-one-dimensional organic crystals.

Professor A.I.Casian is the author of over two hundred scientific works, including two monographs and six textbooks. Under his supervision, 6 doctoral dissertations were defended at the Technical University of Moldova and two in Algeria.

The scientific, pedagogical, organizational work of the scientist A.I.Casian was well appreciated. He was awarded the medal “For Labor Valour”, in 2004 he received the title of Laureate of the National Prize of Moldova in the field of science and technology, in 2017 he was awarded the Honorary Gold Prize of the International Thermoelectric Academy in the nomination “For fundamental contribution to thermoelectricity”.

The International Thermoelectric Academy, the Institute of Thermoelectricity of the National Academy of Sciences and the Ministry of Education and Science of Ukraine express their sincere condolences to the family and friends of Anatoliy Irradionovich, as well as the administration of the Technical University of Moldova and the Department of Theoretical Mechanics of this university and share with them the grief of the great loss.

ARTICLE SUBMISSION GUIDELINES

For publication in a specialized journal, scientific works are accepted that have never been printed before. The article should be written on an actual topic, contain the results of an in-depth scientific study, the novelty and justification of scientific conclusions for the purpose of the article (the task in view).

The materials published in the journal are subject to internal and external review which is carried out by members of the editorial board and international editorial board of the journal or experts of the relevant field. Reviewing is done on the basis of confidentiality. In the event of a negative review or substantial remarks, the article may be rejected or returned to the author(s) for revision. In the case when the author(s) disagrees with the opinion of the reviewer, an additional independent review may be done by the editorial board. After the author makes changes in accordance with the comments of the reviewer, the article is signed to print.

The editorial board has the right to refuse to publish manuscripts containing previously published data, as well as materials that do not fit the profile of the journal or materials of research pursued in violation of ethical norms (for instance, conflicts between authors or between authors and organization, plagiarism, etc.). The editorial board of the journal reserves the right to edit and reduce the manuscripts without violating the author's content. Rejected manuscripts are not returned to the authors.

Submission of manuscript to the journal

The manuscript is submitted to the editorial office of the journal in paper form in duplicate and in electronic form on an electronic medium (disc, memory stick). The electronic version of the article shall fully correspond to the paper version. The manuscript must be signed by all co-authors or a responsible representative.

In some cases it is allowed to send an article by e-mail instead of an electronic medium (disc, memory stick).

English-speaking authors submit their manuscripts in English. Russian-speaking and Ukrainian-speaking authors submit their manuscripts in English and in Russian or Ukrainian, respectively. Page format is A4. The number of pages shall not exceed 15 (together with References and extended abstracts). By agreement with the editorial board, the number of pages can be increased.

To the manuscript is added:

1. Official recommendation letter, signed by the head of the institution where the work was carried out.

2. License agreement on the transfer of copyright (the form of the agreement can be obtained from the editorial office of the journal or downloaded from the journal website – Dohovir.pdf). The license agreement comes into force after the acceptance of the article for publication. Signing of the license agreement by the author(s) means that they are acquainted and agree with the terms of the agreement.

3. Information about each of the authors – full name, position, place of work, academic title, academic degree, contact information (phone number, e-mail address), ORCID code (if available). Information about the authors is submitted as follows:

authors from Ukraine - in three languages, namely Ukrainian, Russian and English;

authors from the CIS countries - in two languages, namely Russian and English;

authors from foreign countries – in English.

4. Medium with the text of the article, figures, tables, information about the authors in electronic form.

5. Colored photo of the author(s). Black-and-white photos are not accepted by the editorial staff. With the number of authors more than two, their photos are not shown.

Requirements for article design

The article should be structured according to the following sections:

- *Introduction*. Contains the problem statement, relevance of the chosen topic, analysis of recent research and publications, purpose and objectives.
- *Presentation of the main research material* and the results obtained.
- *Conclusions* summing up the work and the prospects for further research in this direction.
- *References*.

The first page of the article contains information:

1) in the upper left corner – UDC identifier (for authors from Ukraine and the CIS countries);

2) surname(s) and initials, academic degree and scientific title of the author(s);

3) the name of the institution where the author(s) work, the postal address, telephone number, e-mail address of the author(s);

4) article title;

5) abstract to the article – not more than 1 800 characters. The abstract should reflect the consistent logic of describing the results and describe the main objectives of the study, summarize the most significant results;

6) key words – not more than 8 words.

The text of the article is printed in Times New Roman, font size 11 pt, line spacing 1.2 on A4 size paper, justified alignment. There should be no hyphenation in the article.

Page setup: "mirror margins" – top margin – 2.5 cm, bottom margin – 2.0 cm, inside – 2.0 cm, outside – 3.0 cm, from the edge to page header and page footer – 1.27 cm.

Graphic materials, pictures shall be submitted in color or, as an exception, black and white, in .opj or .cdr formats, .jpg or .tif formats being also permissible. According to author's choice, the tables and partially the text can be also in color.

Figures are printed on separate pages. The text in the figures must be in the font size 10 pt. On the charts, the units of measure are separated by commas. Figures are numbered in the order of their arrangement in the text, parts of the figures are numbered with letters – a, b, .. On the back of the figure, the title of the article, the author (authors) and the figure number are written in pencil. Scanned images and graphs are not allowed to be inserted.

Tables are provided on separate pages and must be executed using the MSWord table editor. Using pseudo-graph characters to design tables is inadmissible.

Formulae shall be typed in Equation or MatType formula editors. Articles with formulae written by hand are not accepted for printing. It is necessary to give definitions of quantities that are first used in the text, and then use the appropriate term.

Captions to figures and tables are printed in the manuscript after the references.

Reference list shall appear at the end of the article. References are numbered consecutively in the order in which they are quoted in the text of the article. References to unpublished and unfinished works are inadmissible.

Attention! In connection with the inclusion of the journal in the international bibliographic abstract database, the reference list should consist of two blocks: CITED LITERATURE and REFERENCES (this requirement also applies to English articles):

CITED LITERATURE – sources in the original language, executed in accordance with the

Ukrainian standard of bibliographic description DSTU 8302:2015. With the aid of VAK.in.ua (http://vak.in.ua) you can automatically, quickly and easily execute your "Cited literature" list in conformity with the requirements of State Certification Commission of Ukraine and prepare references to scientific sources in Ukraine in understandable and unified manner. This portal facilitates the processing of scientific sources when writing your publications, dissertations and other scientific papers.

REFERENCES – the same cited literature list transliterated in Roman alphabet (recommendations according to international bibliographic standard APA-2010, guidelines for drawing up a transliterated reference list "References" are on the site http//www.dse.org.ua, section for authors).

To speed up the publication of the article, please adhere to the following rules:

- in the upper left corner of the first page of the article – the UDC identifier;
- family name and initials of the author(s);
- academic degree, scientific title;

begin a new line, Times New Roman font, size 12 pt, line spacing 1.2, center alignment;

- name of organization, address (street, city, zip code, country), e-mail of the author(s);

begin a new line 1 cm below the name and initials of the author(s), Times New Roman font, size 11 pt, line spacing 1.2, center alignment;

- the title of the article is arranged 1 cm below the name of organization, in capital letters, semi-bold, font Times New Roman, size 12 pt, line spacing 1.2, center alignment. The title of the article shall be concrete and possibly concise;
- the abstract is arranged 1 cm below the title of the article, font Times New Roman, size 10 pt, in italics, line spacing 1.2, justified alignment in Ukrainian or Russian (for Ukrainian-speaking and Russian-speaking authors, respectively);
- key words are arranged below the abstract, font Times New Roman, size 10 pt, line spacing 1.2, justified alignment. The language of the key words corresponds to that of the abstract. Heading "Key words" - font Times New Roman, size 10 pt, semi-bold;
- the main text of the article is arranged 1 cm below the abstract, indent 1 cm, font Times New Roman, size 11 pt, line space spacing 1.2, justified alignment;
- formulae are typed in formula editor, fonts Symbol, Times New Roman. Font size is "normal" – 12 pt, "large index" – 7 pt, "small index" – 5 pt, "large symbol" – 18 pt, "small symbol" – 12 pt. The formula is arranged in the text, center aligned and shall not occupy more than 5/6 of the line width, formulae are numbered in parentheses on the right;
- dimensions of all quantities used in the article are represented in the International System of Units (SI) with the explication of the symbols employed;
- figures are arranged in the text. The figures and pictures shall be clear and contrast; the plot axes – parallel to sheet edges, thus eliminating possible displacement of angles in scaling; figures are submitted in color, black-and-white figures are not accepted by the editorial staff of the journal;
- tables are arranged in the text. The width of the table shall be 1 cm less than the line width. Above the table its ordinary number is indicated, right alignment. Continuous table numbering throughout the text. The title of the table is arranged below its number, center alignment;

• references should appear at the end of the article. References within the text should be enclosed in square brackets behind the text. References should be numbered in order of first appearance in the text. Examples of various reference types are given below.

Examples of LITERATURE CITED

Journal articles

Anatychuk L.I., Mykhailovsky V.Ya., Maksymuk M.V., Andrusiak I.S. Experimental research on thermoelectric automobile starting pre-heater operated with diesel fuel. *J.Thermoelectricity*. 2016. №4. P.84–94.

Books

Anatychuk L.I. *Thermoelements and thermoelectric devices. Handbook.* Kyiv, Naukova dumka, 1979. 768 p.

Patents

Patent of Ukraine № 85293. Anatychuk L.I., Luste O.J., Nitsovych O.V. Thermoelement.

Conference proceedings

Lysko V.V. *State of the art and expected progress in metrology of thermoelectric materials.* Proceedings of the XVII International Forum on Thermoelectricity (May 14-18, 2017, Belfast). Chernivtsi, 2017. 64 p.

Authors' abstracts

Kobylianskyi R.R. *Thermoelectric devices for treatment of skin diseases*: extended abstract of candidate's thesis. Chernivtsi, 2011. 20 p.

Examples of REFERENCES

Journal articles

Gorskiy P.V. (2015). Ob usloviakh vysokoi dobrotnosti i metodikakh poiska perspektivnykh sverhreshetochnykh termoelektricheskikh materialov [On the conditions of high figure of merit and methods of search for promising superlattice thermoelectric materials]. *Termoelektrichestvo - J.Thermoelectricity,* 3, 5 – 14 [in Russian].

Books

Anatychuk L.I. (2003). *Thermoelectricity. Vol.2. Thermoelectric power converters*. Kyiv, Chernivtsi: Institute of Thermoelectricity.

Patents

Patent of Ukraine № 85293. Anatychuk L. I., Luste O.Ya., Nitsovych O.V. Thermoelements [In Ukrainian].

Conference proceedings

Rifert V.G. Intensification of heat exchange at condensation and evaporation of liquid in 5 flowing-down films. In: *Proc. of the 9th International Conference Heat Transfer.* May 20-25, 1990, Israel.

Authors'abstracts

Mashukov A.O. *Efficiency hospital state of rehabilitation of patients with color carcer.* PhD (Med.) Odesa, 2011 [In Ukrainian].